



Australia's National
Science Agency

Water production from CO₂-capture

(RDE 493-28)

Final report

Paul Feron, Ramesh
Thiruvengkatachari, Sanger Huang, Dan
Maher, Phil Green, Jun-Seok Bae,
Debra Fernandes, Ashleigh Cousins,
Nouman Mirza, Ali Pourkhesalian, Ann
Tibbett, Aaron Cottrell, Shuaifei Zhao
(Deakin University)

EP 2023-1113

July 2023

Coal Innovation New South Wales

Citation

Feron P, Thiruvengkatachari R, Huang K, Maher D, Green P, Bae J-S, Fernandes D, Cousins A, Mirza N, Pourkhesalian A, Tibbett A, Cottrell, A., Zhao S (2023) Water production from CO₂-capture (RDE 493-28), Final report, CSIRO, Australia

Copyright

© Commonwealth Scientific and Industrial Research Organisation 2023. To the extent permitted by law, all rights are reserved and no part of this publication covered by copyright may be reproduced or copied in any form or by any means except with the written permission of CSIRO.

Important disclaimer

CSIRO advises that the information contained in this publication comprises general statements based on scientific research. The reader is advised and needs to be aware that such information may be incomplete or unable to be used in any specific situation. No reliance or actions must therefore be made on that information without seeking prior expert professional, scientific and technical advice. To the extent permitted by law, CSIRO (including its employees and consultants) excludes all liability to any person for any consequences, including but not limited to all losses, damages, costs, expenses and any other compensation, arising directly or indirectly from using this publication (in part or in whole) and any information or material contained in it.

CSIRO is committed to providing web accessible content wherever possible. If you are having difficulties with accessing this document please contact [csiro.au/contact](https://www.csiro.au/contact).

Contents

Acknowledgments.....	vii
Executive summary	viii
Lay Summary	xi
1 Introduction	1
1.1 Water consumption in coal fired power stations.....	1
1.2 Coal fired power plants in New South Wales.....	2
1.3 Combined desalination and CO ₂ -capture	4
2 Project objectives, milestones and performance measures	7
2.1 Objectives	7
2.4 Milestones and performance measures.....	9
3 Amine selection	13
4 Forward Osmosis: results from laboratory program and process design	16
4.1 Background.....	16
4.2 Amine losses	17
4.3 Membrane selection	19
4.4 Forward Osmosis experimental methodology	20
4.5 Forward Osmosis experimental results.....	23
4.6 Design of Forward Osmosis process and technical evaluation	30
5 Membrane Distillation: Laboratory program	35
5.1 Background.....	35
5.2 Scope of experimental program.....	36
5.3 Experimental results flat sheet membranes	37
5.4 Experimental results hollow fibre and capillary membrane modules under vacuum operation.....	40
5.5 Results hollow fibre membrane module and capillary membrane modules with sweep gas.....	47
5.6 Overall evaluation of Membrane Distillation experiments.....	56
6 Vales point PCC pilot plant experimental evaluation	59
6.1 Pilot plant operations and modifications	59
6.2 Results MEA PCC pilot plant campaign	62

6.3	Taurate-carbonate PCC pilot plant campaign	65
7	Vales Point Forward Osmosis rig experimental evaluation.....	68
7.1	Forward Osmosis rig design basis	68
7.2	Forward Osmosis rig integration with PCC pilot plant	69
7.3	Forward Osmosis process design	70
7.4	Overview results from Forward Osmosis experimental program.....	77
7.5	MEA-carbonate campaign results	80
7.6	Taurate-Carbonate campaign results.....	86
8	Techno-economic and Greenhouse-Gas life cycle analysis.....	101
8.1	Design basis of combined CO ₂ -capture-desalination process.....	101
8.2	Techno-economic analysis Forward Osmosis process	102
8.3	Greenhouse-gas lifecycle analysis	108
9	Conclusions.....	111
10	Recommendations.....	113
Appendix A	Conference presentations and publications	114
Appendix B	Combined Desalination & CO ₂ capture – Pilot plant equipment specification.	115
Appendix C	Overview of Forward Osmosis experimental results with taurate-carbonate solutions	118

Figures

Figure 1 : CO ₂ -capture integrated with forward osmosis with water recovery in the desorber overhead	5
Figure 2: CO ₂ -capture integrated with forward osmosis with water recovery in the absorber (Membrane Distillation).....	6
Figure 3: Concept of FO process showing the direction of water permeation in the combined CO ₂ capture desalination process	16
Figure 4: Forward Osmosis Heat Exchanger (FOHEX).....	17
Figure 5 Amine loss as a function of water recovery at different values of the Specific Reverse Salt Flux	19
Figure 6: Lab scale flat sheet FO test unit.....	21
Figure 7: Experimental setup for loading CO ₂ in the absorbent solution.....	22
Figure 8: Schematic of hollow fibre FO membrane operation with photo of the Aquaporin hollow fibre membrane used.....	23
Figure 9: Lab scale experimental setup of the hollow fibre FO membrane module.....	23
Figure 10: Experimentally determined water and reverse amine fluxes for 6 amines/amino-acid salts at 20 °C (Porifera membranes); closed symbols: 3.5% aqueous NaCl-solution as feed solution; open symbols: de-ionised water as feed solution; squares: amine solutions; circles: amino-acid salt solutions	27
Figure 11: Experimentally determined water and reverse amine fluxes for 6 amines/amino-acid salts at 20 °C (closed symbols) and 40 °C (open symbols) using 3.5% NaCl as the feed solution (Porifera membranes); squares: amine solutions; circles: amino-acid salt solutions; one experiment at 55 °C	28
Figure 12: Experimentally determined water and reverse amine fluxes for MEA-solutions at 20 °C (squares) and taurate solutions (circles) using 3.5% NaCl as the feed solution (Porifera membranes).....	29
Figure 13: Porifera membrane module and single membrane element (Porifera Inc)	34
Figure 14 Membrane distillation process applied for the recovery of water from absorber	35
Figure 15 Lab scale hybrid heat and vacuum Membrane Distillation unit with the image of the flat sheet MD cell	38
Figure 16 Photograph showing the four modules used in the current work.	41
Figure 17 Schematic of the Vacuum Membrane Distillation setup used to evaluate the hollow fibre/capillary membrane modules	43
Figure 18 Effect of feed temperature and vacuum pressure on the quantity and quality of produced water using the UNSW module	44
Figure 19 Effect of feed temperature and vacuum pressure on the quantity and quality of produced water using Liqui-Cel® module.....	45

Figure 20 Effect of feed flowrate on the quantity and quality of produced water using Liqui-Cel® module	45
Figure 21 Effect of CO ₂ loading on the quantity and quality of produced water using Liqui-Cel® module	46
Figure 22 Effect of feed temperature and vacuum pressure on the quantity and quality of produced water for loaded absorption liquid using Liqui-Cel® module.....	47
Figure 23 Experimental setup for the Membrane Distillation system	48
Figure 24: Liqui-Cel® membrane contactor in experimental set-up.....	48
Figure 25 Water flux and feed temperature drop along the membrane module as a function of feed temperature: (a) deionised water as the feed, and (b) CO ₂ -absorbent solution as the feed. Feed flowrate: 50 L/h; vacuum pressure: 10 kPa	49
Figure 26 Water flux and feed temperature drop along the membrane module as a function of feed flowrate. Feed water temperature: 50.2 ± 0.1 °C (water vapour pressure 12.4 kPa); vacuum pressure: 10 kPa.....	50
Figure 27 Water flux and feed temperature drop along the membrane module as a function of vacuum pressure: (a) no gas flow; (b) with gas flow on the vacuum side (deionised water was used as the feed). Feed temperature: 50.4 ± 0.1 °C (water vapour pressure 12.55 kPa); feed flowrate: 50 L/h.....	51
Figure 28 CUT membrane module integrated in experimental set-up at Deakin University.....	52
Figure 29 Water flux and feed temperature drop along the membrane module as a function of vacuum pressure (feed water temperature: 50.2 ± 0.1 °C (water vapour pressure 12.4 ± 0.04 kPa); feed flowrate: 20 L/h)	53
Figure 30 Water flux and feed temperature drop along the membrane module as a function of feed temperature (feed flowrate: 20 - 21 L/h; Vacuum pressure: 10 kPa (top-end of the membrane module was open)).....	54
Figure 31 Water flux and feed temperature drop along the membrane module as a function of vacuum pressure, using the absorption liquid as the feed, and gas flow on the vacuum side (feed water temperature: 50 °C; feed flowrate: 20 L/h)	55
Figure 32 Water flux and feed temperature drop along the membrane module as a function of feed temperature using the absorption liquid as the feed, and gas flow on the vacuum side (Vacuum pressure = 10 kPa)	55
Figure 33 New flue gas flow meter	60
Figure 34 Damaged steam flow meter	60
Figure 35 New steam valve installed	61
Figure 36 Tie-in points for the Forward Osmosis rig	62
Figure 37 Specific steam flow into the reboiler at different values of the liquid/gas ratio in absorber for 5M MEA and 4M MEA + 1M K ₂ CO ₃	63
Figure 38 MEA concentration in desorber condensate at different desorber top temperatures	64

Figure 39 MEA concentration in desorber condensate at different rich loadings	64
Figure 40 MEA concentration in desorber condensate at different steam consumption	65
Figure 41 Specific steam flow into the reboiler at different values of the liquid/gas ratio in absorber for 5M MEA and 3M taurate + 1.5M K ₂ CO ₃	66
Figure 42 Conductivity versus pH of condensate samples from campaign with 3M taurate + 1.5M K ₂ CO ₃	67
Figure 43 Basic Flow Diagram of Forward Osmosis Rig integration into the PCC pilot plant layout	69
Figure 44 Tie in points to Vales Point PCC pilot plant for FO system	70
Figure 45 Process Flow Diagram of Forward Osmosis System	71
Figure 46 Piping and instrumentation diagram for Forward Osmosis unit	72
Figure 47 3D lay-out of Forward Osmosis unit	73
Figure 48 Forward Osmosis rig with half of membrane modules installed (left side of picture). 74	
Figure 49 Forward Osmosis unit delivered on site (with 2 membrane modules installed)	75
Figure 50 Modified P&I diagram of the Forward Osmosis rig	76
Figure 51 : Heater to control solution temperature to the Forward Osmosis unit	77
Figure 52: Orientation of the membrane module	80
Figure 53 FO performance with NaCl solutions mimicking the conductivity of 30 wt.% aqueous MEA and seawater. FS flowrate = 40 lit/min; DS flowrate = 40 lit/min; NaCl concentration in the DS = 8.7 wt.%; NaCl concentration in the FS = 2.7 wt.%.....	81
Figure 54: Variation in the mass of the saline feed solution tank with time.....	82
Figure 55: Variation in Flux, Average DS line conductivity and pH values with time	83
Figure 56: Variation in the mass of the salt solution with time.....	85
Figure 57: Variation in Flux and the conductivities of draw and feed lines	85
Figure 58 Experimentally determined water flux at average differential NaCl concentration levels	87
Figure 59 Water production cost versus CO ₂ -emission intensity	110

Tables

Table 1: Specific water withdrawal and consumption rate per use type	1
Table 2: Overview of operational coal fired power stations in New South Wales.....	2
Table 3: Performance parameters Australian HELE power station ⁴	3
Table 4: Milestone overview.....	10

Table 5: Amine formulations considered for combined CO ₂ -capture/desalination process in this study.....	14
Table 6: Overview of Forward Osmosis equipment suppliers.....	20
Table 7: Overview of FO performance test results using Porifera flat sheet membranes.....	25
Table 8: Overview of FO performance test results using Aquaporin hollow fibre membranes...	30
Table 9: Comparison of options for CO ₂ -absorbents for evaluation in the Vales Point PCC pilot plant	31
Table 10 Results from Membrane Distillation experiments using porous flat sheet PTFE membranes with MEA and taurate solutions	39
Table 11 Specifications of membrane modules used in the current work.....	42
Table 12 Summary of results of Membrane Distillation experiments with absorption liquids ..	58
Table 13 Design basis for Forward Osmosis rig at Vales Point.	68
Table 14 Overview of analytical techniques used for determination of liquid concentrations ...	79
Table 15 Scope of experimental program.....	79
Table 16 Overview of Forward Osmosis experiments using saline solution as draw solution and de-ionised/saline water as the feed solution	89
Table 17 Overview of Forward Osmosis experiments using taurate-carbonate mixtures as draw solution and de-ionised/saline water as the feed solution	94
Table 18 Overview of results from Forward Osmosis experiments using taurate-carbonate mixtures as draw solution and de-ionised/saline water as the feed solution	99
Table 19: Performance overview for ultra-supercritical coal fired power plant with evaporative cooling used in this study; Results for 90% CO ₂ -capture estimated for state-of-the-art PCC process	102
Table 20: Design requirements for Forward Osmosis unit	103
Table 21: Technical and economic premises for a Forward Osmosis and a Reverse Osmosis process	104
Table 22 Estimated capital costs for a Forward Osmosis and a Reverse Osmosis process.....	106
Table 23: Preliminary Forward Osmosis process cost estimate with a Reverse Osmosis process as reference	107
Table 24 Greenhouse gas emission for water production from the Forward Osmosis and Reverse Osmosis process.....	109

Acknowledgments

CSIRO thankfully acknowledges the funding support from Coal Innovation New South Wales (Project number RDE493-28) for this project.

The support from Delta Electricity to this project and other CINSW funded projects by providing access to the Vales Point PCC pilot plant has been instrumental in the advancement of our post-combustion capture research and that of other research providers. We want to express our sincerest gratitude to Delta Electricity over the last 15 years for their assistance and enablement.

The contributions from Deakin University (Shuaifei Zhao & team – Membrane Distillation work) and University of New South Wales (Robert Taylor & team – provision of membrane contactor module) and Newcastle University (Jessica Allen – supervision of Nouman Mirza) have been greatly appreciated.

Executive summary

Coal fired power stations are thermo-electric power stations that use water for cooling purposes, handling of coal ash, as boiler feedwater make-up and for the various amenities on site. The addition of Post-Combustion CO₂-Capture (PCC) results in an increased use of water, not only for the capture process but also for the flue gas cooling and desulphurisation.

The process investigated in this project integrates a desalination process with an amine-based post-combustion CO₂-capture process, thus providing useable water for the power plant. In a methodological manner key technology items and components were investigated, ultimately resulting in a technology demonstration at the Delta Electricity PCC pilot plant at Vales Power Point power station that was a 3000 times larger scale compared to the laboratory size equipment.

Core to the concept is the Forward Osmosis technology that enables the selective transfer of water directly from a saline cooling water stream to the CO₂ absorption liquid. Subsequently the transferred water can be recovered from the absorption liquid loop in the CO₂-desorber by condensation of the steam exiting together with CO₂, as part of the normal operations and hence without additional energy requirement. Water can also be recovered from the absorber using a Membrane Distillation process, making use of the heat generated during the CO₂-absorption process. All aspects of the process concept have been investigated in this project.

Forward Osmosis

The laboratory phase in the project was preceded by the selection of six liquid absorbent formulations for further assessment. The chosen formulations incorporated amines and amino-acid salts as the CO₂-capture agents. These were evaluated in an experimental set-up for flat sheet membranes with a subset also evaluated separately using hollow fibre membranes. A performance specification was developed for the allowable losses of amines/amino-acids to the cooling water based on the integration of the Forward Osmosis process with the capture plant and its anticipated performance. This resulted in the definition of the Specific Reverse Amine Flux (SRAF) as an important performance parameter in addition to the membrane water flux.

The laboratory experiments indicated a better performance for the amino-acid salt formulations, both in terms of water flux and SRAF, that could be augmented by the addition of carbonates to the formulation. It was therefore decided to go forward towards the pilot plant demonstration with the best performing amino-acid salt formulation (taurate) and the worst performing amine solution (MEA-Mono-ethanolamine) to cover a wide range of potential project outcomes. Carbonates were added to the formulations to improve Forward Osmosis performance.

Based on the laboratory results, a dedicated Forward Osmosis unit was designed for connection with the PCC pilot plant at Vales Point power station. The unit employed membrane modules from Porifera that are based on flat sheet membranes. Prior to the installation of the Forward Osmosis unit, the PCC pilot plant was operated with the chosen absorption liquids to assess the quality of the condensate from the CO₂-desorber. For the experiments with MEA-based absorption liquids there was significant carry-over of MEA into the condensate resulting in concentration levels between 0.05-0.4 mol/L (M). For the experiments with taurate-based absorption liquids there was

negligible carry-over of the absorption liquid. However, the condensate had a conductivity of 700 – 2300 $\mu\text{S}/\text{cm}$ and a varying ammonium concentration between 1000 and 5000 ppm, indicative of degradation of the absorption liquid.

The Forward Osmosis experiments using MEA-carbonate formulations at Vales Point were not successful because of unexpected cross-over of the absorption liquid to the cooling water stream as a result of sealings that were not compatible with MEA. Using a different membrane module supplied by the manufacturer, the experiments with taurate-carbonate mixtures were successfully carried out with demineralised water, 3.5% NaCl solutions and lakewater as the cooling water. The liquid flows could not be operated at the maximum rates due to concerns of high pressure drop causing damage to the membranes. The experimentally determined water fluxes ranged from 4.4 to 10.6 $\text{l}/\text{m}^2\text{h}$, lower than values obtained in the laboratory experiments and the Specific Reverse Amine Flux ranged between 0.3 and 0.75 g/l which was better (lower) than the laboratory experiments and below the required maximum specification of 1 g/l . The hydraulics of the experiment was such that water recoveries were much higher than needed. It is therefore expected that these performances would be better under the actual process conditions.

There was concern around the transfer of salt into the absorption liquids. Salt transfer was expressed as the Specific Forward Salt Flux (SFSF) and ranged from 0.4 to 2.7 g/l (NaCl-basis using Cl^- concentrations) or 0.7 to 6.9 g/l (NaCl-basis using Na^+ concentrations). As this represents a significant influx of salt into the absorption liquid loop this needs to be carefully considered in subsequent work.

Membrane Distillation

The laboratory work on Membrane Distillation has been focused on identifying pathways towards demonstration of the technology in conjunction with the Delta Electricity PCC pilot plant at Vales Point power station. A wide range of membrane geometries (flat sheet, hollow fibre, capillary), membrane modules (Liqui-Cel[®] membrane contactor and filtration shell& tube types) and membrane materials (porous Poly-Tetra-Fluoro-Ethylene-PTFE and Polypropylene-PP) were assessed for their suitability to recover water via evaporation through the membrane and subsequent condensation. While the membrane contactor modules showed good stability with taurate-based absorption liquids and negligible permeation of the absorbent, their water fluxes were quite low. Higher water fluxes were achieved with the flat sheet PTFE membranes. Unfortunately, no suitable suppliers of complete modules were identified. Therefore, it was decided not to progress this work towards a technology demonstration at Vales Point. Using the information gathered in this project it was recommended to pursue the following options for demonstration in subsequent projects:

1. Evaluation of larger size Liqui-Cel[®] membrane contactors
2. Evaluation of a Membrane Distillation module from one of the suppliers identified.

In both cases the evaluation should consider both the performance (water flux, undesired permeation), water quality and robustness for the absorption liquids used.

Techno-economic assessment

The preliminary techno-economic assessment of the overall process indicated a cost of A\$1.82/ m^3 of water produced from a saline water stream, typical of seawater, 37% lower cost than the

equivalent Reverse Osmosis desalination plant. The water production of 4,368 m³/day would be able to supply 60% of the plant's cooling water needs.

Lay Summary

Water consumption in thermal power stations, like coal fired power plants, is a focal point of attention on a dry continent like Australia. The plants require significant amounts of cooling that is most effectively provided by the evaporation of water in a cooling tower or by flow-through cooling using seawater. The addition of CO₂-capture to a coal-fired power station to reduce emissions will increase the cooling water requirement even further as water is needed to cool down the flue gases and the capture plant itself will require water for cooling and other functions.

This project has investigated a new concept that is able to extract water from a saline cooling water stream, such as seawater, into the aqueous absorption liquids that are used to capture CO₂. It does this using a membrane that is water permeable but far less permeable to other components dissolved in the solutions. This so-called Forward Osmosis process works on the principle that water will naturally move from a dilute (low osmotic pressure) solution to a more concentrated (higher osmotic pressure) solution, when separated by a water permeable membrane.

The water that is transferred to the CO₂-absorption liquid can be recovered by evaporation and condensation, which is easiest to do in the CO₂-desorber where the solution is heated up to the boiling point to release CO₂. So, water can be recovered at that point as part of the CO₂-capture process without additional energy expense.

In this project we have researched various combinations of absorption liquids and Forward Osmosis membranes in the laboratory and selected two combinations for trials with Delta Electricity's CO₂-capture pilot plant at Vales Point power station. One combination was successful and provided significant information and insights that have prepared us for the next development steps.

We have quantified possible losses of the absorbents to the cooling water and also found that some salt is transferred from the saline cooling water to the absorption liquids. Both will need to be minimised, which can be achieved with very selective membranes but also by process design.

Our technical approach in this project can be used to assess the application of other absorption liquids and other membrane for this application. Our next steps will target the full integration of the Forward Osmosis system into a capture pilot plant as part of the pathway towards commercial application of this innovative process.

1 Introduction

1.1 Water consumption in coal fired power stations

Coal fired power stations are thermo-electric power stations that use water at various points. Cooling is needed in the steam cycle for the condensation of water, resulting in a cooling water demand that is met by either by flow-through cooling or evaporative cooling. In case of flue gas desulphurisation using limestone slurries or other aqueous solutions, the flue gases will be cooled down resulting in water losses through evaporation in the flue gas. Water is further used for handling of coal ash, boiler feedwater make-up and for the various amenities on site. Table 1 gives a quantitative overview of the water use types. Water withdrawal indicates the amount of water that is extracted from the source; Water is considered to be consumed if it is not returned to the source. Water is generally only returned to the source in case of flow-through cooling. The largest water consumption originates from evaporative cooling towers where water is lost to the ambient air. Flue gas desulphurisation is the next largest consumer, albeit one order of magnitude lower, with minor amounts used for ash handling, boiler feed water make-up and the amenities on a power plant site. Often the cooling tower blow-down water is used for ash handling. In case the power plant is air-cooled, flue gas desulphurisation will emerge as the largest water consumption. Dry processes may be used for flue gas desulphurisation in case of severely constrained water availability.

Table 1: Specific water withdrawal and consumption rate per use type¹

Type of water use	Water withdrawal [m ³ /MWh]	Water consumption [m ³ /MWh]
Flow-through cooling	95 - 170	0
Evaporative cooling	2 – 3	2 – 3
Flue gas desulphurisation	0.15 – 0.30	0.15 – 0.30
Ash handling	0.015 – 0.15	0.015 – 0.15
Boiler feedwater make-up	0.02 – 0.04	0.02 – 0.04
Amenities	< 0.01	< 0.01

¹ Water Use for Electric Power Generation. EPRI, Palo Alto, CA: 2008. 1014026.

The addition of post-combustion CO₂-capture results in a significant increase of the specific water consumption and withdrawals, due to the decrease in output of the power plant and the net-increase of cooling demand resulting from the PCC process, including CO₂-compression. Depending on the PCC technology the specific cooling water will increase by 49 – 83% after implementation of PCC².

1.2 Coal fired power plants in New South Wales

Coal fired power plants in New South Wales use a variety of cooling systems as shown in Table 2. Currently there are no coal fired power plants that use air cooling. Air cooled power stations typically have a 1-2% lower efficiency than a water-cooled power station. The ongoing constraints on water availability make air cooling an increasingly likely option for a new coal fired power station. In Queensland the youngest power stations, Millmerran and Kogan Creek, use air cooling.

Table 2: Overview of operational coal fired power stations in New South Wales

Power Station	Capacity [MW]	Commissioned	Closure (anticipated)	Cooling type
Liddell	1680	1971-73	2023	Flow through cooling from freshwater lake
Vales Point	1320	1978-79	2028	Flow through cooling with saltwater from lake
Eraring	2880	1982-84	2034	Flow through cooling with saltwater from lake
Bayswater	2640	1985-86	2035	Evaporative cooling using river water
Mount Piper	1400	1992-1993	2043	Evaporative cooling using dam water

In this study we have used the HELE (High-Efficiency, Low-Emission) power station defined by GHD in their report to Solstice Development Services³, who were engaged by ACA Low Emissions Technologies, as a representative power station. The plant uses a high-quality Hunter Valley coal in an ultra-supercritical coal fired power station. The high-pressure steam conditions are 275 bar and 604 °C with the intermediate pressure conditions at 59 bar and 604 °C. The plant uses an electrostatic precipitator for particulate removal, with no other emission controls in place. The performance parameters are given in Table 3 for the cases with evaporative cooling and air cooling.

² Global CCS Institute 2016, Water use in thermal power plants equipped with CO₂ capture systems, Melbourne, Australia.

³ Solstice Development Services, June 2017. HELE power station, Cost and Efficiency Report

The air-cooled power plant has a lower efficiency because of the auxiliary consumption of the cooling fans and a slightly higher condenser pressure.

Table 3: Performance parameters Australian HELE power station⁴

	Evaporative cooling	Air cooling
Coal input [t/h]	195.6	201.4
Gross electric output [MW _e]	675.5	678.8
Auxiliary consumption [MW _e]	25.5	28.8
Net electric power output [MW _e]	650	650
Net electrical efficiency, LHV [%]	42.88	41.64
Net electrical efficiency, HHV [%]	41.36	40.16
Specific CO ₂ emissions [tonne/MWh]	0.777	0.800
Specific cooling requirement [MWth/MWe]	1.115	1.174
Specific water consumption [m ³ /MWh]	1.777 (cooling and boiler feedwater)	0.05 (only boiler feed water)

The Solstice Development Services report did not discuss the implications of integrating an amine-based PCC process on either power stations, in particular in relation to the water use. Retrofitting the power plant will have the following effects:

- Assuming that the steam needed to regenerate the amine solutions is extracted from the power station steam cycle, it will result in less cooling needed for the power station as the steam is condensed in the reboiler of the PCC process.
- The flue gas (~ 140 °C) will need to be cooled down for effective CO₂-capture. A direct contact cooler may be used for this purpose which will result in a higher water content of the flue gas that will leave the capture plant or be condensed in the wash water section resulting in an equivalent water use for cooling at point.
- The capture plant requires cooling for the lean absorption liquid prior to entering the absorber and for cooling the CO₂ product that leaves the desorber. Depending on the level

of integration with the power station, the compression of CO₂ might also require additional cooling.

- Water is also needed for the formulation of amines in aqueous solutions, with the degradation products discarded in a wastewater stream.

In a study carried out for the IEAGHG programme⁴ we calculated the cooling requirement for a state-of-the-art PCC process, including CO₂-compression to 120 bar, to be 3.01 GJ/tonne CO₂, which is equivalent to 1.25 m³/t CO₂. It must be borne in mind that a significant fraction of this cooling requirement replaces part of the cooling requirement for the power station. At the specific reboiler duty of 2.46 GJ/tonne CO₂, it is estimated that only 22% (= (3.01-2.46)/2.46x100%) is an additional cooling duty requiring more cooling water. The overview study carried out by the GCCSI indicated absolute cooling water requirements were increased by 19-31% after retrofitting PCC to a coal fired power station, which is consistent with our estimate.

The power plant modelled in the IEAGHG study had a flue gas desulphurisation system installed, which is not standard for power plants in Australia. The water make-up requirement was estimated to be equal to 0.064 m³/MWh. This is lower than the literature values that can be derived from the data ranges provide in Table 1, most likely because the flue gas is cooled before the flue gas desulphurisation which reduces the evaporative cooling load.

1.3 Combined desalination and CO₂-capture

The process investigated in this project integrates a desalination process with an amine-based post-combustion CO₂-capture process, thus providing useable water for the power plant. It involves the replacement of the lean absorption liquid cooler in an amine-based CO₂-capture process by a Forward Osmosis (FO) membrane module. In an FO operation, two solutions with different osmotic pressures flow on either side of the semipermeable membrane and water is selectively transferred through the membrane from a solution of lower osmotic pressure (the cooling water) to a solution of higher osmotic pressure (the amine solution). The FO operation might utilise any saline water source such as, seawater or an aquifer that is unsuitable for direct use. As the solutions used for CO₂-capture are usually aqueous solutions with a higher concentration than seawater there will be a driving force for transfer of water from its source to the absorption liquid. The water can be recovered from the solution at no additional heat input to the CO₂-capture process in the top of the desorber as shown in Figure 1. The wet CO₂-product leaving the desorber is supplied to a condenser or other heat exchanger with the condensate removed from the absorption liquid loop.

⁴ IEAGHG, "Further assessment of Emerging CO₂ capture technologies for the Power Sector and their Potential to Reduce Costs, 2019-09, September, 2019

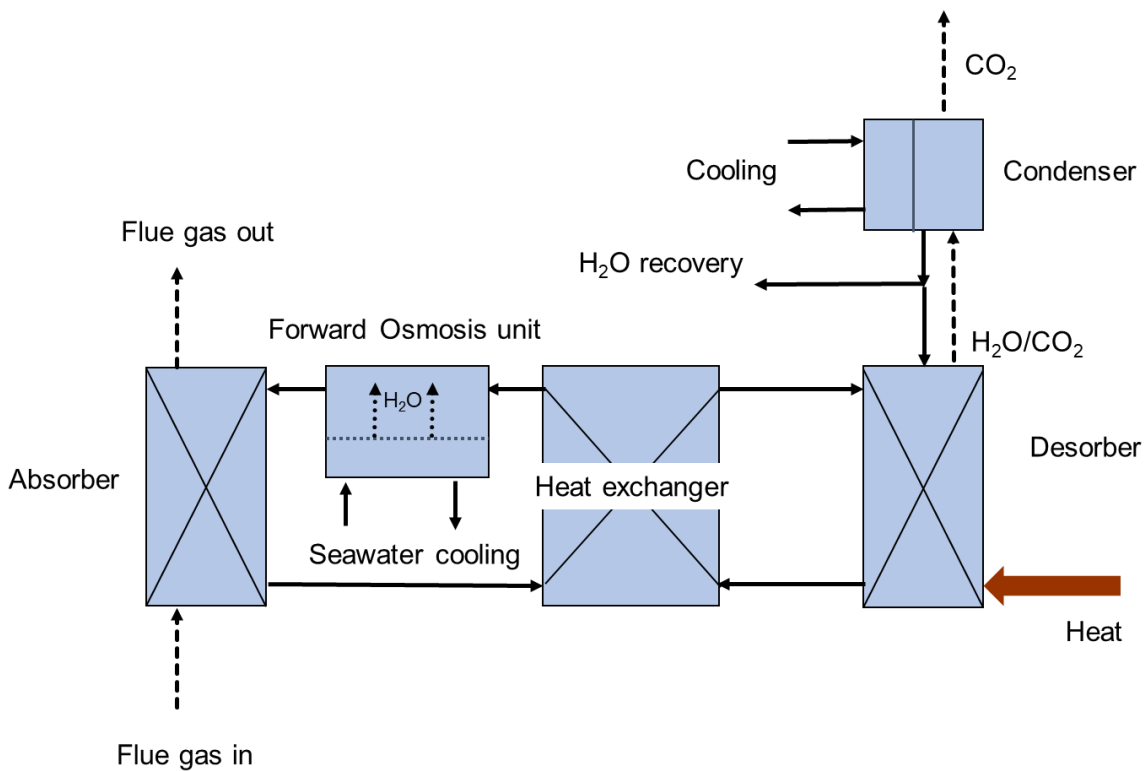


Figure 1 : CO₂-capture integrated with forward osmosis with water recovery in the desorber overhead

Water can also be recovered from the absorber by a vacuum membrane condenser which enables evaporation of water across a membrane with water recovery in a condenser under vacuum, as shown in Figure 2. This Membrane Distillation-based recovery route makes use of the exothermic nature of the reaction between CO₂ and the amine solution, which results in a sizeable temperature increase in the absorber. It has motivated technology suppliers to utilise so-called intercooling to maintain the driving force for CO₂- transfer to the liquid. With the proposed water recovery route, the reaction enthalpy released can be advantageously used to produce water. It is a more complicated recovery process and requires the development of dedicated process equipment. In essence, this water recovery process is achieved through the application of a Membrane Distillation process.

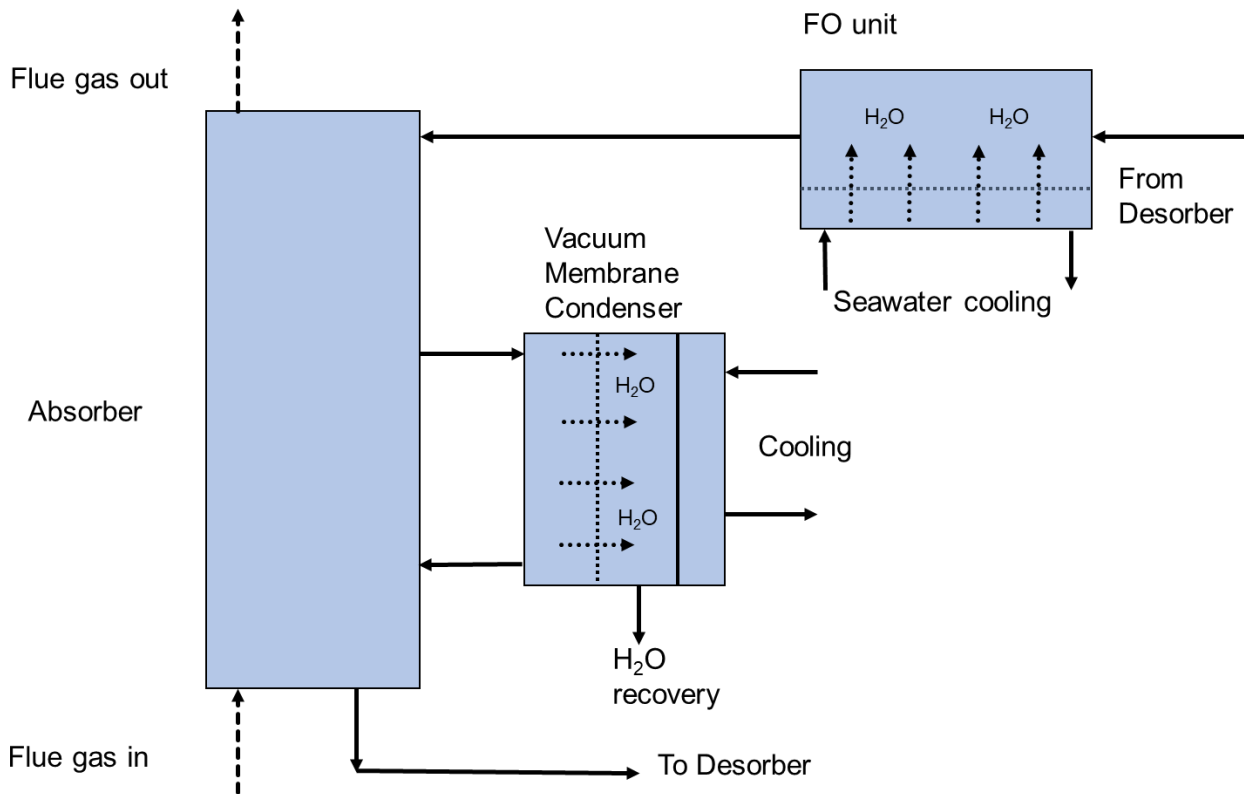


Figure 2: CO₂-capture integrated with forward osmosis with water recovery in the absorber (Membrane Distillation)

The source of saltwater can be seawater, water from aquifers, lakewater or brines from reverse osmosis desalination operations. The concentration of absorption liquids used in CO₂-capture is invariably higher than the salt concentration in these source streams, i.e. there will always be a driving force for water transfer.

2 Project objectives, milestones and performance measures

2.1 Objectives

This project aimed to demonstrate CSIRO's membrane-based process technology⁵ for production of freshwater from saline water with the Delta Electricity PCC pilot plant at Vales Point. The technology is based on the use of a Forward Osmosis membrane unit to transfer water from the saline cooling water to the amine solution, effectively replacing the lean absorption liquid cooler in an amine-based capture process. Subsequent recovery of freshwater is possible either from the CO₂-desorption process or via a vacuum Membrane Distillation process in the absorber.

The technology development challenges are in the application of the two membrane processes, Forward Osmosis and Membrane Distillation. For these two applications suitable membranes and membrane modules needed to be selected, characterised and evaluated under representative conditions during the first laboratory-based stage. This activity provided the necessary design information for a larger unit that was subsequently evaluated at Vales Point.

2.2 Goals

The overall project goals were:

1. Demonstration of the integrated desalination – CO₂ capture concept under realistic circumstances
2. Establishment of principles that underpin the process and equipment design
3. Identification of most suitable or best performing membrane – absorption liquid combinations
4. Techno-economic evaluation of process concept for NSW coal fired power plants

2.3 Methodology/Experimental design

The methodology was based on laboratory research that underpinned the conduct of two targeted pilot plant campaigns with the PCC pilot plant at Vales Point power station. A techno-economic evaluation was also performed.

The project consisted of the following four activities:

⁵ Water production through CO₂ capture in coal-fired power plants, Paul Feron, Ramesh Thiruvenkatachari, Ashleigh Cousins, Energy Science and Engineering 2017; 5(5): 244–256

1. Laboratory research to underpin the overall process design and equipment selection focused on the forward osmosis process

This involved:

- Screening and selection of suitable absorption liquids with high osmotic pressure,
- FO membrane type and module selection, suitable membrane and module for the membrane contactor,
- Performance evaluation of the most suitable combinations (maximum water permeability, minimum amine permeability, heat exchange efficiency over a range of conditions),
- Process and equipment design for use with the PCC pilot plant at Vales Point.

2. Laboratory research that supported the process and equipment design for recovery of water from the absorber

This involved:

- Design and construction of a vacuum membrane condenser that could be operated with amine solutions,
- Experimental performance assessment of vacuum membrane condenser (condenser configuration, water permeability, water quality as a function of temperature and CO₂-loading).

3. Pilot plant research that demonstrated the technical viability

This involved:

- Approvals and permitting for PCC pilot plant operation including the FO unit, use of water source and water discharge,
- Construction and installation of pilot FO unit on existing PCC pilot plant,
- Modifications of existing PCC pilot plant to enable experimental campaigns (water collection, tie in points for FO modules, control system modifications),
- Construction and installation of vacuum membrane condenser unit and integration with the pilot plant,
- Two experimental campaigns over a range of relevant PCC process conditions (Water recovery, water quality, amine transfer to saline water) one focused on the use of the FO unit, one focused on water recovery from the absorber. In both experimental campaigns, membrane performance optimization and stability were evaluated.

4. Techno-economic evaluation

This involved:

- Assessment of investment cost and PCC plant design changes,

- Potential uses of water produced (literature assessment, power plant owners' feedback),
- Formulation of technology deployment plan for NSW.

2.4 Milestones and performance measures

An overview of the project milestones and results achieved is given in Table 4.

Table 4: Milestone overview

Milestone	Milestone Description	Results
M1	Selection of suitable amines for further investigation	<p>3 aqueous amine and 3 amino-acid salt solutions were selected from a list of 10 options, based on their potential use in a PCC process and their suitability for the combined desalination process.</p> <p>This is further described in Section 3.</p>
M2	Selection of suitable FO membranes and modules	<p>Porifera flat sheet and Aquaporin hollow fibre FO membranes were selected based on their compatibility with the high pH amine solutions used as the draw solutions. The Porifera membrane modules are stacked modules and the Aquaporin hollow fibre membranes are assembled in shell and tube modules.</p> <p>This is further described in Section 4.</p>
M3	Selection of suitable membranes and modules for water recovery from the absorber	<p>For the recovery of water two types of commercially available poly-tetrafluorethylene (PTFE) flat sheet membranes were chosen for their hydrophobic characteristics and thermal/chemical robustness. As an alternative a commercially available membrane contactor with polypropylene (PP) hollow fibre membranes was also selected for evaluation at Deakin University and at CSIRO in Newcastle. Several alternatives, commercially available or developmental, were also evaluated. Some of them use capillary membranes.</p> <p>This is further described in Section 5.</p>
M4	Performance results from laboratory experiments indicating the most suitable amine – FO membrane combinations	<p>Laboratory experiments with the Porifera membranes were carried out for the 6 selected CO₂-absorbent solutions using demineralised water and 3.5wt% sodium-chloride solutions at different temperatures. An adequate body of experimental data for the water flux and reverse amine flux was accumulated, sufficient for design purposes.</p>

		<p>Aquaporin hollow fibre FO membranes were also evaluated with 2 selected CO₂-absorbent solutions using demineralised water and 3.5wt% sodium-chloride solutions at two different temperatures.</p> <p>Experimental results are provided in Section 4.</p>
M5	FO process and equipment design for use with the PCC pilot plant at Vales Point	<p>The FO process and equipment design was based on Porifera membrane modules, that are available commercially. The standard design required further detailing and incorporate a separate heater for inclusion into the PCC pilot plant at Vales Point to mimic the desired conditions.</p> <p>This is further described in Section 8.</p>
M6	Modifications and preparations for operation and integration of the pilot plant with the infrastructure at the Vales Point PCC pilot plant facility	<p>Replacement items (steam control valve and flue gas flow meter) were received and installed on the Vales Point PCC pilot plant. The pilot plant control system was also updated. The tie-in points with Vales Point PCC pilot plant were prepared for connection to the Forward Osmosis unit.</p> <p>This is further described in Section 6.</p>
M7	Process and equipment design for absorber water recovery process application with the PCC pilot plant at Vales Point	<p>Recovery of water from the absorber via the Membrane Distillation process at the scale of the PCC pilot plant at Vales Point was not pursued in this project after the evaluation of different membranes and membraned configurations, as the technology was considered not to be sufficiently reliable to conduct trials.</p> <p>This is further discussed in Section 5.</p>
M8	Results from first experimental campaign with the PCC pilot plant at Vales Point power station	<p>MEA-carbonate mixtures were chosen for the first experimental campaign. The campaign entailed the assessment of water quality from the desorber as well as an assessment of the FO process performance. The latter campaign had to be terminated because of cross-over of absorption liquid to the cooling water.</p> <p>This is further described in Section 6 and 7.</p>

M9	Results from the second experimental campaign with the PCC pilot plant at Vales Point power station	<p>Taurate-carbonate mixtures were chosen for the second experimental campaign. The campaign entailed the assessment of water quality from the desorber as well as an assessment of the FO process performance using a new membraned module. These campaigns were successfully completed.</p> <p>This is further described in Section 6 and 7.</p>
----	---	--

3 Amine selection

Suitable amines were selected from a list of common amines that are likely to be used in CO₂-capture processes. In addition to that we also considered amino-acid salt solutions as they have benefits for the operation of the combined CO₂-capture-desalination process as show in our previous work¹. Amino-acid salt solution are expected to have higher water flux at the same concentration as a result of their higher ionic strength. They also have negligible amine vapour pressure, making it easier to produce a high quality of water produced from this process. Amino-acid salt solutions are, however, more prone to precipitation as a result of changes in the CO₂-concentration and temperature. Generally, they are also more viscous than amine solutions. An overview of the amine formulations considered is provided in Table 5.

Table 5: Amine formulations considered for combined CO₂-capture/desalination process in this study

Amine formulation	Comment
Mono-ethanolamine (MEA)	Base line; used in many pilot plants – primary amine
Piperazine (PZ)/amino-methyl-propanol (AMP)	Improved amine formulation – secondary (di-)amine + sterically hindered amine; representative of current state of the art ⁵
CAL008	CSIRO proprietary absorption liquid ⁶
Methyl-diethanolamine (MDEA)	Tertiary (alkanol)amine used in gas treating ⁷
Taurine with equimolar amount of KOH	Representative sulphonic amino-acid – primary amine ⁸
β-Alanine with equimolar amount of KOH	Highly soluble amino-acid – primary amine ⁹
Glycine with equimolar amount of KOH	Amino-acid available in process simulator ProTreat [®] used as a proxy for amino-acid salt solutions - primary amine ¹⁰
Sarcosine with equimolar amount of KOH	Very reactive amino-acid – secondary amine ¹¹
Proline with equimolar amount of KOH	Highly reactive - high solubility secondary amino-acid, cyclic ¹¹
Lysine with equimolar amount of KOH	Highly reactive di-amino-acid ¹²

The list in Table 5 was reduced to a shortlist of six amine solutions: three based on alkanol-alkylamines and three amino-acid salt solutions to cover a wide range of options. The selection was based on their suitability for use in PCC and robustness in PCC based on experience available in-house.

The formulations selected for the lab-based Forward Osmosis experiments were:

- 5 M Mono-ethanolamine (MEA)
- 4.5 M Piperazine(PZ)/amino-methyl-propanol(AMP) (1:2 molar ratio)

⁶ “Performance of CSIRO Absorbent Liquid 008 (CAL008): parametric study and 5000-hour campaign”, Cottrell, A. et al., GHGT14, 21-25 October 2018, Melbourne, Australia

⁷ “Advanced Gas Treating: The Engineering Science, Weiland, R.H., Hatcher, N.A., 2nd edition, Optimised Gas Treating Inc., Houston, Texas, 2012

⁸ “Amino-acid based solvent Vs. Traditional Amine Solvent: a Comparison” Moiola S., et al. Chemical Engineering Transactions, Vol. 69, pp 157-162, 2018

⁹ “Carbon dioxide absorption characteristics of aqueous amino acid salt solutions”, Song H.-J., et al. / International Journal of Greenhouse Gas Control 11 (2012) 64–72

¹⁰ “Carbon dioxide capture by solvent absorption using amino acids: A review”, Hu, G., et al., Chinese Journal of Chemical Engineering 26 (2018) 2229–2237

¹¹ “Bench-scale experimental tests and data analysis on CO₂ capture with potassium proline solutions for combined cycle decarbonization, Conversano, A., et al., International Journal of Greenhouse Gas Control, 93(2020)102881

¹² “CO₂ absorption using aqueous potassium lysinate solutions: Vapor – liquid equilibrium data and modelling, Shen, S. et al., J. Chem. Thermodynamics 115 (2017) 209–220

- 6 M CAL008 amine solution
- 3 M Taurine with equimolar amount of KOH giving a 3 M Taurate solution
- 5 M β -Alanine with equimolar amount of KOH giving a 5 M Alanate solution
- 4 M Sarcosine with equimolar amount of KOH giving a 4 M Sarcosate solution.

The concentrations of the amino-acid salt solutions were limited by their propensity to form precipitates when absorbing CO₂.

4 Forward Osmosis: results from laboratory program and process design

4.1 Background

The FO process operates using the principle of water separation through concentration gradients: a highly concentrated solution and a low concentration solution are placed on either side of a water permeable membrane and due to the concentration gradient water will naturally traverse the semi-permeable membrane, from a lower solute concentration feed solution (in this case, sea water) to a higher solute concentration solution (aqueous absorbent - amine or amino acid solution) (Figure 3).

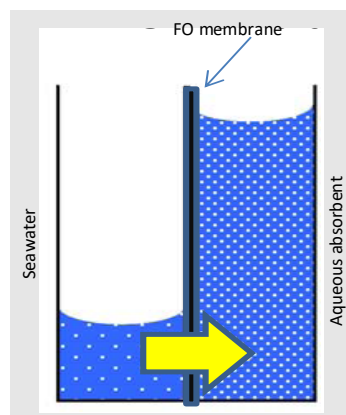


Figure 3: Concept of FO process showing the direction of water permeation in the combined CO₂ capture desalination process

Besides the utilisation of the driving force for the transfer of water, the aqueous absorption solution will also be cooled by the feed water and the water permeating into the absorbent solution. In the combined CO₂ capture desalination process the FO unit will also replace the trim cooler and operate as a Forward Osmosis Heat Exchanger (FOHEX) unit, as shown in Figure 4.

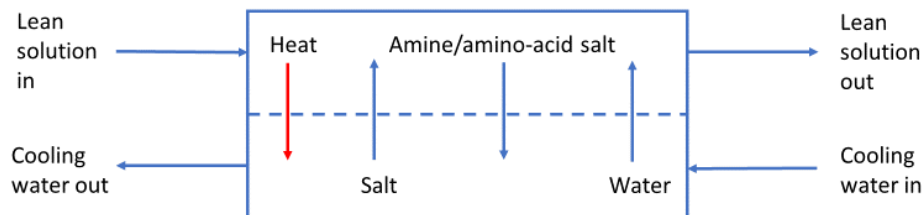


Figure 4: Forward Osmosis Heat Exchanger (FOHEX)

The rate of permeation of water through the membrane is expressed through the water flux, which is defined as the amount of water traversed through the membrane in one hour per unit of membrane area (L/m^2h often abbreviated to LMH). In the Forward Osmosis process, with the currently available commercial membranes, a certain amount of solute is also transported in the reverse direction to the water permeation. In this case, from absorbent solution to seawater. This is measured as reverse solute flux, related to the solution flux and is represented as specific reverse solute flux SRSF (Solute flux/ solution flux – unit: g/L). Reported values for the SRSF are typically between 0.1 and 0.55 g/L¹³. In the present Forward Osmosis application, the SRSF is aimed to be kept as low as possible to minimise the absorbent solute loss and avoid the introduction of this solute into the cooling water. For the purposes of the combined desalination – CO₂-capture process we express this as the Specific Reverse Amine Flux (SRAF). Another aspect is the transportation of salt from the cooling water to the amine solution, together with the water transport. This should also be kept at a minimum as the build-up of salts in the amine solution would increase the load on the reclaiming process. It can be described as the Specific Forward Solute Flux, SFSF (Salt flux/solution flux – unit: g/L).

4.2 Amine losses

The SRAF is not only determined by the membrane type and the type of amine but also by operational conditions such as temperature and amine concentration. Publicly available data on the SRAF is currently scarce. Experimental values determined with the amino-acid glycine and MEA by the University of Technology Sydney¹⁴ show a wide range between 1 and 200 g/L. Other

¹³ Forward Osmosis Membranes – A Review: Part I, Eyvaz et al., <http://dx.doi.org/10.5772/intechopen.72287>, Chapter 2 in “Osmotically Driven Membrane Processes - Approach, Development and Current Status”, edited by Hongbo Du, 2018

¹⁴ Simultaneous cooling and provision of make-up water by forward osmosis for post-combustion CO₂ capture, Zheng, et al., *Desalination* 476 (2020) 114215

researchers¹⁵ have indicated SRAF values for MEA that are as low as 0.37 g/L, where both water flux and amine flux were quite dependent on the CO₂-loading of the amine solution.

We adopted a performance criterion that the amine loss should not exceed 0.1 kg/tonne CO₂ or 0.1 g/kg CO₂. The SRAF is a determining factor for the amine loss resulting from the implementation of the FO process. However, the amine loss per unit of CO₂-captured is a specific loss criterion and it is therefore also determined by the amount of water removed from the saltwater solution, i.e. at lower water recovery relative to the amount of CO₂-captured the specific amine loss will be lower. This relationship has been further explored algebraically for the purpose of translation of the specific amine loss criterion into a desired value for the SRAF. Our previous work¹ indicates that up to 1 m³ water per tonne CO₂ may be produced without additional energy consumption for the capture process. This assumes that water is recovered from the desorber and the absorber. A value of around 0.4 m³/tonne CO₂ was estimated to be achievable from the desorber, only. A water production of 0.1 m³/tonne CO₂ would suffice to cover the water requirement for the Flue Gas Desulphurisation (FGD) in a coal fired power plant.

Figure 5 gives the specific amine loss as a function of the water recovery at different values for the SRAF. The specific amine loss criterion can be met by accepting a lower water recovery in the process. The results show that for the amine losses to be less than 0.1 kg/tonne CO₂ the SRAF will have to be lower than 0.25 at a water recovery of 0.4 m³/tonne CO₂ and lower than 1 at a lower water recovery of 0.1 m³/tonne CO₂. These points are indicated by the blue arrows in Figure 5.

¹⁵ An integrated system for CO₂ capture and water treatment by forward osmosis driven by an amine-based draw solution, Gwak, et al., *Journal of Membrane Science* 581 (2019) 9–17

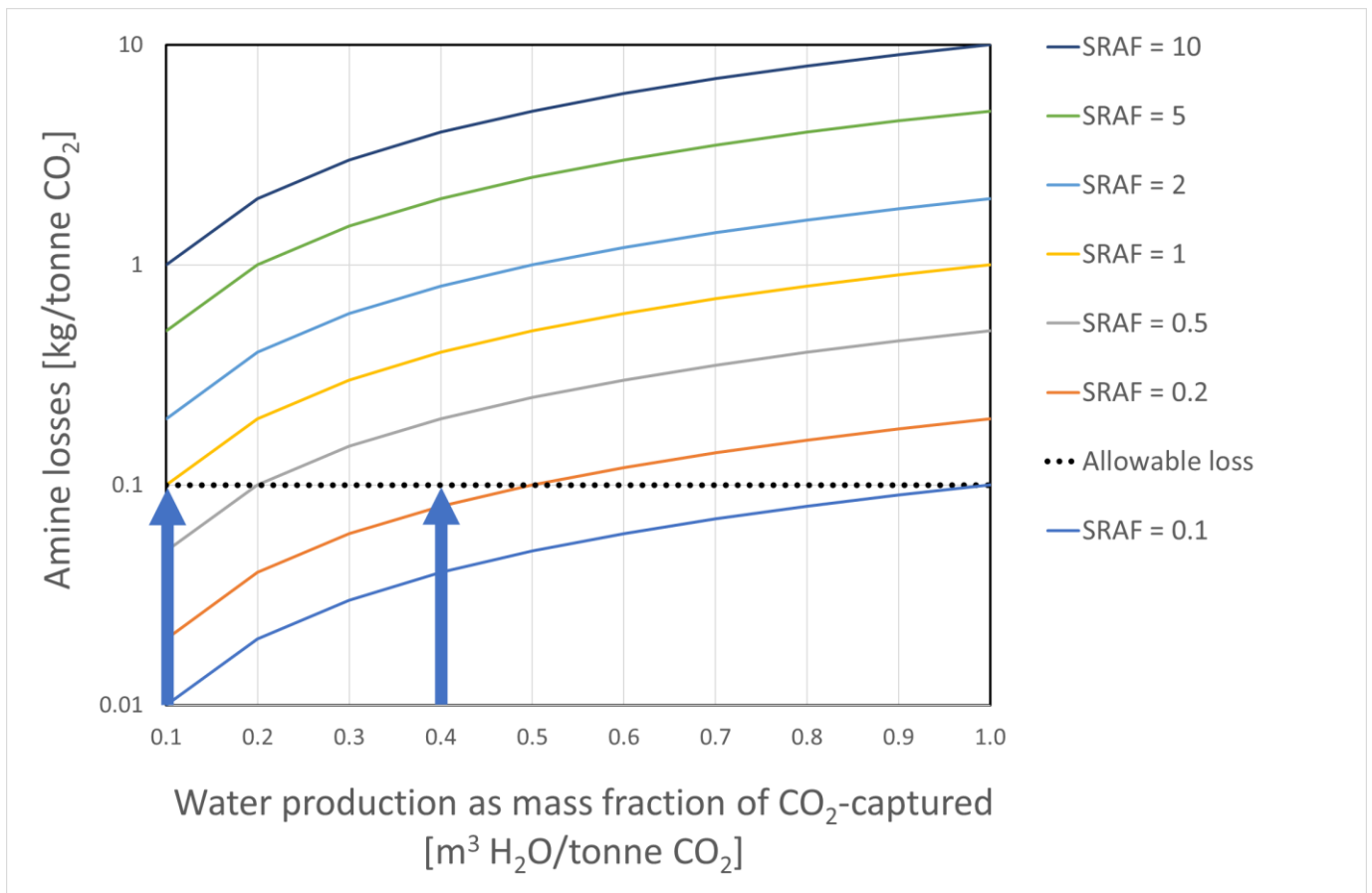


Figure 5 Amine loss as a function of water recovery at different values of the Specific Reverse Salt Flux

4.3 Membrane selection

The selection of membranes was determined by their commercial availability and applicability in the process. Forward Osmosis¹⁶ is not yet a process that is fully established in the market in the same way that reverse osmosis is. Perhaps not surprising the membrane materials are quite similar to those used in reverse osmosis, mainly cellulose tri-acetate (CTA) and polyamide thin film composites (TFC). Earlier studies indicated that the water flux through the TFC membranes is almost twice that of CTA and that they have higher rejection and lower reverse solute permeation^{17,18}. Membrane properties like hydrophilicity, thickness and chemical heterogeneity are also more favourable for the TFC membranes. The TFC membrane generally has a greater tolerance to temperature and wider operating pH range. One drawback of the TFC based membranes are they are not tolerant to chlorine as they consist of polyamide as an active surface.

¹⁶ "Recent developments in forward osmosis: Opportunities and challenges", Zhao, S. et al., Journal of Membrane Science 396 (2012) 1–21

¹⁷ Ren J. and McCutcheon J.R. 2014. Desalination, 343, 187-193

¹⁸ Thiruvengkatachari R., Francis M. Cunningham M., Su S. 2016. Sep Sci and Technol, 163, 181-188

There are a handful of suppliers of membrane and modules that could be evaluated for the application of the combined CO₂-capture and desalination process. We stipulated two main criteria for the membrane/modules:

1. The membrane and modules need to be chemically compatible with the amine solutions used. As the lean amine solutions are quite alkaline the membranes/modules need to be resistant to high pH (at least 9).
2. The membrane and modules need to be stable at the desired operational temperature, i.e., they need to be thermally compatible. As the forward osmosis modules will be effectively used as a heat exchanger, they will be exposed to a temperature of around 60 °C, which mimics the exit temperature of the lean absorption liquid from the lean-rich heat exchanger in an amine-based CO₂-capture process.

The suitability of the FO membranes and modules for this application is not known a priori and will need to be determined in the experimental program in the laboratory and on pilot plant location.

Table 6 provides information on FO membrane equipment for three suppliers that had publicly available information on their website. Only the FO membranes from Porifera and Aquaporin qualify from the chemical compatibility perspective. No information could be found on the maximum temperature for the Porifera FO technology, and the other options had a temperature limit of 50 °C. It is thought the TFC membranes would have higher temperature tolerance than CTA membranes. Both the Porifera and Aquaporin FO membranes were therefore selected for the experimental evaluation.

Table 6: Overview of Forward Osmosis equipment suppliers

Supplier	Fluid Technology Solutions	Porifera	Aquaporin
Membrane material	Cellulose acetate	Polyamide thin film composite	Polyamide thin film composite with integrated aquaporin proteins
Membrane type	Flat sheet	Flat sheet	Hollow fibre
Module type	Spiral wound	Stacked elements in plate and frame modules	Shell and tube
pH range	3 – 7	2 – 11	3 – 10
Maximum temperature	50 °C	n.a.	50 °C

4.4 Forward Osmosis experimental methodology

The FO lab-scale setup used for the flat sheet membrane performance characterisation is shown in Figure 6. The FO unit consists of a membrane cell with an effective membrane area of 0.014 m². A flat sheet FO membrane from Porifera was used in this study. A set of peristaltic pumps circulated the solutions on either side of the membrane with a set flow rate of 1 L/min. Simulated seawater as feed solution and CO₂ absorption liquid as the draw solution are circulated in a counter-current

mode. The orientation of the active layer of the FO membrane was toward the absorbent solution. The change in weights of the feed and draw solutions was monitored using weighing balances and were data logged with a time interval of 10 seconds. This enabled us to measure the amount of water permeation through the membrane and is reported as a water flux (L/m^2h). Other parameters measured were the solution temperatures, conductivities and pH. Solution samples, collected before and after the test, were analysed to evaluate the composition to understand the reverse amine and the forward salt permeation through the membrane. The determination of amine concentrations in the saline water was based on a total nitrogen method carried out by an external lab. The determination of salt in the amine solution was based on both the determination of the sodium and chloride ions in the amine solution. It appeared that for the amino-acid salt solutions a significant concentration of sodium was present in the solution prior to the FO experiments. This was not the case for the amine solutions where sodium was below the detection limit before the start of FO experiments. It was concluded that the determination of the chloride concentrations was preferable.



Figure 6: Lab scale flat sheet FO test unit

A systematic testing methodology has been adopted. Simulated sea water solutions (35 g/L NaCl) were tested against the selected amine absorbent solutions. Initial testing also involved experiments using deionised water.

The effect of the following parameters on process performance was investigated:

- Temperature

The experiments were carried out at room temperature (for convenience) and elevated temperatures reflecting likely operational temperature in the CO_2 -capture process (typically $40^\circ C$ in the experiments). The seawater side was maintained at ambient temperature.

- CO_2 -loading

To simulate the lean absorbent solution loading, CO_2 was then loaded into the solution at different concentrations (0.2-0.4 mol CO_2 /mol amine). The experimental setup for charging the solution with CO_2 is shown in Figure 7.



Figure 7: Experimental setup for loading CO₂ in the absorbent solution.

A set of experiments was also carried out with a different FO membrane configuration using a hollow fibre membrane module instead of a flat sheet FO membrane setup (Figure 8 and Figure 9). This would allow us to compare the performance of two different FO membranes and module configurations for this application. Hollow fibre modules are similar to tubular modules with much higher packing densities. However, the difference is that the dimensions of the hollow fibre are much smaller than the tubular membrane components. Hollow fibre modules would have a much smaller footprint compared to plate and frame configuration used with flat sheet membranes. The Aquaporin hollow fibre membrane is used with an active membrane area of 2.3 m². Inside diameter of the fibre (lumen side) is 195 µm. The feedwater flows through the membrane lumen side and the absorbent solution through the shell side. The large membrane area meant that experiments could only be carried out in the once-through mode, as a significant amount of water would be removed in a single pass.

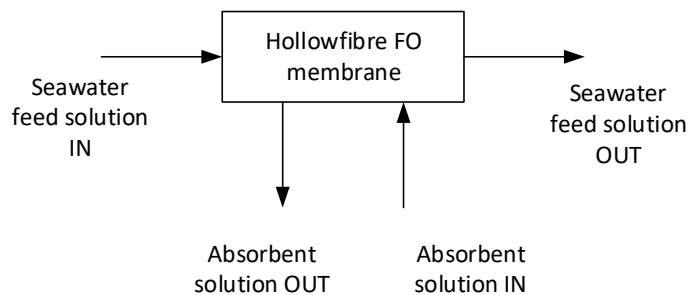


Figure 8: Schematic of hollow fibre FO membrane operation with photo of the Aquaporin hollow fibre membrane used

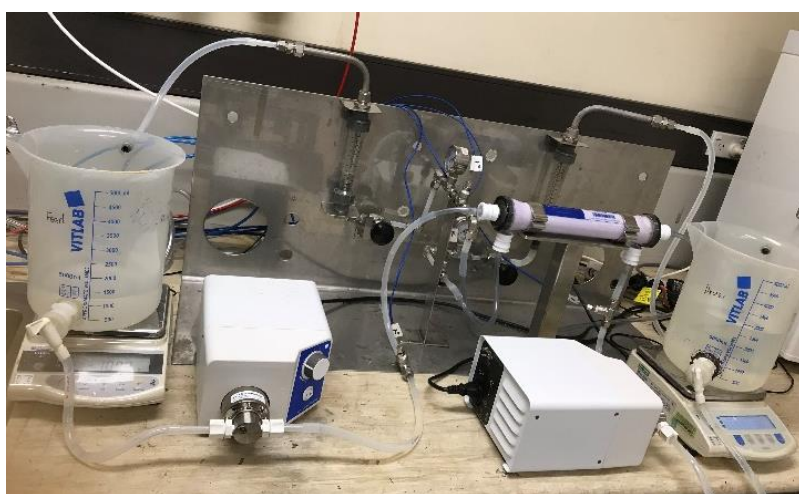


Figure 9: Lab scale experimental setup of the hollow fibre FO membrane module.

4.5 Forward Osmosis experimental results

The forward osmosis performance can be expressed by the following:

- Water transfer dependent on the type of absorption liquid, saline water concentration and type of membrane,
- Transfer of amines to the saline water solution, and,
- Transfer of salts to the amine solution.

Ideally only water is transferred from the saline water, i.e. no transfer of ions and amines.

The research output consists of the performance data that are necessary for the design of the FO process and equipment and its subsequent evaluation of scaled-up trials at the Vales Point PCC pilot plant.

The full range of amine solutions defined in chapter 3 were initially evaluated using the Porifera flat sheet membranes. The experiments were carried with water and a 3.5% NaCl, representing seawater, at temperatures of 20 °C and 40 °C. Some amine/amino-acid salt solutions were also partially loaded with CO₂ and some used additional Na₂CO₃ to increase the osmotic pressure of the solution. A typical experiment would take 90 minutes, operated in a recirculation mode, during

which 40% of the water in the feed solution transferred to the amine/amino-acid salt solution. This meant that concentrations changed significantly both in the feed (~60% increase in concentration when using a salt solution) and the amine/amino-acid salt solutions (~30% decrease in concentration). The reported flux values are averaged over the duration of the experiments.

Results for the water flux, salt flux and Specific Reverse Amine Flux (SRAF) for the Porifera flat sheet membranes are shown in Table 7. The data in

Table 7 are also graphically displayed in Figure 10, Figure 11 and Figure 12 to aid in the interpretation of results.

Table 7: Overview of FO performance test results using Porifera flat sheet membranes

Amine/Amino-acid absorbent draw solution	Temperature °C	Feed solution	Average water flux [L/m ² h]	Average reverse amine flux [g/m ² h]	SRAF [g/L]
MEA (5M)	20	De-ionised water	21.4	204	9.5
			19.5	222	11.4
	20	3.5% NaCl solution	7.3	583	79.9
	40	3.5% NaCl solution	7.8	654	83.8
	55	3.5% NaCl solution	7.6	828	109
MEA (5M) + 0.2 mol CO ₂ /mol MEA	20	3.5% NaCl solution	8.7	170	19.5
MEA (5M) + 0.4 mol CO ₂ /mol MEA	20	3.5% NaCl solution	10.2	97.5	9.6
MEA (4M) + 1M Na ₂ CO ₃	20	De-ionised water	27.4	110	4.0
MEA (5M) + 0.5M Na ₂ CO ₃ + 0.2 mol CO ₂ /mol MEA)	20	3.5% NaCl solution	10.4	171	16.4
PZ/AMP (4.5M)	20	De-ionised water	18.7	13.9	0.74
			19.8	16.7	0.84
	20	3.5% NaCl solution	9.6	15.5	1.6
	40	3.5% NaCl solution	10.8	31.8	2.9

CAL008 (6M)	20	De-ionised water	10.2	28.6	2.8
			10.5	22.0	2.1
	20	3.5% NaCl solution	5	23.9	4.8
	40	3.5% NaCl solution	9.0	67.0	7.4
Alanate (5M)	20	De-ionised water	54.8	13.5	0.25
	20	3.5% NaCl solution	22.9	27.9	1.2
	40	3.5% NaCl solution	28.5	72.7	2.6
Sarcosate (4M)	20	De-ionised water	49.8	8.1	0.16
	20	3.5% NaCl solution	16.7	6.1	0.37
	40	3.5% NaCl solution	21.4	29.2	1.36
Taurate (3M)	20	De-ionised water	45.3	10.7	0.24
	20	3.5% NaCl solution	17.2	8.2	0.48
	40	3.5% NaCl solution	20.8	21.5	1.0
Taurate (3M) + 0.17 mol CO ₂ /mol taurate	20	3.5% NaCl solution	15.2	11.8	0.78
Taurate (3M) + 0.5M Na ₂ CO ₃	20	De-ionised water	47.4	8.7	0.18
Taurate (3M) + 0.5M Na ₂ CO ₃ + CO ₂ (0.17 M/M)	20	3.5% NaCl solution	15.4	23.2	1.51

Figure 10 provides a comparison of water and reverse amine fluxes for 6 amine/amino-acid salt solutions at room temperature using two different feed solutions: an aqueous NaCl solution representing seawater (closed symbols) and de-ionised (DI) water (open symbols). As anticipated the water fluxes are higher for the cases using DI-water because of the higher osmotic pressure difference, while the specific reverse amine fluxes (SRAF) are lower. The amino-acid salt solutions gave highest water fluxes and lowest reverse amine fluxes, which is consistent with our previous work using MEA and glycinate¹. The ionic strength of the amino-acid salt solution is higher than the amine solution and this results in a higher osmotic pressure of the solution and therefore higher water flux. As the amino-acid salts are present as charged molecules they are more strongly rejected by the membrane.

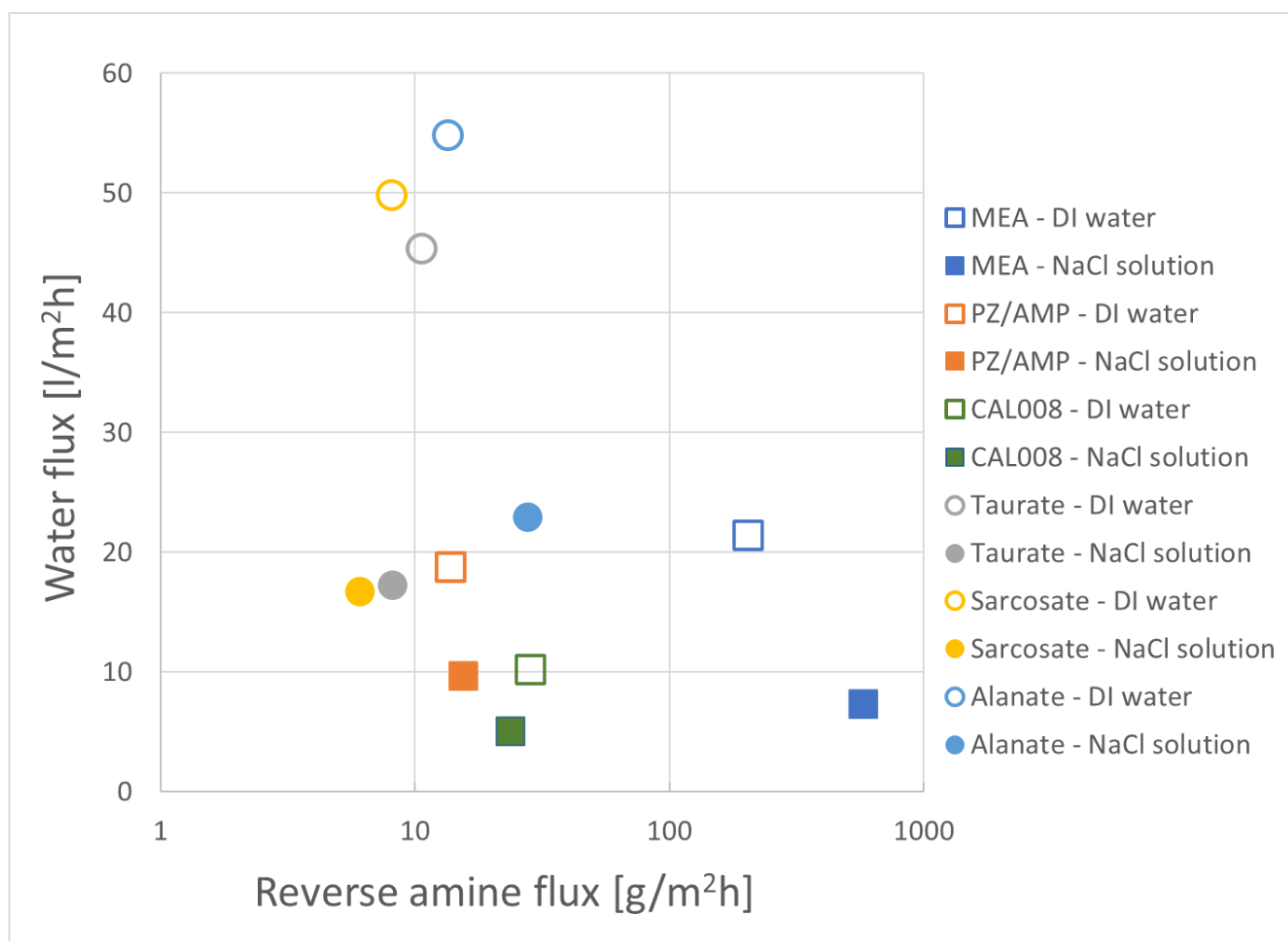


Figure 10: Experimentally determined water and reverse amine fluxes for 6 amines/amino-acid salts at 20 °C (Porifera membranes); closed symbols: 3.5% aqueous NaCl-solution as feed solution; open symbols: de-ionised water as feed solution; squares: amine solutions; circles: amino-acid salt solutions

Figure 11 provides a comparison of water and reverse amine fluxes for 6 amine/amino-acid salt solutions at 20 °C and 40 °C, using an aqueous 3.5% NaCl solution representing seawater as the feed solution. One experiment was carried out at 55 °C using an MEA solution. It shows water fluxes and specific reverse amine fluxes (SRAF) are higher at increased temperature. The amino-acid salt solutions give highest water fluxes and lowest reverse amine fluxes. The reverse amine fluxes showed a larger increase than the water fluxes with a temperature increase. The taurate solution

possessed the smallest increase in reverse amine flux with increasing temperature. The change in both fluxes is mostly caused by the change in fluid properties such as viscosity, which will impact upon the diffusion processes.

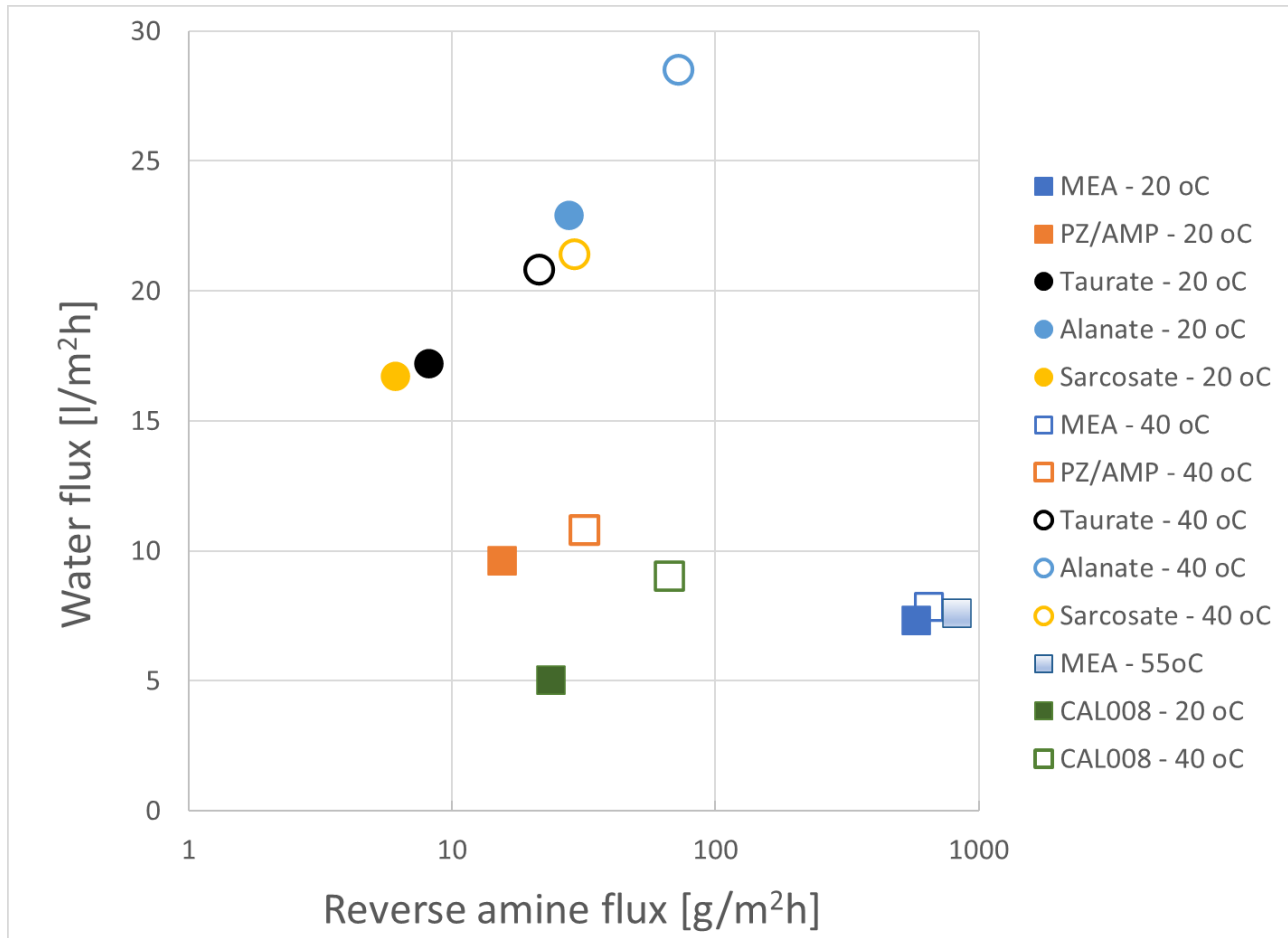


Figure 11: Experimentally determined water and reverse amine fluxes for 6 amines/amino-acid salts at 20 °C (closed symbols) and 40 °C (open symbols) using 3.5% NaCl as the feed solution (Porifera membranes); squares: amine solutions; circles: amino-acid salt solutions; one experiment at 55 °C

The absorption of CO₂ into the solutions will impact the water flux and amine flux. In the next series of experiments the impact of CO₂-loading was therefore investigated. MEA and taurate solutions were selected for these experiments as these were the most likely candidates, from a practical perspective, to be used in the Delta Electricity PCC pilot plant at Vales Point power station. Figure 12 presents experimental results for MEA and taurate solutions that have been partially loaded to represent lean loading conditions. Also, the impact of adding an additional alkaline salt, i.e. sodium carbonate, to the solution is shown. Both the presence of CO₂ and the additional of salt were anticipated to increase the water fluxes and decrease the reverse amine fluxes because of the increased osmotic pressure. This appeared to be the case, in particular for the MEA-solutions, but less so for the taurate solutions, which showed little variation in the water fluxes.

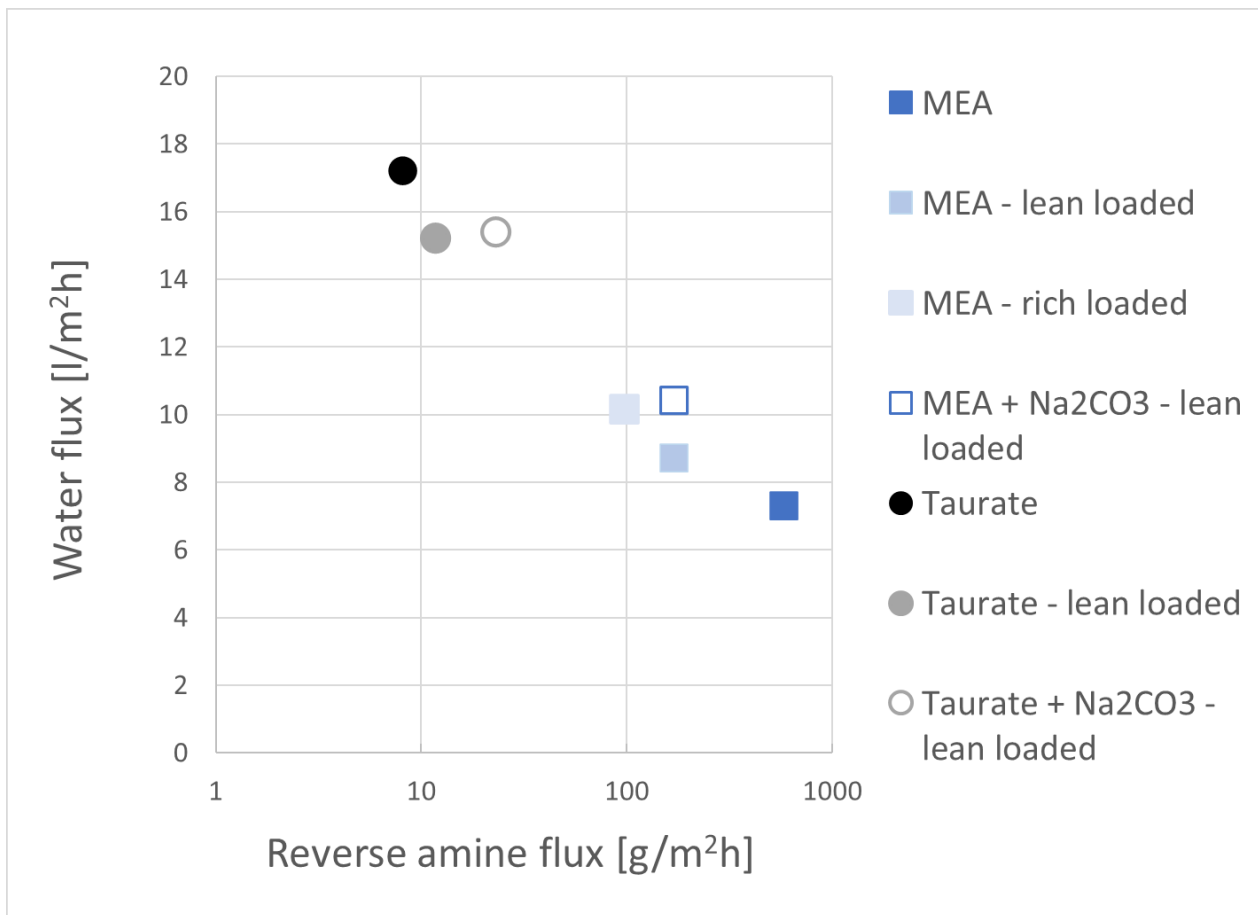


Figure 12: Experimentally determined water and reverse amine fluxes for MEA-solutions at 20 °C (squares) and taurate solutions (circles) using 3.5% NaCl as the feed solution (Porifera membranes)

The results in Table 7 indicated that values for the Specific Reverse Amine Flux (SRAF) were mostly higher than the expected minimum of <math><1</math> (at 0.1 m³/tonne CO₂ water recovery) with the exception of the taurate solutions. SRAF values for the amino-acid salt solutions were generally lower than for the amine solutions and will also depend on the concentration of amine/amino-acid salts in solution and the CO₂-loading.

A limited number of experiments, i.e., only using MEA and taurate solutions at two different temperatures were carried out with the hollow fibre membranes from Aquaporin with results presented in Table 8. The experiments used a 3.5% NaCl solution as the feed. For both absorption liquids the water flux is higher compared to the Porifera membranes with a lower specific reverse amine flux (SRAF). At the higher temperature the specific reverse amine flux was significantly higher. The Aquaporin recommended operating temperature is between 5 and 30 °C with maximum allowable temperature of 50 °C for short periods, perhaps somewhat consistent with the increased reverse amine fluxes. As with the Porifera membranes the water flux was higher for the taurate solution, and the specific reverse amine flux was lower.

Table 8: Overview of FO performance test results using Aquaporin hollow fibre membranes

Amine/Amino-acid salt solution	Temperature °C	Feed solution	Average water flux [L/m ² h]	Average reverse amine flux [g/m ² h]	SRAF [g/L]
MEA (5M)	20	3.5% NaCl solution	13.6	157	11.5
	40	3.5% NaCl solution	12.8	885	69.2
Taurate (3M)	20	3.5% NaCl solution	20.4	0.69	0.03
	40	3.5% NaCl solution	23.2	27.7	1.20

4.6 Design of Forward Osmosis process and technical evaluation

The principles for design of the FO process and the technical evaluation were based on the following:

- 1) Enable evaluation of both amine solutions and amino-acid salt solutions

Performance results from the laboratory experiments indicated that amino-acid salt solutions are preferred for the combined CO₂-capture/desalination process. As amino-acid salt solutions are only available from a small number of suppliers, the evaluation of amine solutions was also deemed necessary. The project plan was therefore based on the evaluation of two CO₂-absorbents: one amine solution and one amino-acid salt solution. A comparison between the 6 types of CO₂-absorbents based on their practical use in the PCC pilot plant and in the Forward Osmosis process is shown in Table 9.

Table 9: Comparison of options for CO₂-absorbents for evaluation in the Vales Point PCC pilot plant

Amine/Amino-acid salt solutions	PCC pilot plant performance	Forward Osmosis process operation
MEA	<ul style="list-style-type: none"> - Ample operational experience in pilot plant operation (primarily obtained at AGL Loy Yang and Stanwell Tarong power stations; limited at Vales Point) - Will exhibit oxidative degradation but thermal degradation is expected to be low - Process simulation models available and validated with pilot plant data 	<ul style="list-style-type: none"> - Adequate water flux - Highest amine losses in FO experiments (SRAF >1 in all experiments) - Long term effect on membrane at high pH is not known
PZ/AMP	<ul style="list-style-type: none"> - Limited operational experience in pilot plant operation (at AGL Loy Yang) - Anticipated to be more resistant to oxidative and thermal degradation than MEA - Process simulation models available but not validated with pilot plant data - PZ will form nitrosamines in solution - Handling of PZ on site will require additional permits 	<ul style="list-style-type: none"> - Adequate water flux - Low amine losses in FO experiments (SRAF <1 was not met in all experiments) - Long term effect on membrane at high pH is not known
CAL008	<ul style="list-style-type: none"> - Ample operational experience in pilot plant operation (at AGL Loy Yang) - Thermal robustness equivalent to MEA; oxidative robustness better than MEA - Process simulation models available that can be validated with pilot plant data - Most expensive amine formulation - Handling of CAL008 on site will require additional permits 	<ul style="list-style-type: none"> - Adequate water flux - Medium amine losses (SRAF >1) - Long term effect on membrane at high pH is not known

Alanate	<ul style="list-style-type: none"> - Some operational experience in pilot plant (at AGL Loy Yang) - Anticipated thermal robustness less than MEA; anticipated oxidative robustness equivalent to MEA - Process simulation models not available - High solubility of amino-acids, i.e. low operability risk 	<ul style="list-style-type: none"> - High water flux - Low amine losses in FO experiments (SRAF <1 was not met in all experiments) - Long term effect on membrane at high pH is not known
Sarcosate	<ul style="list-style-type: none"> - No operational experience in pilot plant - Anticipated oxidative and thermal robustness less than MEA - Process simulation models not available - Good solubility of amino-acids, i.e. medium operability risk - As a secondary amine will form nitrosamines in solution 	<ul style="list-style-type: none"> - High water flux - Low amine losses in FO experiments (SRAF <1 was not met in all experiments) - Long term effect on membrane at high pH is not known
Taurate	<ul style="list-style-type: none"> - No operational experience in pilot plant - Anticipated oxidative and thermal robustness equivalent to MEA - Process simulation models not available - Limited solubility of amino-acids, i.e. high operability risk - Non-hazardous chemical 	<ul style="list-style-type: none"> - High water flux - Lowest amine losses in FO experiments (SRAF <1 was met in all experiments) - Long term effect on membrane at high pH is not known

To provide best insights into the practical operation of the combined CO₂-capture desalination the following absorption liquids were utilised in the PCC pilot plant:

- MEA-solutions; building on the significant available PCC pilot plant experience with this solution will enable the investigation of the least performing amine solution for the combined CO₂-capture desalination process. The performance can be augmented by the replacement of part of the MEA by carbonates in solution.
- Taurate solutions; as the best performing solution for the combined CO₂-capture desalination process, the formulation will be adjusted to avoid conditions where precipitation is likely to occur. Here, the performance can be augmented by the addition of carbonates to the solution.

2) Experimental conditions to reflect reality of a full-scale process

It is required that the PCC pilot plant is operated in such a way that it represents the reality of a full-scale process, in particular that it generates absorption liquids that have a composition typical of a lean solution that can be used in the FO process or MD process. To this effect a parametric study will be carried out for the chosen absorption liquid during which the capture rate is maintained at 90% while liquid flow rates are varied. For MEA, this can be compared with process simulations using ProTreat[®]. A process model was established for evaluation purposes. For taurate solutions, the PCC process evaluation was experimental with extrapolation of performances from the MEA experiments.

It was recognised that while the PCC pilot plant will be able to generate absorption liquids of the desired composition, the temperature conditions will be affected by heat losses that are common with small-scale pilot plants, like the Vales Point PCC pilot plant. It was therefore decided to vary the temperature of the absorption liquids by the inclusion of a heater as part of the experimental rig to be able to bring the temperature to the desired level. This will also facilitate the most convenient tie-in point for the experimental FO rig.

3) Use of commercially available components for the FO equipment

The development of the combined CO₂-capture/desalination process will be aided by the use equipment that is already commercially available. This will facilitate deployment and scale-up. The applications for forward osmosis are manifold and can mostly be found in the need for dehydration of fluids. Water is transferred from a fluid to a higher osmotic draw solution which can be regenerated either thermally or by other means. In most applications the objective is to remove as much water as possible and the commercially available equipment is designed with this background.

Unique to the combined CO₂-capture/desalination process the removal of water from the feed solution will be comparatively small because of its relationship to the amount of CO₂ captured. Maximisation of the water transfer is not the objective. Instead recovering water without additional energy consumption to the CO₂-capture process is strived for. This results in water recoveries that are likely to be dependent on the capture technology used and much smaller than customary for seawater desalination, for example.

The FO equipment would therefore benefit from a flexible design that can be fine-tuned to these applications. This flexibility can be achieved more easily with the Porifera membrane modules that can be assembled like plate and frame heat exchangers (Figure 13). The elements can be connected in parallel or in series or any combination of this to match the desired water recovery.



Figure 13: Porifera membrane module and single membrane element (Porifera Inc)

5 Membrane Distillation: Laboratory program

5.1 Background

Membrane distillation is a thermal-based membrane separation process applied here to recover the water from the absorber. In this process, the driving force for water separation is the vapour pressure difference induced by the temperature difference across the porous hydrophobic membrane. This membrane separates the feed solution and the permeate. The feed solution is in direct contact with the membrane surface and a liquid-vapour interface is formed. Due to the vapour pressure gradient across the membrane, volatile compounds of the feed solution evaporate and the vapour molecules pass through the membrane pores from the feed to the permeate side. As the driving vapour pressure gradient is induced by a temperature difference from the feed side to the permeate side, the feed solution must have higher temperature than the permeate in order to achieve a positive driving force. On the permeate side a circulating solution at lower temperature than the feed can be passed directly in contact with the membrane by applying a sweep gas or vacuum. Pore wetting happens when the liquid feed permeates the membrane pores and this is influenced by the feed solution and membrane characteristics, and the operating conditions. In our operation, absorbent feed solution flows through one side directly contacting the membrane, an air gap is provided in the permeate side separated from the cooling circulating fluid and a vacuum is applied to the permeate side to collect the condensate (Figure 14).

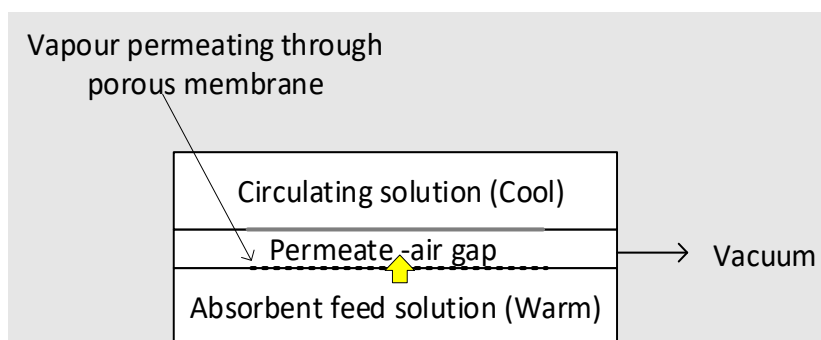


Figure 14 Membrane distillation process applied for the recovery of water from absorber

The absorption of CO₂ is exothermic and as a result the temperatures can be in excess of 70 °C in certain parts of the absorber. In the Membrane Distillation process, the absorption liquid is extracted from the CO₂-absorber at a point where the temperature is high. It is then fed to the membrane unit where water will evaporate under vacuum conditions and condense on a surface that is cooled before being recovered from the vacuum. The temperature of the absorption liquid is reduced, meaning that the Membrane Distillation has the additional function of an intercooler. Intercooling is used to ensure that the absorption of CO₂ is not limited by the increased temperature. It is not only limited to one location in the absorber and might be performed at multiple locations.

5.2 Scope of experimental program

MEA solutions and taurate solutions were initially targeted from the selection process for the Forward Osmosis experimentation and also used in the Membrane Distillation experiments. Most of the experimental work, however, has been carried out with the taurate solutions as the distillate from an MEA solution would contain MEA, which is not desired. Moreover, there was significant concern over possible leakage of the MEA solutions through the porous membrane as result of membrane wetting. Membrane wetting is less likely to occur when using ionic solutions like amino-acid salt solutions.

5.2.1 Experimental parameters

The following experimental parameters were varied to characterise the membrane and module performance:

- CO₂-content

The CO₂-content of the absorption liquid was chosen to be representative of the intermediate conditions in the absorber. The most likely location of the liquid extraction point is in the upper half of the absorber where CO₂-mass transfer is fast, and a significant temperature increase will occur.

- Temperature

The absorption liquid typically enters the absorber at 40 °C and depending on its CO₂-reaction enthalpy (determined by the type of amine) reaction rate, the temperature in the absorption liquid can increase considerably up to 70 °C.

- Vacuum pressure

The vacuum pressure should be below the water vapour pressure of the solution to achieve sizeable evaporation. The lower the pressure the more water will be recovered and the larger the temperature decrease will be.

5.2.2 Output data and information

The objective of the laboratory experiments is to gather data and information on the following:

- Water flux through the membranes under the range of operational conditions

This information is needed for design purpose and general understanding/validation of this method for water recovery.

- Water quality

The process modelling carried out previously has indicated that the water can contain significant amounts of amine, but this is dependent on the type of amine, their vapour pressure (amino-acid salts have essentially zero vapour pressure), the CO₂ loading and the temperature. A coarse measure of water quality is a conductivity measurement, and this was used as a proxy for water quality.

5.2.3 Membranes and membrane modules

It was recognised that Membrane Distillation is an emerging technology, mainly used to produce freshwater from seawater or brackish water by thermal means. The experimental program has considered a wide range of membranes and membrane modules, all of them porous and hydrophobic, as a starting point for assessment and further development of the application. These included the following:

- Flat sheet membranes
Flat sheet membranes can be used in spiral wound membrane modules and stacked modules (similar to plate frame heat exchangers). We evaluated one type of flat sheet membrane (Section 5.3) using MEA solutions and taurate solutions.
- Capillary membranes
Capillary membranes are available in shell and tube membrane modules. Their usual field of application is in micro-filtration. We obtained two types of capillary membranes and evaluated their suitability using the modules as purchased and a module specially designed by colleagues at the University of New South Wales. Taurate solutions were used during these experiments which are reported in Section 5.4 and 5.5.
- Hollow fibre membrane modules
Hollow fibre membrane modules developed for membrane contactor applications to remove O₂ from water are potentially suitable for recovery of water under (partial) vacuum. Taurate solutions were used during these experiments which are reported in Section 5.4 and 5.5.

Section 5.4 reports results obtained under vacuum only whereas Section 5.5 also reports on results with a sweep gas (air).

5.3 Experimental results flat sheet membranes

The lab scale MD unit used in the experiments is shown in Figure 15. An MD cell purchased from Sterlitech consists of feed cell, permeate and cooling water cells. A 2.5 mm air gap was maintained in the permeate cell. The permeate cell was modified to adopt vacuum to operate as a hybrid heat and vacuum Membrane Distillation unit.

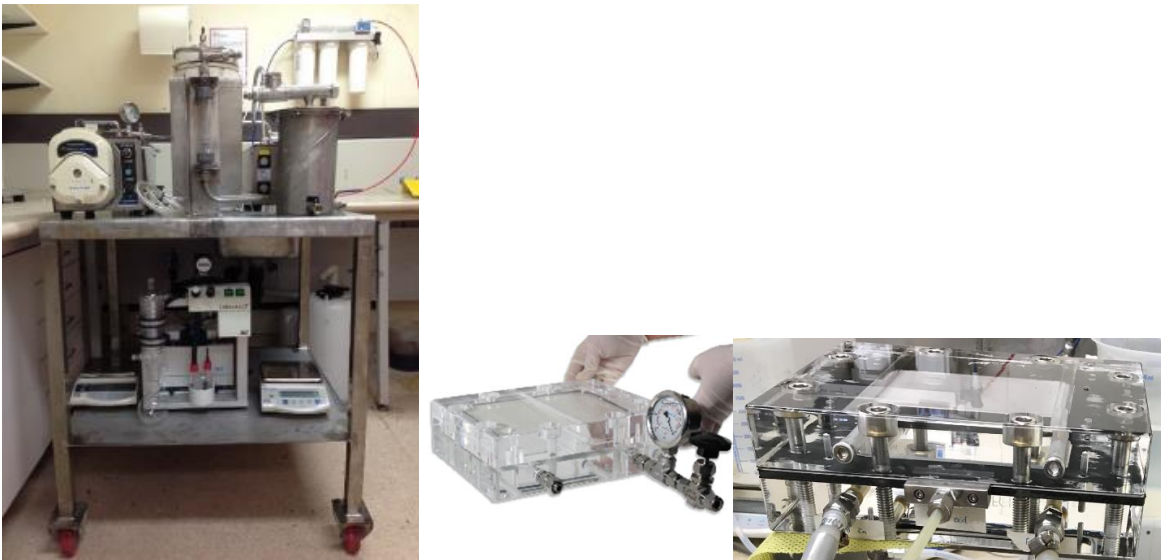


Figure 15 Lab scale hybrid heat and vacuum Membrane Distillation unit with the image of the flat sheet MD cell

Commercially available Poly-Tetra-Fluor-Ethylene (PTFE) membranes from Sterlitech were used in this study. PTFE Membranes are extremely hydrophobic and exhibit very high chemical compatibility. This type of membrane is generally used for gas filtration to remove dust and was used here for our gas/liquid application. They also show high thermal stability and can be operated well over 70 °C (stable up to 260 °C) to withstand the typical reaction temperatures encountered in the absorption column. Different membrane pore sizes from 0.1-0.45 micron are also available. A membrane pore size of 0.2 micron was selected for this study considering the application of vacuum for the extraction of water. The Sterlitech PTFE membranes were obtained as unlaminated (without the polypropylene netting/backing layer) to increase the water permeation.

MEA and taurate solutions were used as CO₂ absorbents for these experiments in which the efficiency of the water recovery was determined. Permeate water quality (amine content) and the variation in flux permeation with the change in feed solution, water temperature, CO₂ loading, vacuum pressure were investigated. The diluted absorbent solution from the forward osmosis process was also used as the feed solution. Feed solution flow rate was maintained at 1 L/min. Feed solution temperature was varied. Vacuum pressure was set at 950 mbar absolute. CO₂ loading varied between 0.2-0.4 mol/mol. A single experiment normally lasted 90 minutes, with condensate samples taken every 30 minutes, at which also the weight was also measured. The results were averages from these three points.

The experimental results, water flux, conductivity of product water, amine concentration in product water, forward amine flux and specific forward amine flux are provided in Table 10. Apart from made-up absorbent solutions, product solutions from the FO experiments, i.e. diluted mixtures, were also used. Several experiments were also run as duplicates.

Table 10 Results from Membrane Distillation experiments using porous flat sheet PTFE membranes with MEA and taurate solutions

Absorption liquid	Temperature °C	Water flux [l/m ² h]	Conductivity product water [mS/cm]	Amine concentration in product [g/l]	Forward amine flux [g/m ² h]	Specific forward amine flux [g/l]
5 M MEA 0.4 mol CO ₂ /mol MEA	55	9.4	2.17	14.6	185	19.7
	55	11.0	2.05	8.7	88	8.0
	55	11.0	2.03	9.1	91	8.3
	55	9.5	1.85	9.9	53	5.6
5 M MEA 0.4 mol CO ₂ /mol MEA	65	14.2	4.61	15.7	244	17.2
Diluted MEA solution from FO experiments	55	17.1	0.80	Not determined	-	-
Diluted MEA solution from FO experiments	55	20.6	0.66	9.9	192	9.3
Diluted MEA solution from FO experiments	55	18.4	0.64	11.8	232	12.6
3 M Taurate 0.17 mol CO ₂ /mol Taurate	55	10.2	0.84	2.9	30.4	3.0
	55	9.4	0.18	0.15	1.0	0.1
3 M Taurate 0.2 mol CO ₂ /mol Taurate	65	14.5	0.40	0.80	5.6	0.4
Diluted Taurate solution from FO experiments	55	22.5	0.05	0.10	2.4	0.1
Diluted Taurate solution from FO experiments	55	19.9	0.07	0.15	3.2	0.2

The water fluxes for 5M MEA solutions and taurate solutions were quite similar, as these are driven by the water vapour pressure at a given temperature. Although only two experiments were carried out at the higher temperature of 65 °C, both resulted in a higher water flux as expected from the high water vapour pressure at higher temperature. For the experiments with taurate the carry-over of amino-acid was significantly less than for the MEA solution. As MEA solutions have an amine vapour pressure, amine is evaporated together with water and subsequently is absorbed into the condensate. For taurate solutions the transfer mechanism is only through membrane defects. This results in significantly lower transfer of amines to the condensate. This points towards amino-acid salt solutions being preferred for this type of water recovery. The experiments also indicated that water fluxes were significantly higher for the diluted mixtures for both MEA solutions and taurate solutions, i.e., the water flux is influenced by the concentration of amine or amino-acid salt.

In our subsequent Membrane Distillation experiments we focused on the use of taurate solutions as they provide a significantly higher water quality and pose lowest risk in membrane wetting and hence undesired permeation of absorption liquid to the vacuum side.

5.4 Experimental results hollow fibre and capillary membrane modules under vacuum operation

Four different membrane modules (named herein as UNSW module, CUT module, MicroDyn module and Liqui-Cel® module after the names of their suppliers) were used in the next stage of the Membrane Distillation work. These membrane modules incorporated hollow fibre and capillary membranes. Apart from the UNSW module, all membrane modules were sourced commercially, and larger membrane modules were available from the suppliers.

The CUT and MicroDyn modules are microfiltration test modules. We selected those modules as larger size microfiltration modules were available from these suppliers that could potentially be used in subsequent pilot plant trials for the MD application.

The Liqui-Cel® module is a membrane contactor module used for evaluation of degassing applications that work under vacuum or with a sweep gas. The module design is therefore proven for vacuum desorption processes and larger modules are also available from the supplier.

The UNSW module is a prototype, shell and tube Membrane Distillation module from a local university that showed promise for MD application. Its swirling flow design was expected to result in high mass transfer. It is potentially scalable to larger sizes by increasing tube size and stacking of multiple tubes.

All membrane modules consisted of polypropylene membrane materials, housed within a polyvinyl chloride shell. Figure 16 shows an overview of the membrane modules used. The membrane module characteristics are presented in Table 11. The polypropylene membranes in the CUT, MicroDyn and the UNSW modules were thought to be the same type.

The absorption liquid used in the experiments consisted of taurine, potassium carbonate, potassium hydroxide and water (3M taurine, 3M KOH, and 1.5M K₂CO₃). The study was conducted at laboratory scale under vacuum operation.

It was anticipated that the experimental results, in particular the water fluxes, could be used for scale-up studies that would provide a design for subsequent work at pilot plant scale. However, this does not mean that similar water fluxes would be achieved in large scale modules if the scale up leads to different hydraulic regimes. This is an unknown with membrane module designs that do not allow for any flexibility, as is the case with commercially available membrane modules.

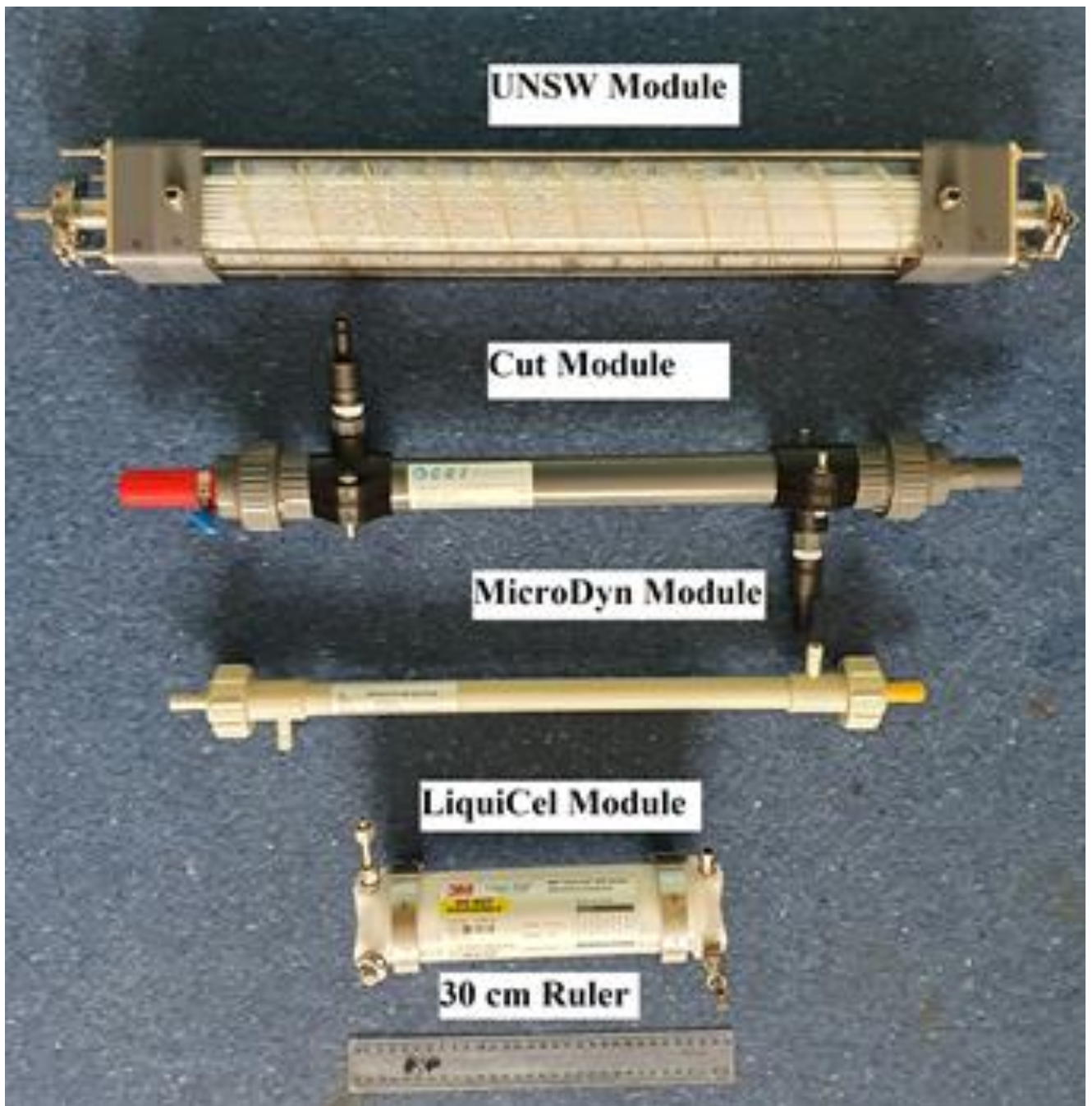


Figure 16 Photograph showing the four modules used in the current work.

Table 11 Specifications of membrane modules used in the current work

Parameters	Values for various modules			
Name used in the current work	MicroDyn Module	CUT Module	UNSW Module	Liqui-Cel® Module
Suppliers	MICRODYN-NADIR GmbH, Germany.	CUT Membrane Technology GmbH, Germany.	The University of New South Wales (UNSW), Australia.	3M Company, USA.
Model	MD 020 CP 2N	MF 002-018 040-0500 PVC	Built in-house at UNSW	EXF-2.5x8
Materials (membrane/housing /potting)	PP/PVC/PU	PP/PVC/PU	PP/PVC/Epoxy	PP/ND*/PE
Number of fibres	40	ND	50	9950
Fibre internal diameter (mm)	1.8	1.8	1.8	0.24
Fibre length (mm)	420	500	ND	150
Effective pore size (µm)	0.2	0.2	0.2	0.03
Porosity (%)	70	70	70	40
Effective surface area (m ²)	0.1	0.31	0.19	1.4
Maximum allowable temperature (°C)	40	ND	80	70

*ND means no data available. PP = Polypropylene; PVC = Polyvinyl chloride; PU = Polyurethane; PE = Polyethylene

5.4.1 Experimental setup

The experimental setup consisted of a feed tank, a feed heater, a feed pump, a condenser, a weighing balance and a vacuum pump, as shown in Figure 17. Membrane modules were used successively to characterize the performance (flux of the produced water) of each of them. Moreover, vacuum on the lumen side of membrane modules was controlled using a vacuum controller.

In a typical experiment, the feed (absorption liquid used in the MD process) was heated to a certain temperature using the feed tank and feed heater. The heated feed was pumped through a flow meter to the shell side of the membrane module. Water vapours would pass through the membranes and end up on the lumen side, where they would be sucked using vacuum and passed through the condenser. The weight of the condensed liquid or permeate was continuously monitored and used to determine the produced flux. The inlet and outlet temperatures around the membrane module were continuously monitored using thermocouples. Moreover, the salt removal and dissolved oxygen removal performances of the modules were determined by monitoring the electrical conductivities and dissolved oxygen contents of feed and permeate, respectively. In

addition, the pH of the permeate was also continuously monitored and used as another index to determine the quality of the produced water.

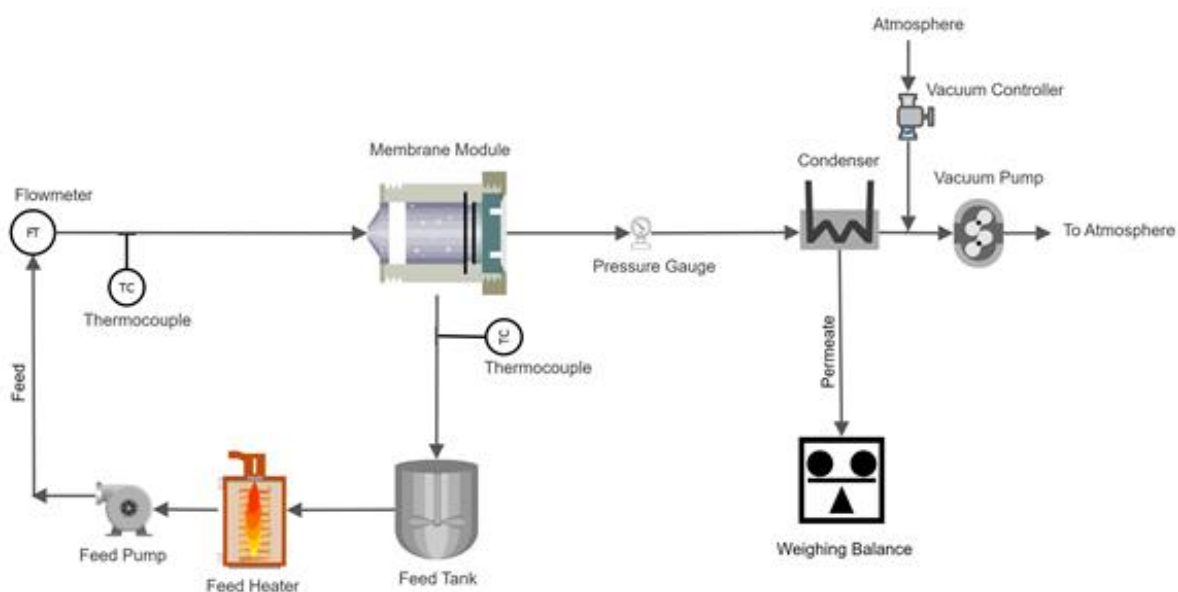


Figure 17 Schematic of the Vacuum Membrane Distillation setup used to evaluate the hollow fibre/capillary membrane modules

During the experiments, the effects of feed temperature, vacuum pressure, feed flowrate, and CO₂ loading of the absorption liquid on the performance of membrane modules to produce water were analysed. These factors were chosen as the conditions along the absorber column are spatially transient. Various conditions, such as temperature, flowrate and CO₂ loading of the slip stream that would be taken for water production would depend on its location in the absorber column. Therefore, a comprehensive study of these factors on the performance of membrane modules to produce water is needed for developing reasonable and rational practical applications.

5.4.2 Experimental results

Out of the four membrane modules, the CUT and MicroDyn modules were wetted during the initial experiment testing, most likely due to the aggressive chemical nature and high pH of the absorption liquid (feed). The liquids might have interacted with the PU potting material. Other materials used, i.e., membranes and housing were known to be quite stable as determined by separate exposure experiments. Therefore, no results are reported for these membrane modules. However, the UNSW and Liqui-Cel[®] modules were durable enough to produce water from the absorption liquid under various conditions. Their performances are separately reported as below.

Performance of the UNSW module

For the UNSW module, the feed inlet temperature was varied through values of 50, 55 and 60 °C, whereas the vacuum pressure on the lumen side, feed flowrate and CO₂ loading were maintained at values of 7 kPa (abs.), 17.6 lit/hr and 0, respectively. The results obtained for the produced water are shown in Figure 18.

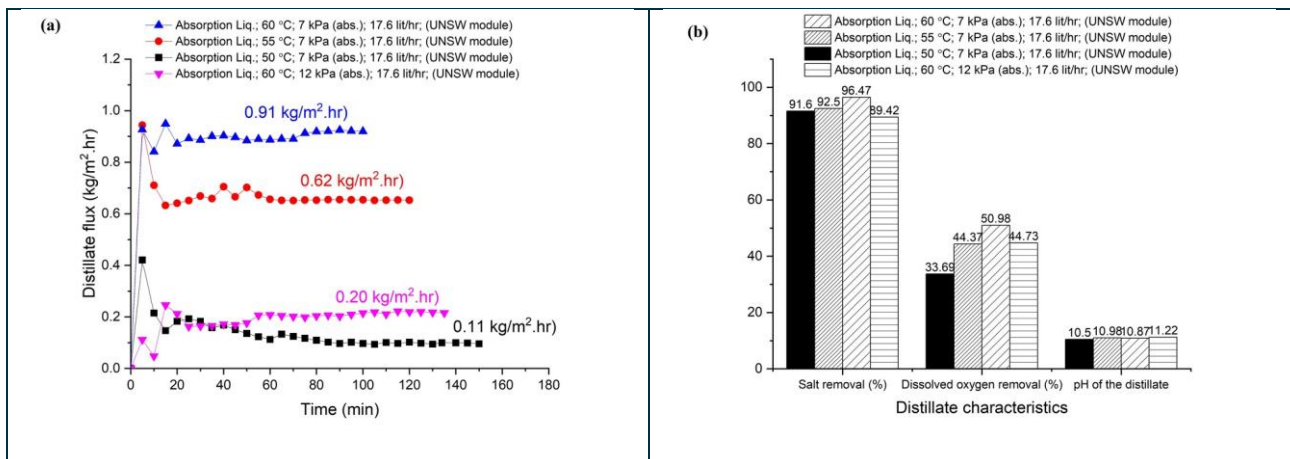


Figure 18 Effect of feed temperature and vacuum pressure on the quantity and quality of produced water using the UNSW module

The results showed that, with the increase in feed temperature, the amount of produced water increased. When the feed temperatures were 50, 55 and 60 °C, the produced water flux had steady state values of 0.11, 0.62 and 0.91 kg/m²hr, respectively. Moreover, the salt removal and dissolved oxygen removal increased with the increase in feed temperature. For example, for the feed temperature of 50 °C, the salt removal and dissolved oxygen removal had values of 91.6% and 33.6%, whereas for the feed temperature of 60 °C, the salt removal and dissolved oxygen removal increased to 96.47% and 50.98%, respectively. When the feed temperature was varied within the range of 50 – 60 °C, the pH value of the produced water varied within the range of 10.5 - 10.8. In a follow-up experiment, the vacuum pressure on the lumen side was increased from 7 kPa (abs.) to 12 kPa (abs.), whereas the feed temperature, feed flowrate and CO₂ loading were maintained at the values of 60 °C, 17.6 lit/hr and 0, respectively. The results showed that the flux of produced water decreased from 0.91 kg/m².hr to 0.20 kg/m².hr, highlighting the significant impact of lumen-side vacuum pressure on the flux of produced water. Moreover, the values of salt removal and dissolved oxygen removal decreased to 89.4% and 84.7%, respectively, whereas the pH value of the collected water increased to 11.2 compared to those of the distillate collected at a higher vacuum pressure under the same feed temperature, flowrate and CO₂ loading conditions. At this stage, the UNSW module got wet, and therefore, no further experiments could be performed using the module.

Performance of the Liqui-Cel® module

Liqui-Cel® module was the most robust and durable, and therefore, a more detailed investigation for water production from the absorption liquid using a MD process could be conducted.

In the first set of experiments, the feed temperature was varied through values of 50, 55 and 60 °C, while the values of feed flowrate, vacuum pressure and CO₂ loading were maintained at 17.6 lit/hr, 7 kPa (abs.) and 0, respectively. The corresponding results are shown in Figure 19.

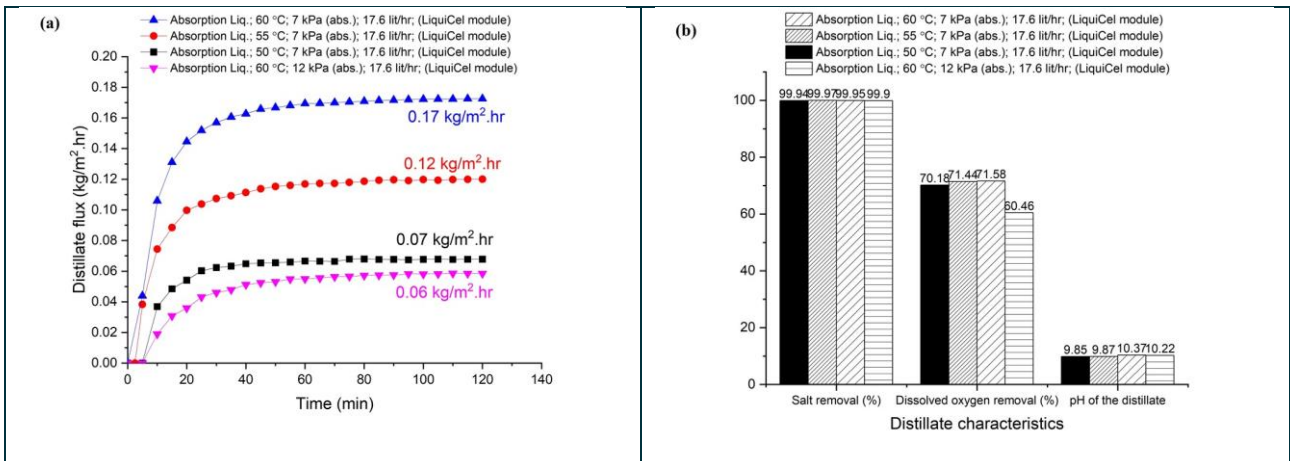


Figure 19 Effect of feed temperature and vacuum pressure on the quantity and quality of produced water using Liqui-Cel® module

When the feed temperature was varied from 50 °C to 60 °C, the flux of produced water increased from 0.07 to 0.17 kg/m².hr. Meanwhile, the salt removal, dissolved oxygen removal and pH of the produced water remained within the ranges of 99.94 - 99.95%, 70.18 - 71.58% and 9.85 - 10.37 for the studied feed temperature range (50 – 60 °C). When the vacuum pressure on the lumen side was increased from 7 kPa to 12 kPa for the feed temperature of 60 °C, the flux of produced water decreased from 0.17 to 0.06 kg/m².hr. Interestingly, the salt removal remained as high as 99.9%, however the dissolved oxygen removal dropped by around 10 percentage points to a value of 60.5%. The pH of the produced water also increased from 9.85 to 10.22, indicating that the produced water has some basic species in it.

In the follow-up experiments, the feed flowrate was varied through values of 7.6, 12.6 and 17.6 lit/hr while keeping the feed temperature, vacuum pressure and CO₂ loading constant at values of 60 °C, 7 kPa (abs.) and 0, respectively. The corresponding results are shown in Figure 20.

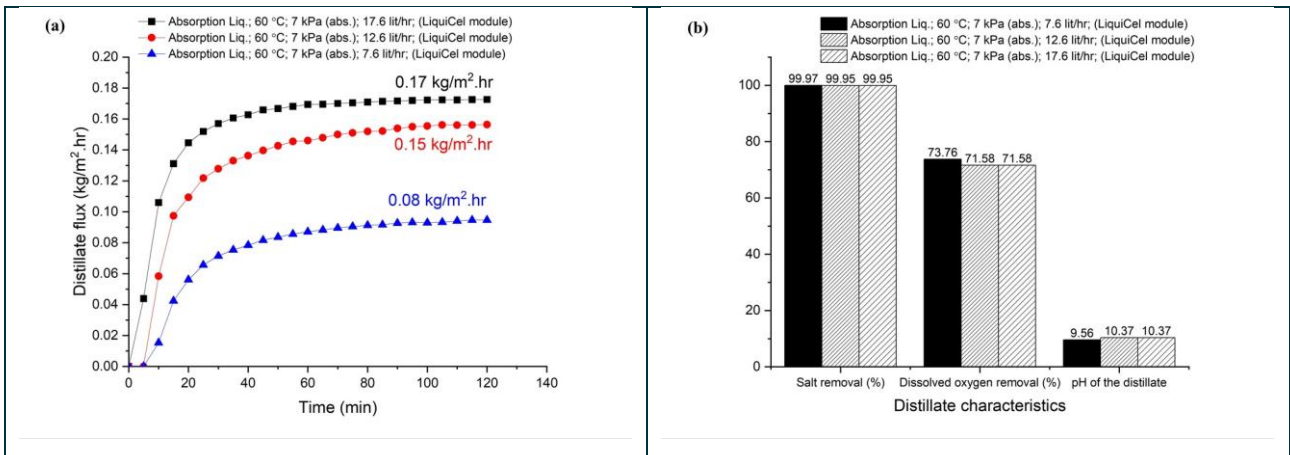


Figure 20 Effect of feed flowrate on the quantity and quality of produced water using Liqui-Cel® module

When the feed flowrate was changed from 7.6 lit/hr to 17.6 lit/hr, the steady state flux of produced water increased from 0.08 kg/m².hr to 0.17 kg/m².hr. Meanwhile, within the feed flowrate range of 7.6 - 17.6 lit/hr, the salt removal, dissolved oxygen removal and pH values remained within the ranges of 99.95 - 99.97%, 71.58 - 73.76% and 9.56 - 10.37, respectively.

In another set of experiments, the feed solution was loaded with CO₂ to different degrees to study the production of water. The CO₂ loading of the absorption liquid was varied through values of 0, 0.15 and 0.3 while the feed flowrate, vacuum pressure and feed temperature were maintained constant at values of 17.6, 7 kPa (abs.) and 60 °C, respectively. The corresponding results are shown in Figure 21.

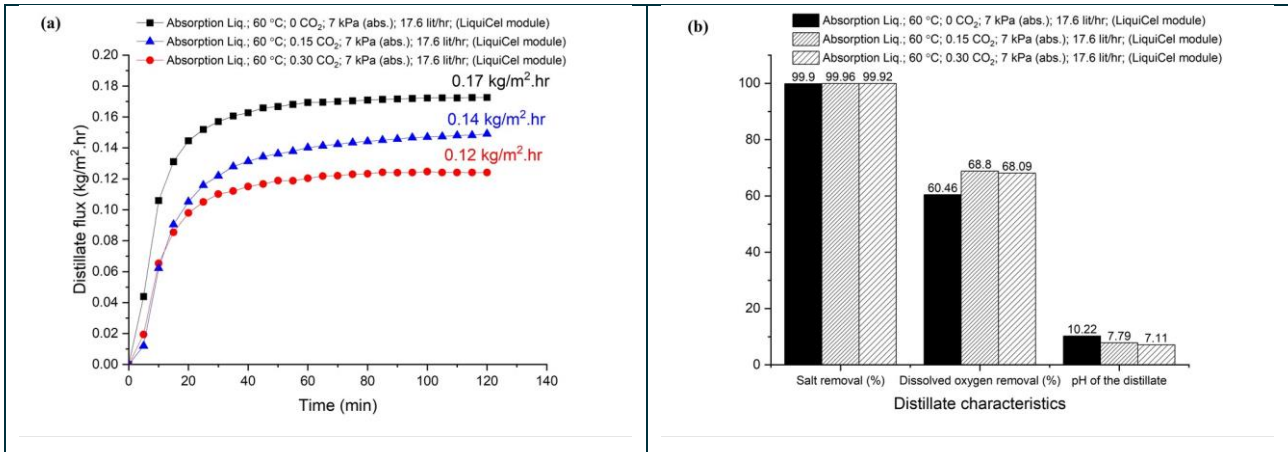


Figure 21 Effect of CO₂ loading on the quantity and quality of produced water using Liqui-Cel® module.

When the CO₂ loading of the absorption liquid was increased from 0 to 0.3, the flux of produced water decreased from 0.17 kg/m².hr to 0.12 kg/m².hr. Meanwhile, the salt removal and dissolved oxygen removal remained within the ranges of 99.9 - 99.92%, 60.46 - 68.09%, respectively. The distillate pH was higher at lower CO₂-loading, which can be explained by a small amount of absorption liquid permeating through the membrane and being mixed with the condensate. Small amounts of permeating liquid can affect the pH considerably. These results clearly indicated that CO₂ loading affected the quantity and quality of produced water. Therefore, further experiments were performed to study the impact of feed temperature and vacuum pressure on the quantity and quality of produced water from loaded absorption liquid using Liqui-Cel® module.

In this set of experiments, the absorption liquid was loaded to the loading of 0.3. The feed temperature was varied through values of 50, 55 and 60 °C, whereas the feed flowrate, vacuum pressure and CO₂ loading were maintained at 17.6 lit/hr, 7 kPa (abs.) and 0.3, respectively. The corresponding results are shown in Figure 22.

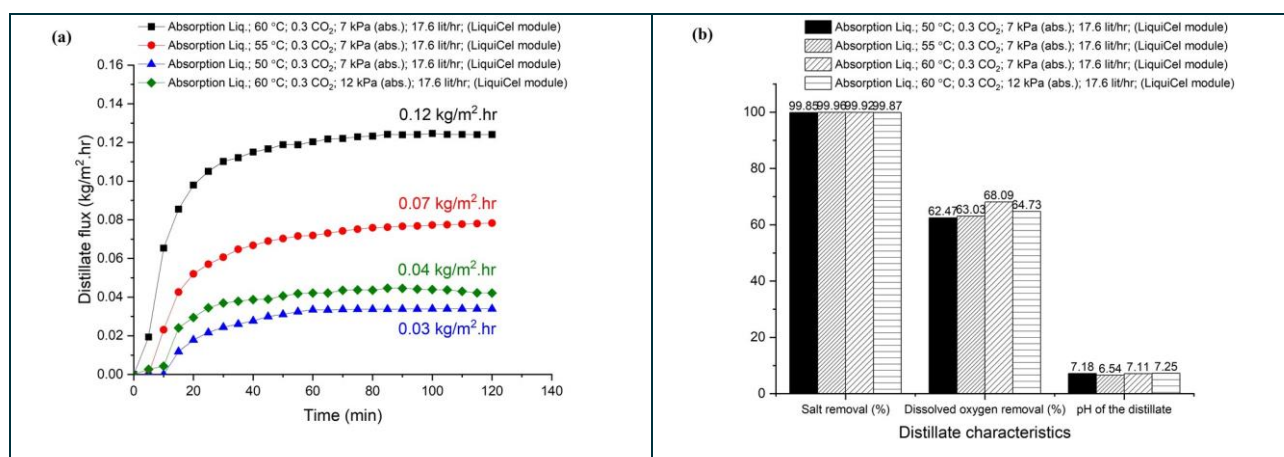


Figure 22 Effect of feed temperature and vacuum pressure on the quantity and quality of produced water for loaded absorption liquid using Liqui-Cel® module

When the feed temperature was increased from 50 °C to 60 °C for the loaded solvent, the flux of produced water increased from 0.03 kg/m².hr to 0.12 kg/m².hr. Meanwhile, the salt removal and dissolved oxygen removal were within the ranges of 99.85 - 99.92% and 62.4 - 68.09%, respectively. When the vacuum pressure on the lumen side was decreased from 7 to 12 kPa, the flux of produced water decreased from 0.12 to 0.04 kg/m².hr. The salt removal remained stable at around 99.8%, whereas the dissolved oxygen removal increased from 62.47% to 64.73%. The pH values of the produced water for this set of experiments remained within the range of 6.54 - 7.25, indicating that relatively clean water was produced during this set of experiments.

5.5 Results hollow fibre membrane module and capillary membrane modules with sweep gas

Membrane distillation experiments were also carried out at Deakin University, Geelong, Victoria, using the commercially available Liqui-Cel® membrane contactor and the CUT module (for specifications see Table 11). The Liqui-Cel® membrane contactor modules are commercially available in a range of module sizes that would facilitate further development and scale up of the process, whereas the CUT module was a standard micro-filtration module that could also be scaled-up.

The experiments were performed using deionised water or a CO₂-absorbent solution mixture of 3 M taurine, 3 M KOH and 1.5 M K₂CO₃ as the feed with the setup shown in Figure 23. On the liquid side, a feed solution (water or the absorbent) was heated to a certain temperature (40 - 60 °C) and circulated on the shell side of the hollow fibre membrane. The liquid flowrate was monitored by a flowmeter. The inlet and outlet temperatures of the feed solution were monitored by two thermocouples. The temperature drop between the inlet and outlet was used to evaluate the heat transfer and cooling performance of the vacuum Membrane Distillation system. The weight loss of the feed solution was recorded to evaluate the mass transfer performance (water flux) across the membrane. On the gas side, a water-circulation multifunction vacuum pump (Lichen Bangxi Equipment, Shanghai) with pressure reading was used to provide the vacuum pressure. The vacuum pressure could be adjusted to the desirable values by Valve 1 and/or Valve 2. The transferred water vapour was condensed into a bottle by a cold trap. Figure 24 shows the actual set-up in the

laboratory with the Liqui-Cel® membrane contactor. Different from the experiments reported in Section 5.4, these experiments were predominantly carried out in a sweep gas mode, i.e. air was allowed to flow through the module to aid in the evaporation process under partial vacuum.

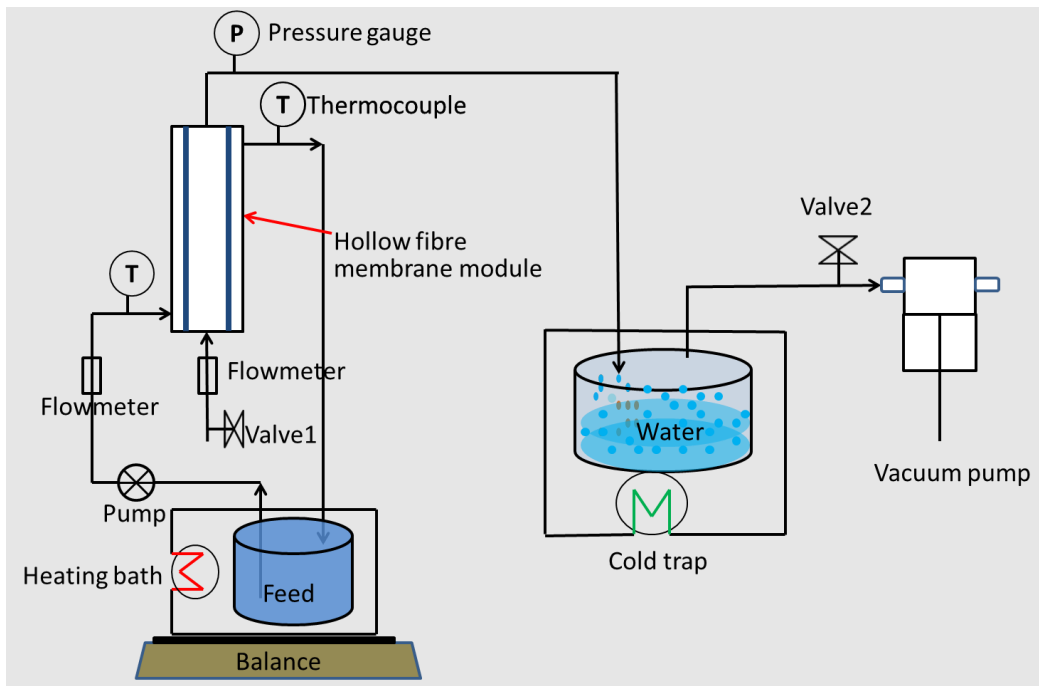


Figure 23 Experimental setup for the Membrane Distillation system

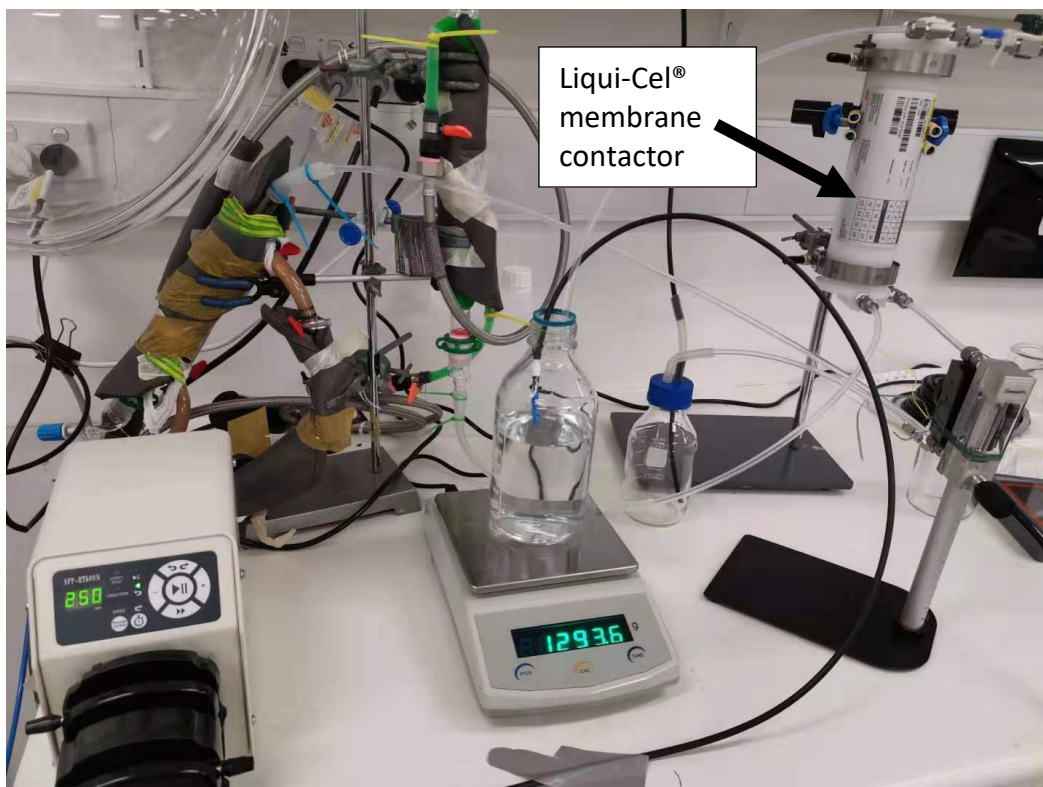


Figure 24: Liqui-Cel® membrane contactor in experimental set-up

5.5.1 Experimental results with Liqui-Cel® membrane contactor

Initial experiments were conducted with deionised water. As shown in Figure 25, with the rise in feed temperature, the change trends of the water flux and temperature drop of the feed along the membrane module were very similar, suggesting that the heat loss from the feed was mainly used to evaporate and drive the water vapour across the membrane.

When the feed water temperature increased from 40 to 60 °C, the corresponding water vapour pressure increased from 7.5 to 20.0 kPa. As a result, the water flux increased exponentially from 27 to 81 g/m²h Figure 25(a). Similarly, when the mixture solution was used as the feed, a similar change trend in water flux with the increase of the feed temperature was observed (Figure 25(b)). However, compared with the water vapour flux using pure water as the feed, the water flux using the mixture solution as the feed was slightly lower due to the decreased water vapour pressure (driving force).

Higher water vapour flux across the membrane often requires more evaporative heat to drive the process to happen. Therefore, higher water flux led to larger feed temperature drop along the membrane module. Compared with the feed temperature drop using pure water, the feed temperature drop using the mixture feed solution was much larger. This was mainly caused by the difference between the specific heat capacities of the solutions. When the specific heat capacity of the mixture solution is lower, a larger temperature drop along the membrane module difference is expected, which is desirable in using MD for heat exchanging purposes.

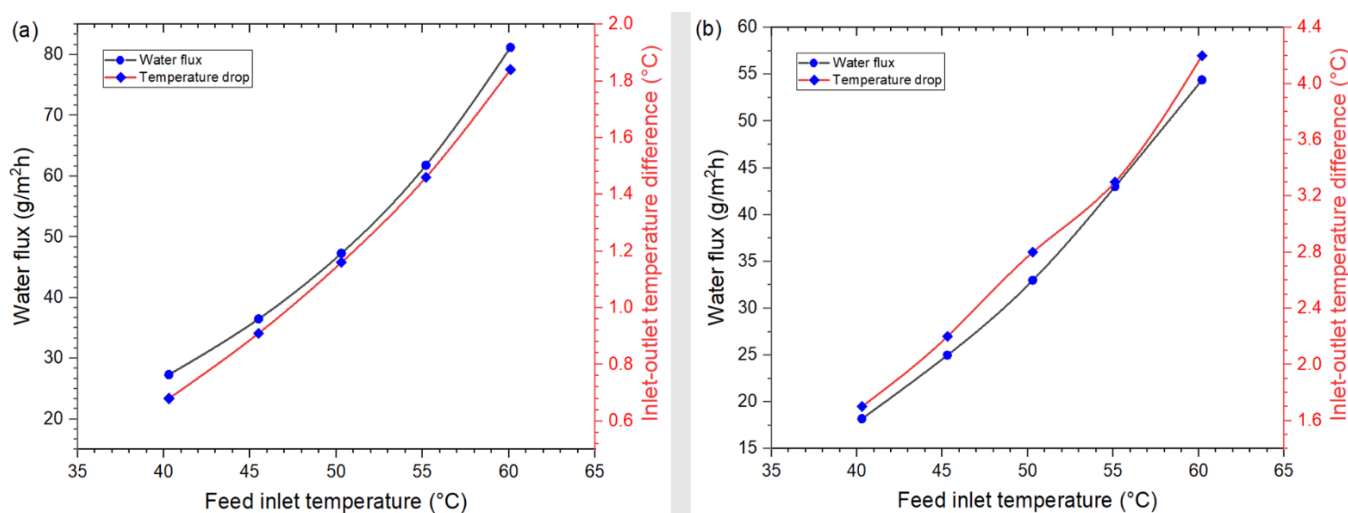


Figure 25 Water flux and feed temperature drop along the membrane module as a function of feed temperature: (a) deionised water as the feed, and (b) CO₂-absorbent solution as the feed. Feed flowrate: 50 L/h; vacuum pressure: 10 kPa

Next, we investigated the effect of feed flowrate on the water vapour flux. When the feed flowrate increased from 10 to 50 L/h, the water fluxes were fairly constant, only varying between 42.4 and 44.6 g/m²h (Figure 26). This suggested that there was a negligible effect of flow rate on the mass transfer. However, the feed flowrate had a significant impact on the feed temperature drop along the membrane module. As the feed flowrate increased from 10 to 50 L/h, the feed temperature drop reduced from 3 to 1 °C. When using the Membrane Distillation process as an intercooler, it is desirable to have a larger feed temperature drop along the membrane module that provides a better cooling performance. Therefore, maintaining a relatively low feed flowrate would be desirable.

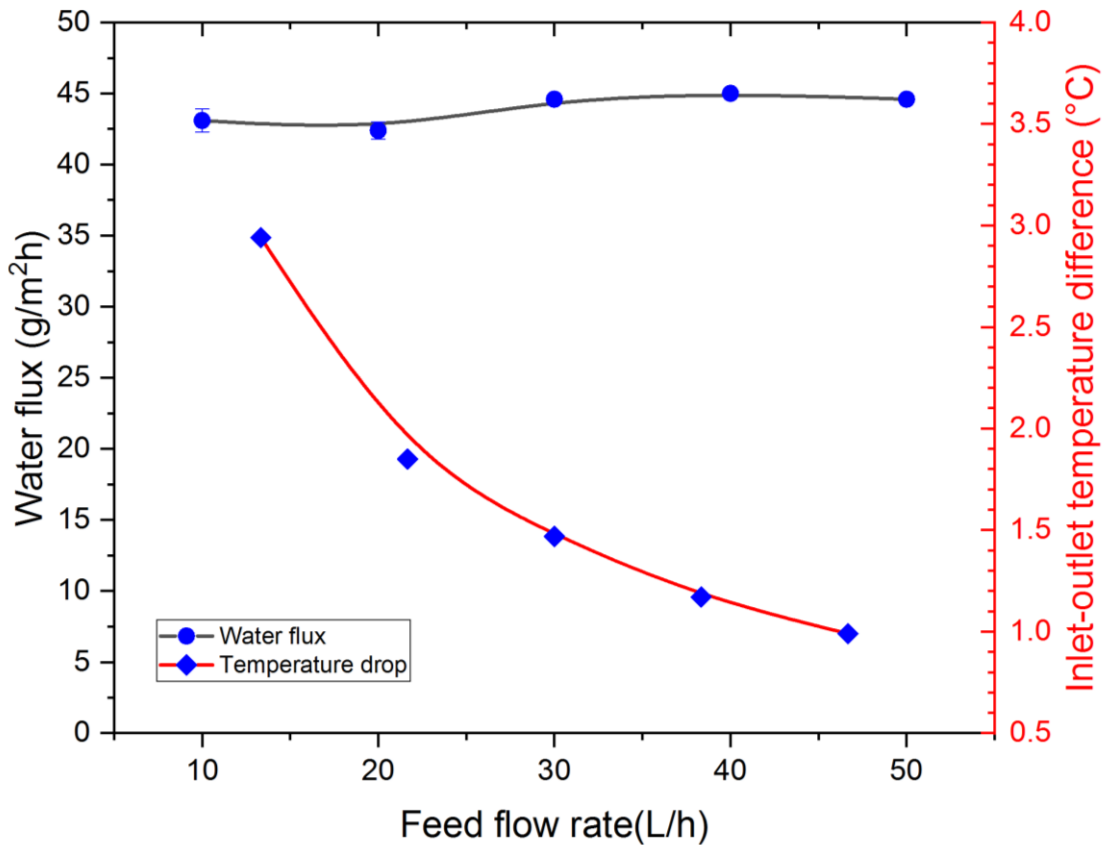


Figure 26 Water flux and feed temperature drop along the membrane module as a function of feed flowrate. Feed water temperature: 50.2 ± 0.1 °C (water vapour pressure 12.4 kPa); vacuum pressure: 10 kPa

When Valve 1 before the membrane module was completely closed (see Figure 23), there was no gas flow on the vacuum side and the vacuum pressure change could be adjusted by the valve at the bottom-end of the membrane module. The water flux was relatively stable; gradually increased from 3.9 to 6.5 g/m²h as the vacuum pressure varied from 5 to 15 kPa, and then decreased to 4.6 g/m²h at 20 kPa (Fig. 5a). This result suggests that the mass transfer performance (i.e. water flux) in our study was not sensitive to the vacuum pressure change. This might be because of hydraulic pressure drop in the hollow fibres which, at the low vacuum pressure might result in a limitation of driving forces. Similar to the water flux, the temperature drop along the membrane module was also stable in the Membrane Distillation process (~ 0.37 °C at a liquid flowrate of 50 L/h).

When Valve 1 before the membrane module was completely open, air flowed into the membrane module and the vacuum pressure change was adjusted by Valve 2 at the other end of the membrane module (Figure 23). The water flux increased almost linearly from 11.7 to 45.5 g/m²h as the vacuum pressure increased from 2.5 to 10 kPa (Figure 27b). When the vacuum pressure was 10 kPa, Valve 2 at the other end of the membrane module was fully closed. This means that if we want to further increase the vacuum pressure, Valve 2 is fully closed and Valve 1 before the membrane module has to be partially closed. When we further increased the vacuum pressure up to 20 kPa by partially closing valve 1 before the membrane module, the water flux dropped significantly from the peak value (45.5 g/m²h at 10 kPa) to 29.1 g/m²h. These results demonstrate that the gas flow along the membrane module had a significant impact on mass transfer in Membrane Distillation. The gas flow

can destroy, evaporate and strip the condensed water film layer on the vacuum side, thereby improving the mass transfer performance. Higher gas flow rates caused higher water fluxes by reducing the boundary layer effect on the gas side. For example, when the gas flow rates were 0 and 10 L/min, the water fluxes were 5.8 and 45.5 g/m²h, respectively, under the same vacuum pressure of 10 kPa. It was noted that the water flux with gas flow was almost eight times higher than that without gas flow on the vacuum side.

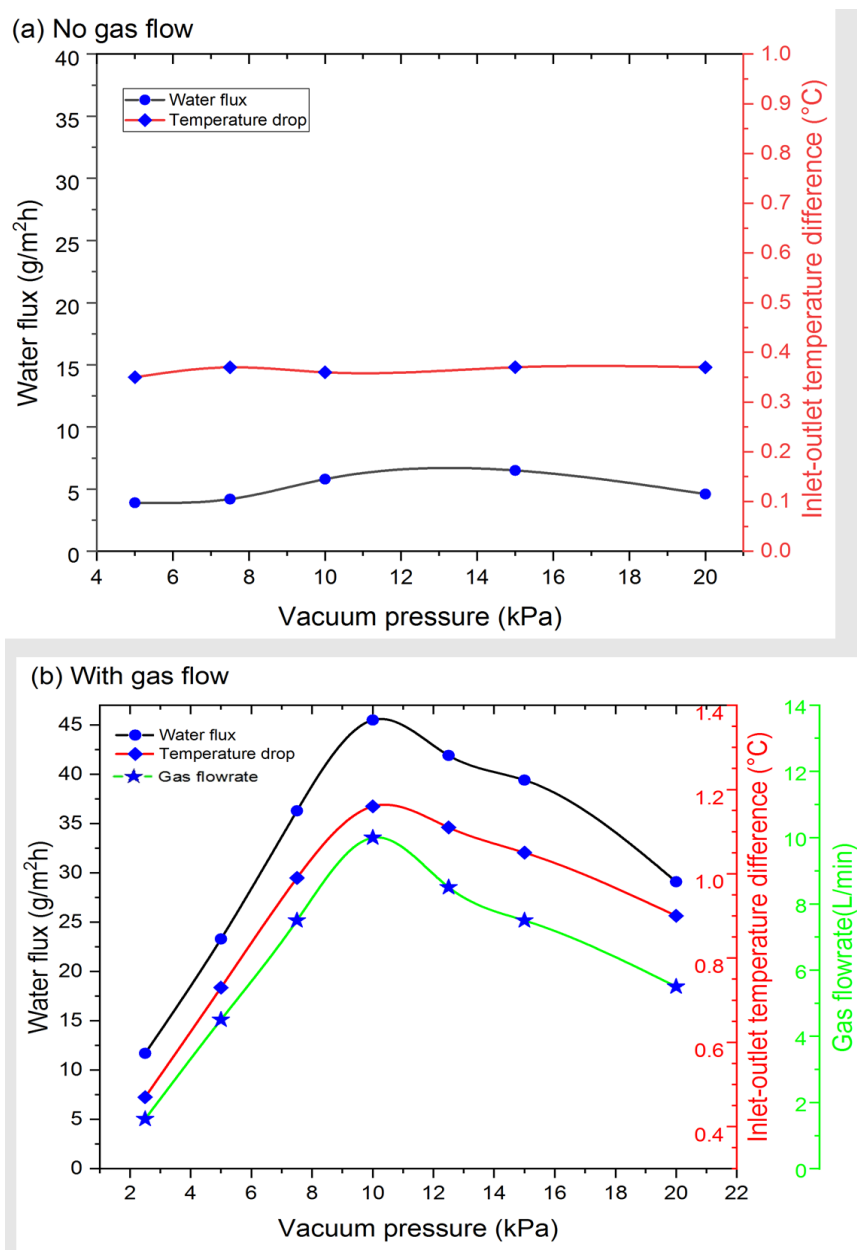


Figure 27 Water flux and feed temperature drop along the membrane module as a function of vacuum pressure: (a) no gas flow; (b) with gas flow on the vacuum side (deionised water was used as the feed). Feed temperature: 50.4 ± 0.1 °C (water vapour pressure 12.55 kPa); feed flowrate: 50 L/h

5.5.2 Experimental results with CUT membrane module

Next the CUT microfiltration membrane module was integrated into the existing experimental set-up at Deakin University (Figure 28). Experiments were first carried out using water and subsequently with the absorption liquid consisting of taurine, potassium carbonate, potassium hydroxide and water (3M taurine, 3M KOH, and 1.5M K_2CO_3).

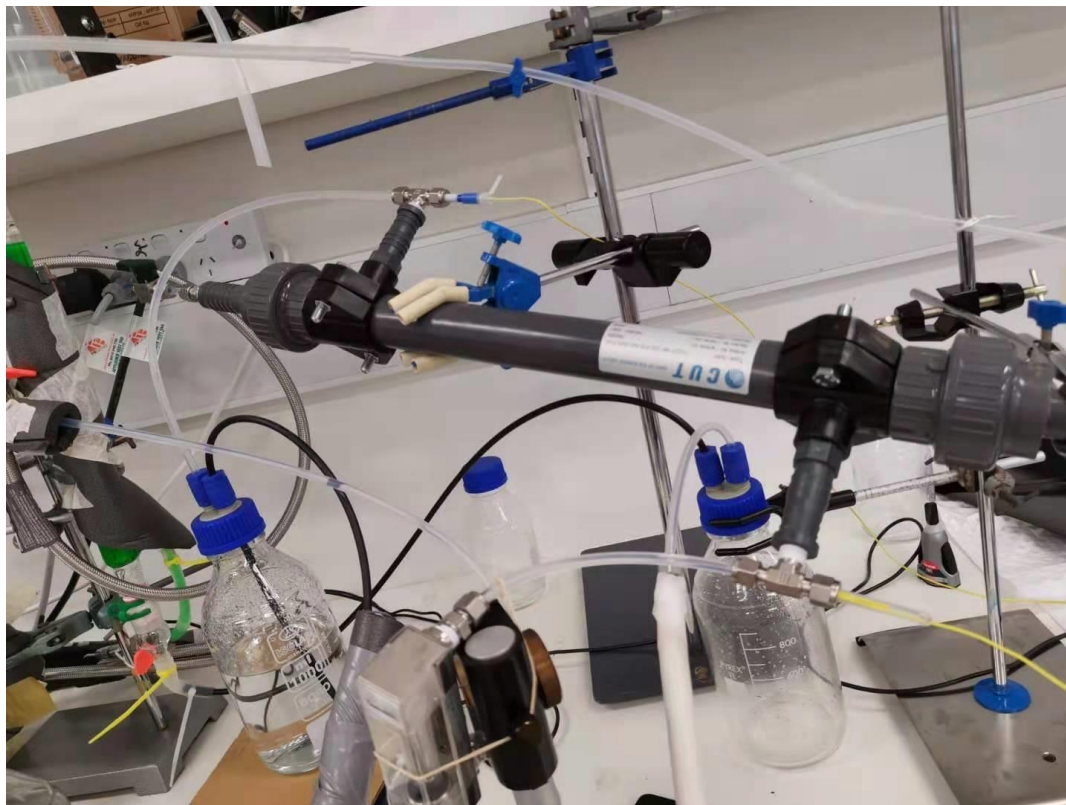


Figure 28 CUT membrane module integrated in experimental set-up at Deakin University

Sweep gas experiments using water as the feed solution

The effect of vacuum pressure on the heat and mass transfer was determined at constant inlet temperature (50.2 ± 0.1 °C) and feed flow rate of 20 L/h. The results in Figure 29 show water flux, temperature change and gas flow to follow the same pattern as a function of vacuum pressure. With the increase of the vacuum pressure as shown in Figure 29, the water flux and temperature drop increased first from 21 to 155 g/m^2h , and then declined to 110 g/m^2h . It suggests that the gas flowrate on the vacuum side played an important role in the membrane module performance. When the vacuum pressure increased from 2.5 to 10 kPa, the valve on one end of the hollow fibre membrane module was almost fully opened (valve 1), which maintained the gas flowing on the vacuum side.

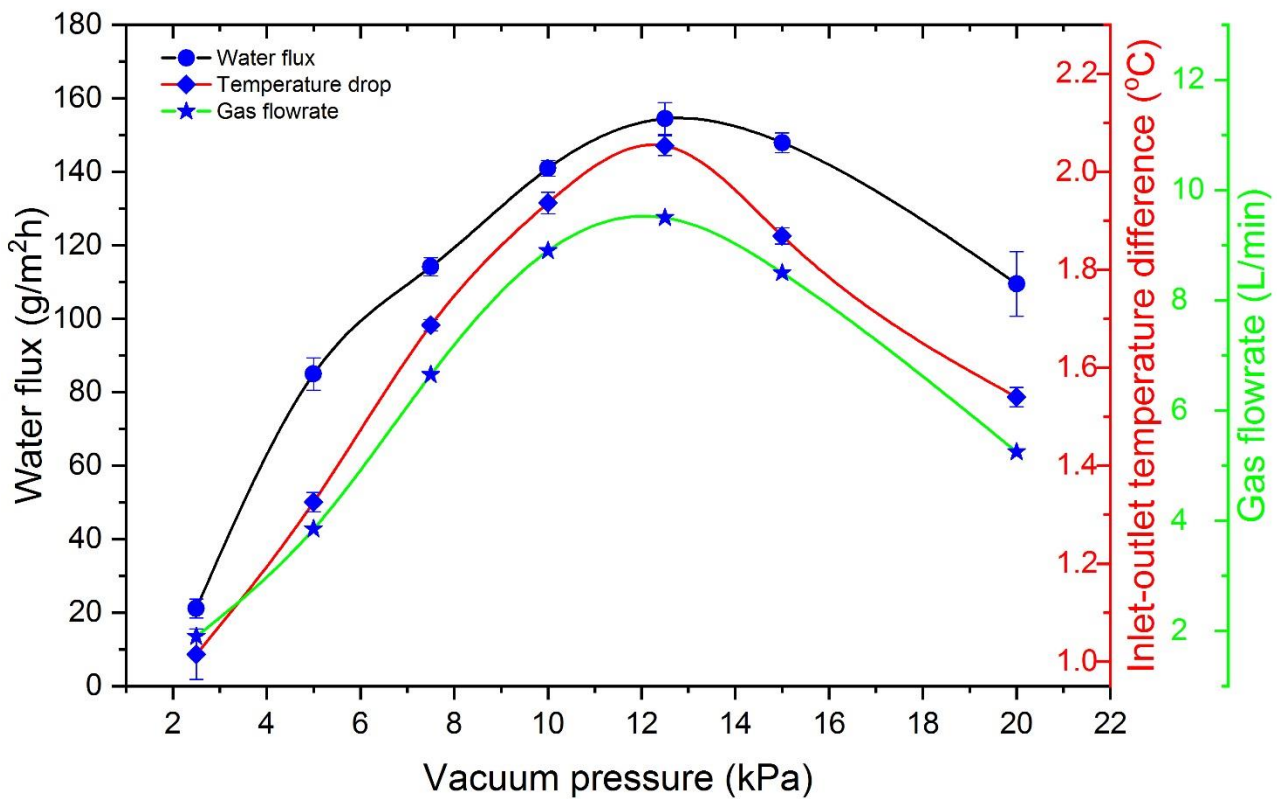


Figure 29 Water flux and feed temperature drop along the membrane module as a function of vacuum pressure (feed water temperature: 50.2 ± 0.1 °C (water vapour pressure 12.4 ± 0.04 kPa); feed flowrate: 20 L/h)

Next the effect of feed temperature variation on heat and mass transfer performance was assessed with results shown in Figure 30 for feed water temperature between 40 and 60 °C at a constant feed flowrate (20 - 21 L/h). When the feed temperature increased from 40 to 60 °C, the corresponding water vapour pressure increased from 7.4 to 20.0 kPa. As a result, the water flux increased from 78 to 238 g/m²h. Higher water vapour flux across the membrane requires more evaporative heat to drive the process to happen. Therefore, higher water flux led to larger feed temperature drop along the membrane module.

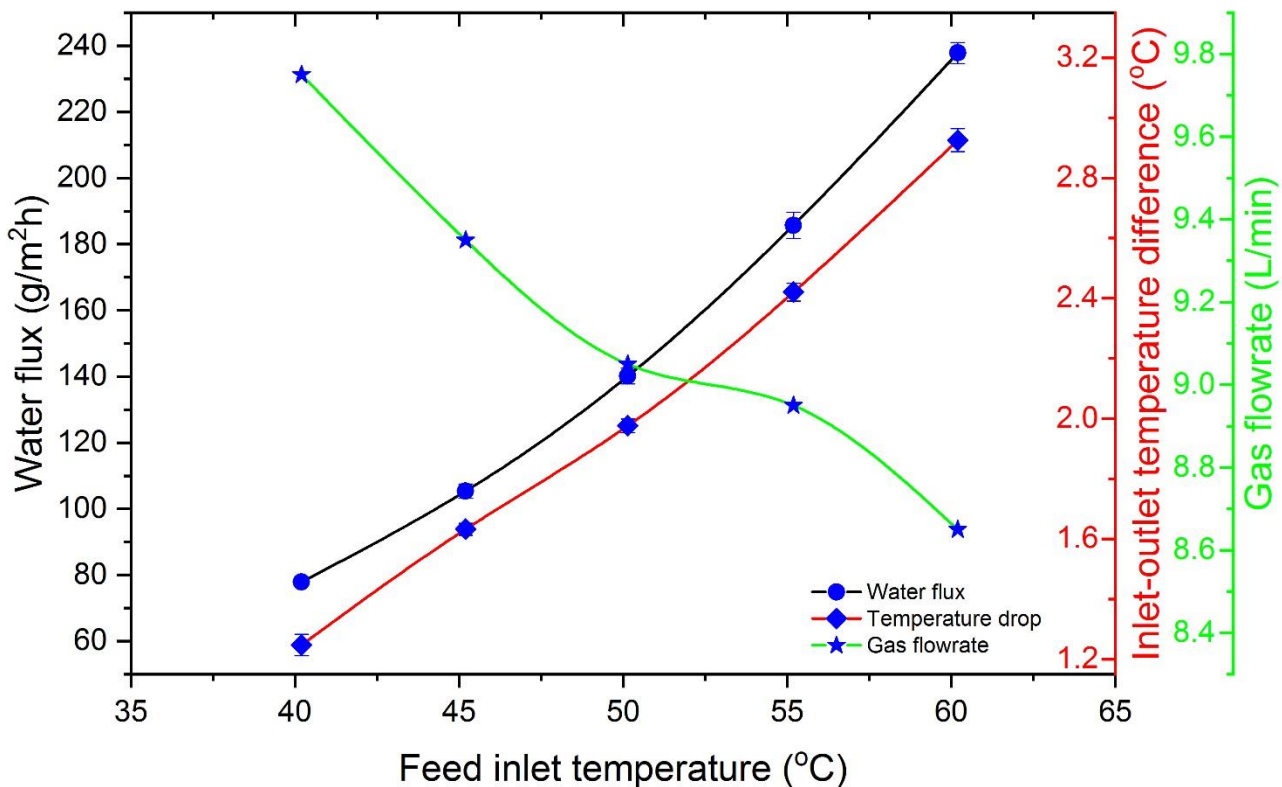


Figure 30 Water flux and feed temperature drop along the membrane module as a function of feed temperature (feed flowrate: 20 - 21 L/h; Vacuum pressure: 10 kPa (top-end of the membrane module was open))

Sweep gas experiments with absorption liquid (3 M Taurine, 3 M KOH and 1.5 K₂CO₃)

The effect of vacuum pressure on the heat and mass transfer was assessed first with the experimental results shown in Figure 31. Compared with the experiments using water as the feed (Figure 29), the water flux at the vacuum pressure of 10 kPa reduced from 140 to 110 g/m²h because the water vapour pressure over the absorbent solution will be lower than that for water. Another difference is the feed temperature drop along the membrane module, which is slightly lower for the mixed absorbent.

A reduction in water flux was also noticed during the experiments in which the temperature of the feed solution was varied, as shown in Figure 32 but only for the high temperature. As more experiments were carried out with the CUT membrane module it was noticed that the conductivity of the product water steadily increased from around 5 μS/cm to over 500 μS/cm. While the latter conductivity is like that of tap water, it was clear that part of the feed water was transferred across the membrane.

The water fluxes for the CUT membrane module are significantly higher (2-3 times) than for the Liqui-Cel®. The membranes used in the CUT module have a higher porosity and pore size (Table 11) which will result in higher flows. Also, the large dimensions of the capillaries in the CUT membrane modules will result in lower pressure drop, which is a significant benefit when working under vacuum, as driving forces can be maintained and energy losses are reduced.

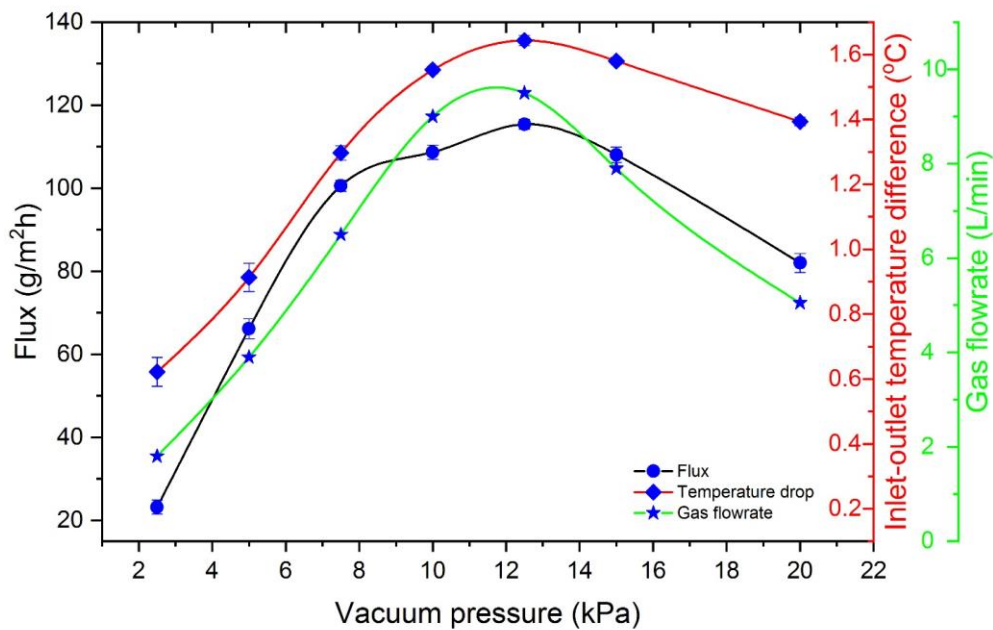


Figure 31 Water flux and feed temperature drop along the membrane module as a function of vacuum pressure, using the absorption liquid as the feed, and gas flow on the vacuum side (feed water temperature: 50 °C; feed flowrate: 20 L/h)

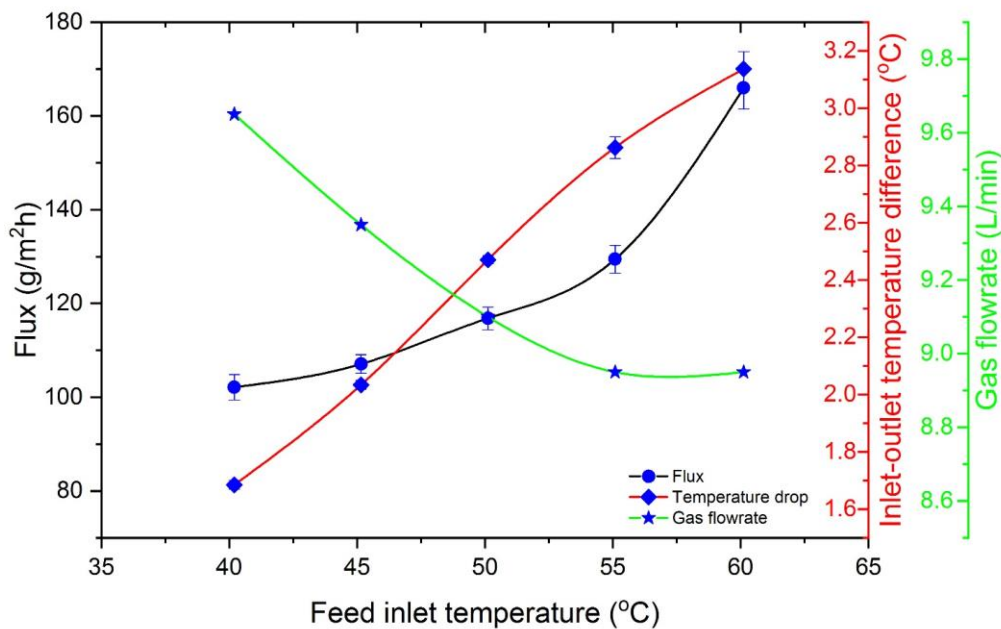


Figure 32 Water flux and feed temperature drop along the membrane module as a function of feed temperature using the absorption liquid as the feed, and gas flow on the vacuum side (Vacuum pressure = 10 kPa)

5.6 Overall evaluation of Membrane Distillation experiments

The experimental Membrane Distillation work covered several membrane materials and membrane module types. Most membrane modules were commercially available with potential for process scale up using large size membrane modules. The experimental conditions, in particular the temperature and vacuum pressure, were also varied. The membrane operation has involved operation under vacuum without and with the use of a sweep gas.

The above choices were made to cover the widest range of options for the laboratory work with a view to assess whether the technology would be suitable for pilot plant evaluation. The performances were therefore influenced by a multitude of factors that made comparison not straightforward. Nevertheless, a summary of performance results is presented in Table 12 for the Membrane Distillation laboratory experiments carried out with absorption liquids.

The range in water fluxes for the individual membranes and membrane modules were mostly determined by the operating conditions (vacuum pressure, temperature) with high liquid temperature and low vacuum pressure giving the highest fluxes, when operating with vacuum only. The operation with sweep gas did not provide benefits in terms of water flux enhancement.

The differences in the experimentally determined water fluxes between the different membranes and modules were large, nearly up to two orders of magnitude, e.g., comparing the water fluxes for the flat sheet PTFE membranes and the Liqui-Cel[®] membrane modules. Largely the result of the much lower porosity and smaller pore size for the hollow fibres used in the Liqui-Cel[®], the water flux is also influenced by the module design. This is because pressure drop under vacuum translates to loss of driving force and, consequently, lower water fluxes and mass transfer limitations might be present in the liquid phase due to poor mixing. It is perhaps best demonstrated through the comparison of water fluxes for the UNSW module, designed for Membrane Distillation applications, and the CUT module, essentially a standard shell and tube micro-filtration module. Both use the same capillary membranes but the water flux for the specially designed Membrane Distillation module from UNSW is significantly higher.

Even more than membrane and membrane module performance, the technology robustness is the decisive factor in scale-up. The robustness is coarsely defined as the prevention of undesired liquid permeation through the membranes, which might occur under the pressure gradient across the membrane and through pinholes (large pores) in the membranes. Without robust membranes and membrane modules, scale-up is not possible, as the permeate quality would be compromised.

In terms of robustness, the PTFE flat sheet membranes and the Liqui-Cel[®] have both outperformed the capillary membranes tested here. The PTFE membranes are more hydrophobic than the PP membranes, which helps in preventing the membrane pores being wetted with the absorption liquid. It is expected that PTFE membranes with smaller pore sizes than the ones tested in this project would have better quality product water. Scale-up would require access to membrane modules for dedicated pilot plant testing. Despite the presence of several companies that can deliver membrane modules for standard Membrane Distillation applications (<https://www.aquastill.nl/>; <https://www.memsys.eu/>; <https://www.memsift.com/>), such modules are not necessarily useful for our process that needs to work with amine solutions and with a vacuum for the driving force. This would require evaluation of the membrane modules and materials in conjunction with the selected absorption liquids, as the Membrane Distillation companies are

focused on seawater desalination and similar applications. There is a lack of practical experience in working high pH feed solutions.

Liqui-Cel® has modules available that could be used for technology scale-up (https://www.3m.com.au/3M/en_AU/liquicel-au/) and have shown adequate robustness in the laboratory experiments. Their relatively low water flux is off set by the compactness of the equipment and typically low cost of the hollow fibre membranes used, in comparison to PTFE. Larger Liqui-Cel® membrane modules use different materials for potting the PP membranes and would have to be evaluated with the absorption liquids first.

It appeared to be quite challenging to bring the Membrane Distillation technology to a demonstration at the Vales Point PCC pilot plant, at this stage. However, the laboratory work indicated that following options could be pursued:

1. Evaluation of larger size Liqui-Cel® membrane contactors

Larger size membrane modules are available from the supplier and the technology has been used for decades in other applications such as degassing. A first step would be to ascertain the material compatibility with the absorption liquids used, as the materials (not the membranes) used in the large modules differ from the modules evaluated in the laboratory in this project.

2. Evaluation of a Membrane Distillation module from one of the identified suppliers

This option would incorporate the evaluation of smaller scale prototypes from any of the suppliers to ascertain the integrity of the system (membranes, potting and other materials). A preference for PTFE membranes has emerged from our work.

In both cases the evaluation should consider both the performance (water flux, undesired permeation) and robustness for the absorption liquids. The results would also underpin the techno-economic analysis of the process. It would be very beneficial to have up-front discussions with the suppliers for both options to ascertain system robustness at an early stage and where possible conduct experiments to ascertain the materials compatibility.

Table 12 Summary of results of Membrane Distillation experiments with absorption liquids

Membrane geometry/ module	Membrane Material	Temperature range	Water flux range	Comments/Observations
Flat sheet/test cell	PTFE	55 – 65 °C	MEA: 9.5 – 20.6 l/m ² h Taurate: 9.4 – 22.5 l/m ² h	<ul style="list-style-type: none"> - Only membranes tested; no modules - No significant liquid leakage
Hollow fibres/Liqui-Cel®	PP	40 – 60 °C	Taurate/Carbonate: 0.02 – 0.17 l/m ² h	<ul style="list-style-type: none"> - Experiments without/with sweep gas - Larger modules commercially available as membrane contactors - No significant liquid leakage
Capillaries/CUT	PP	40 – 60 °C	CUT - Taurate/carbonate: 0.02 – 0.16 l/m ² h	<ul style="list-style-type: none"> - Microfiltration module design - Larger modules commercially available as microfiltration modules - Significant leakage particular under deep vacuum
Capillaries/UNSW	PP	50 – 60 °C	UNSW - Taurate/carbonate: 0.1 – 0.9 l/m ² h	<ul style="list-style-type: none"> - Dedicated Membrane Distillation module design - Prototype module design - Leakage became apparent towards end of experiments

6 Vales point PCC pilot plant experimental evaluation

6.1 Pilot plant operations and modifications

The Delta Electricity PCC pilot plant at Vales Point was mothballed in April 2019. A site inspection was conducted by CSIRO at Vales Point Power Station with the purpose of reviewing the health and safety systems and processes of the rig. The review¹⁹ was conducted with regards to CSIRO HSE requirements and any potential areas of noncompliance, observations and/or suggestions for improvement were noted for further attention. It contained a series of recommendations that were implemented as part of the PCC pilot plant preparations. These related to:

- Induction process to PCC pilot plant
- Operational procedures
- Consultation/Team meetings
- Hazardous chemicals management
- Electrical
- Emergency management
- Equipment maintenance
- Change management

The pilot plant also required several alterations to improve its operability. These were:

- Update of the PCC pilot plant Eurotherm control system

As the licence for the PCC pilot plant control system had expired, an update was required from the supplier. The update also included a new PC to run the updated software.

- Installation of new flue gas flow meter

Accurate flue gas measurements are needed to understand pilot plant operation and control and the provision of reliable information data that will inform process performance. An orifice type flow meter was purchased and installed by external contractors. Figure 33 and Figure 34, respectively, show the newly installed flow meter and the damaged flow meter removed from the pilot plant.

- Installation of new steam control valve for the reboiler

The new steam control valve enabled a smoother regulation of the steam input to the reboiler compared to previous manual control that was also quite labour intensive. Figure 35 shows the new control valve after installation into the pilot plant.

¹⁹ Vales Point HSE Review, Renata Payne, Phil Green, CSIRO internal report 2nd May 2019



Figure 33 New flue gas flow meter



Figure 34 Damaged steam flow meter



Figure 35 New steam valve installed

Provisions were also made for the off takes of lean absorption liquid to and from the Forward Osmosis rig that was separate from the PCC pilot plant as shown in Figure 36. To enable operation at elevated temperatures a heat exchanger was added that used steam for heating.

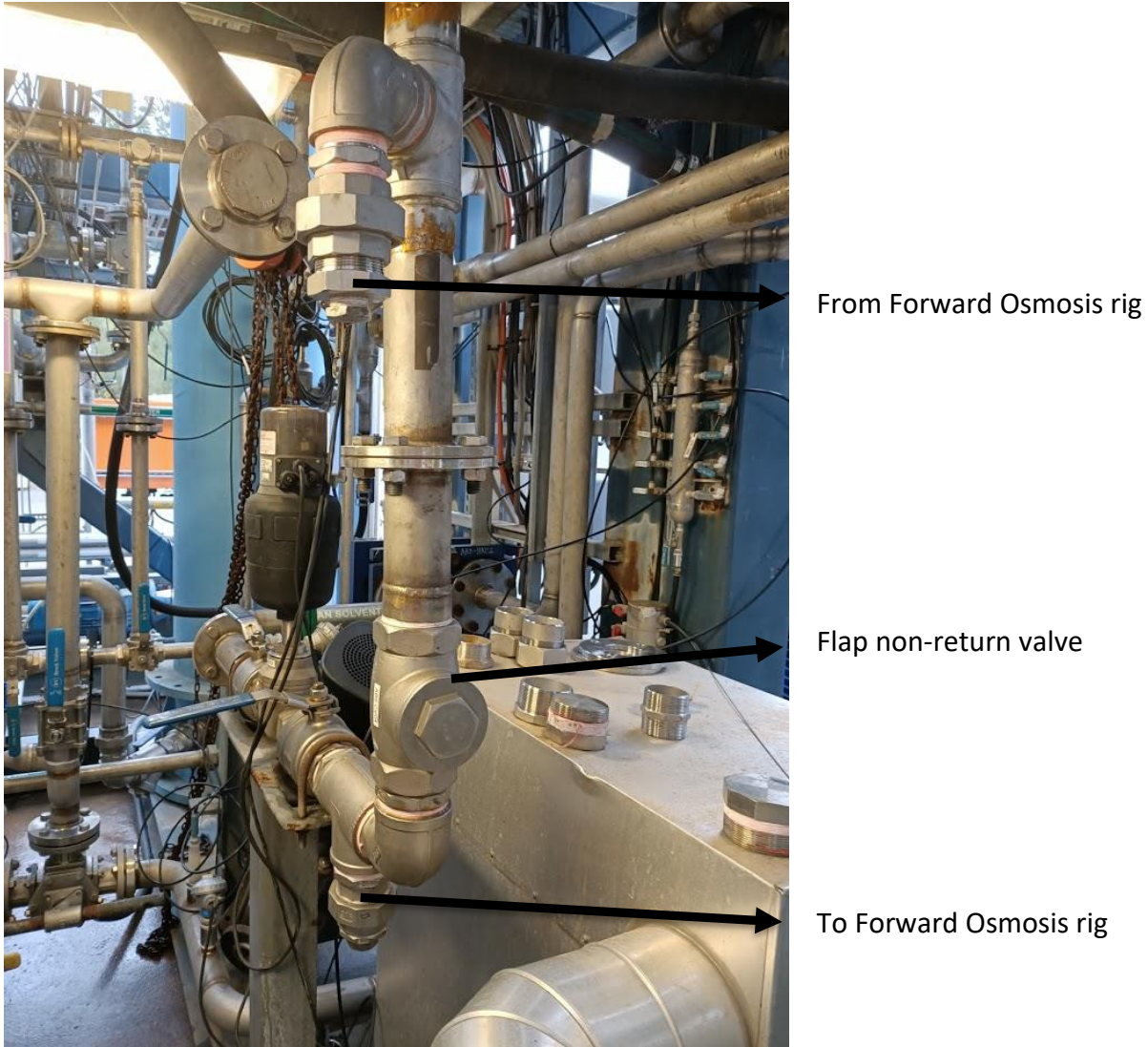


Figure 36 Tie-in points for the Forward Osmosis rig

6.2 Results MEA PCC pilot plant campaign

A total of 26 PCC pilot plant runs, 14 using 5M MEA and 12 using the 4M MEA/1M K_2CO_3 formulation, were carried out with the aim of determining the concentration of MEA in the condensate from the CO_2 desorber. The operational target of most runs was to achieve 90% CO_2 -capture at different settings of the liquid flow rate for a given flue gas flow rate. The average capture rate was ~91% for the MEA runs and 79% for the MEA-carbonate runs. The CO_2 -content in the flue gas typically varied between 9.9% and 11.9% for these runs as determined by the power plant operation.

The amount of steam required for regeneration of the absorption liquid is shown in Figure 37. The data indicates that the MEA-carbonate solution is more difficult to regenerate than MEA and cyclic loadings will be lower. This is mainly because of its higher pH of the solution as a result of the carbonate addition. This hampers the release of CO_2 . The overall steam required is anticipated to be between 1.5 and 2 kg steam/kg CO_2 in a large-scale MEA-based process. This is not achieved in the PCC pilot plant at Vales Point because of heat losses to the environment. The pilot plant is furthermore not optimised for operation with the chosen absorption liquids.

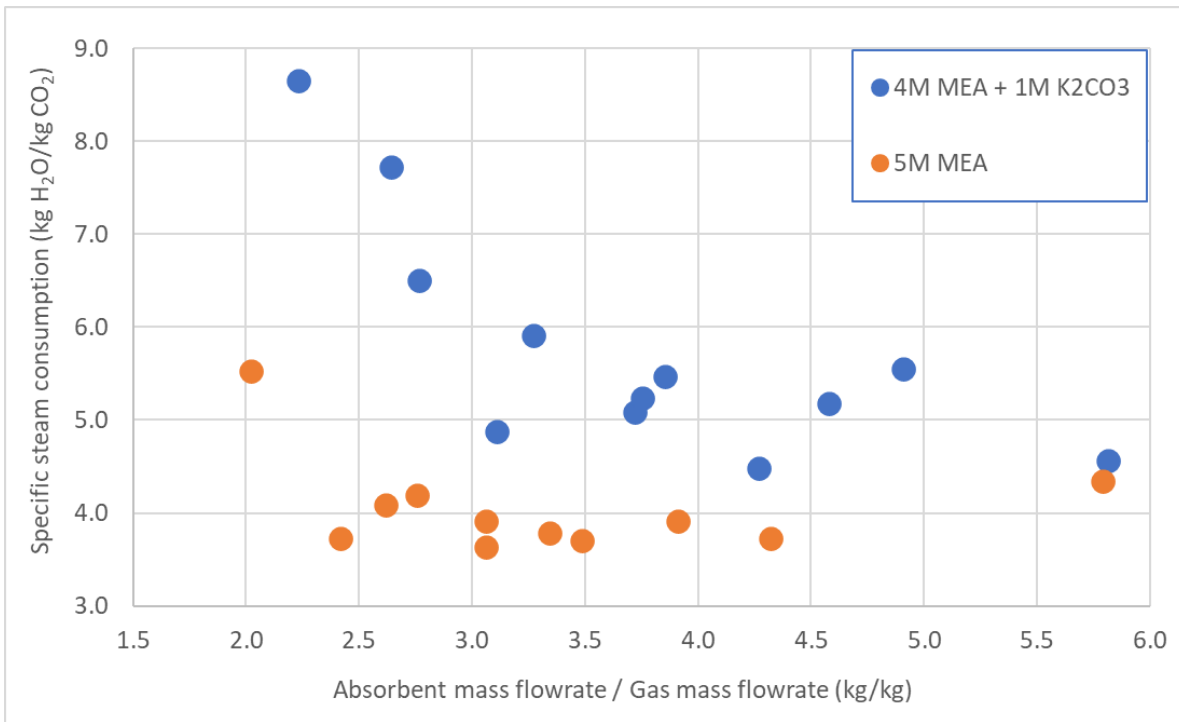


Figure 37 Specific steam flow into the reboiler at different values of the liquid/gas ratio in absorber for 5M MEA and 4M MEA + 1M K₂CO₃

The values for the MEA concentration in the desorber condensate are shown in Figure 38 as a function of desorber top temperature and in

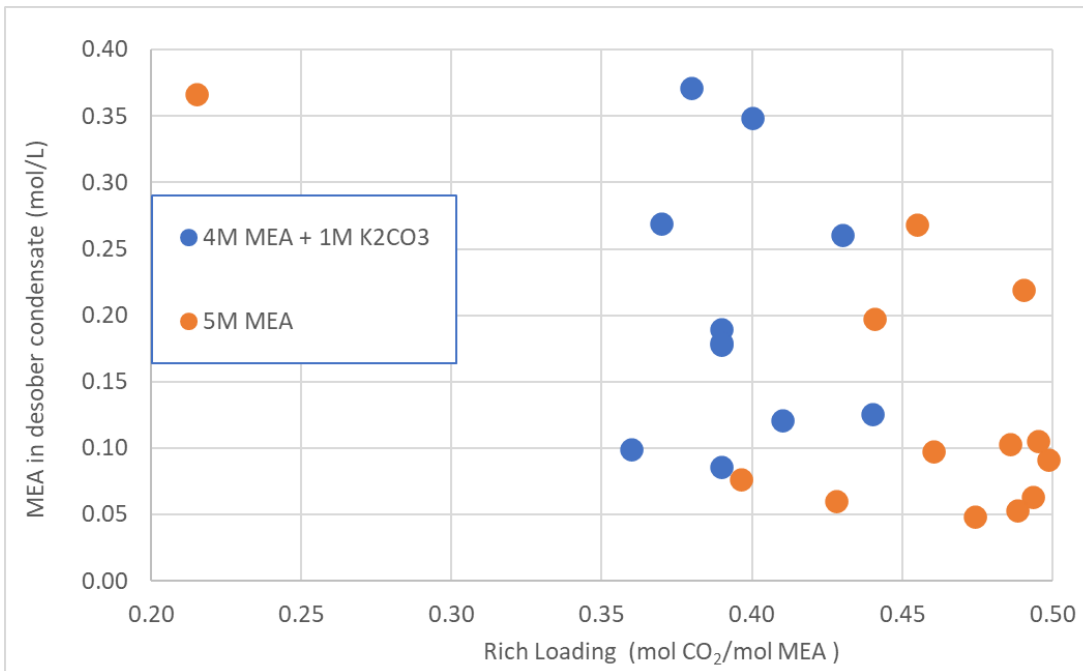


Figure 39 as a function of rich loading. One would expect that at a higher temperature the MEA concentration in the desorber condensate to be higher, as vapour pressure increases with temperature. At high rich loading one would expect that the MEA concentration in the condensate to be lower, because of the lower amount of unbound MEA in solution. While these trends are

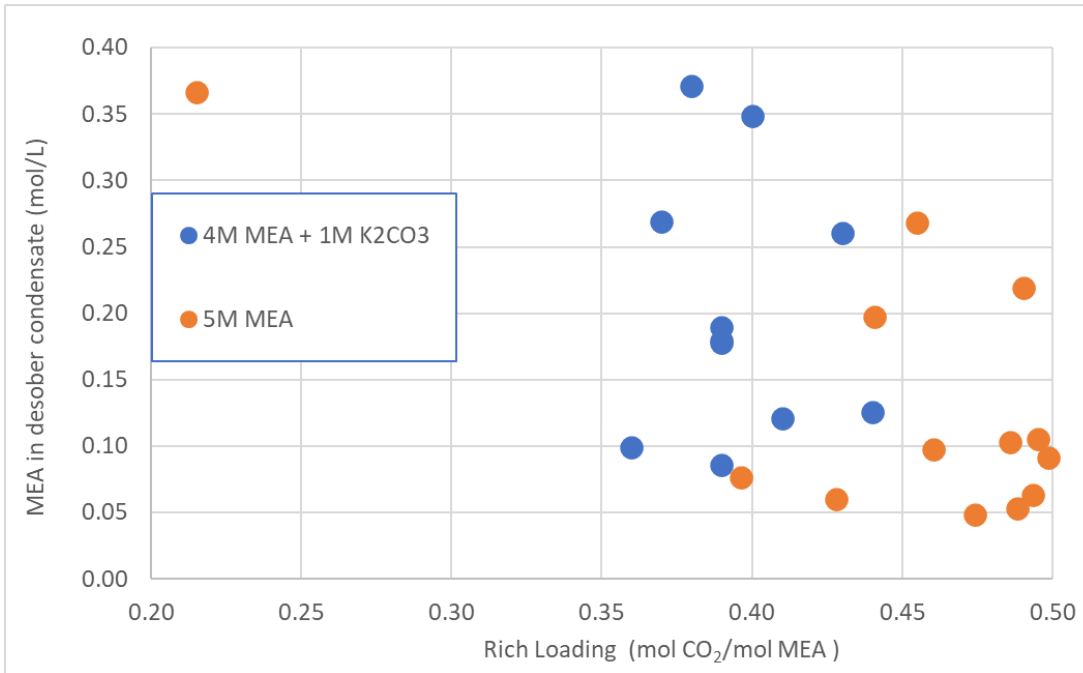


Figure 39 there is also considerable variation in the results. This is because operation conditions, such as steam flow, desorber bottom temperature, desorber pressure are varied to maintain CO₂-capture rate at the desired level as absorption liquid flow is varied. This will impact on the composition of the wet CO₂ stream leaving the desorber. It does appear from Figure 40 that conditions can be selected that provide low steam consumption with MEA concentrations in the desorber condensate below 0.1 mol/l. This is equivalent to be at least 6000 ppm salt content and would require further treatment for most uses except in the circumstance where the water is used for make-up of new absorption liquid.

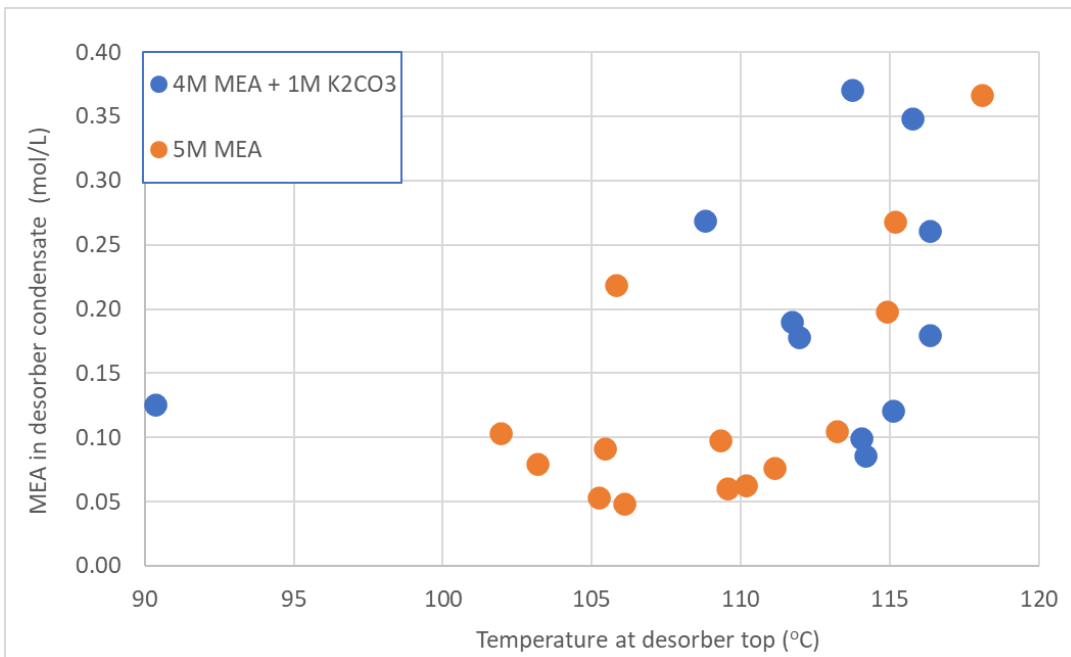


Figure 38 MEA concentration in desorber condensate at different desorber top temperatures

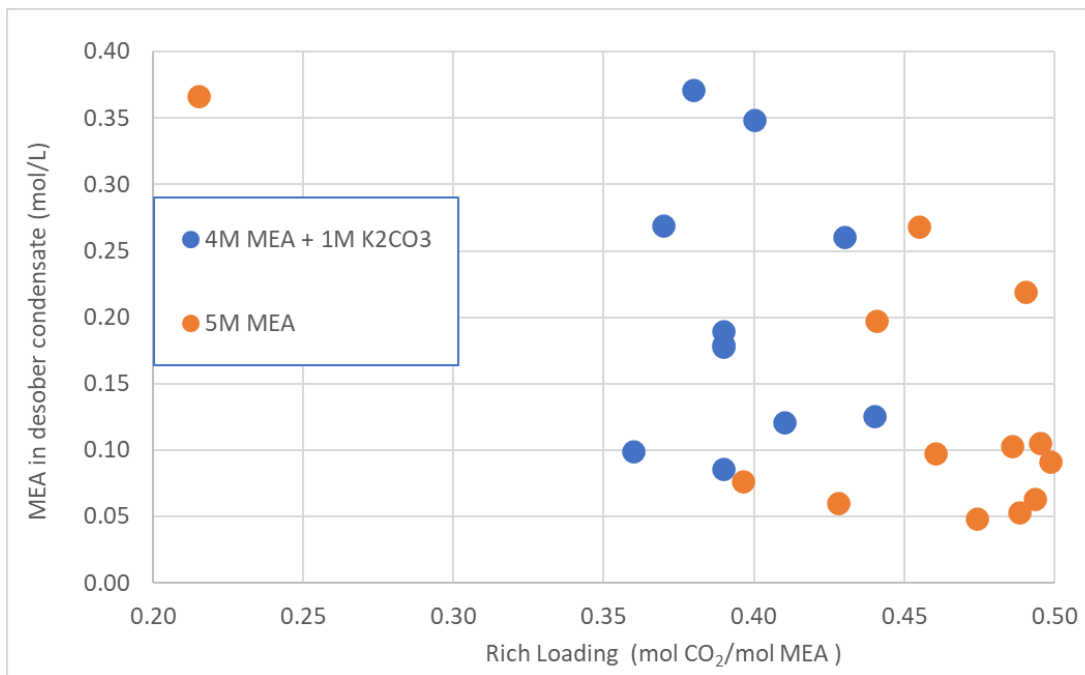


Figure 39 MEA concentration in desorber condensate at different rich loadings

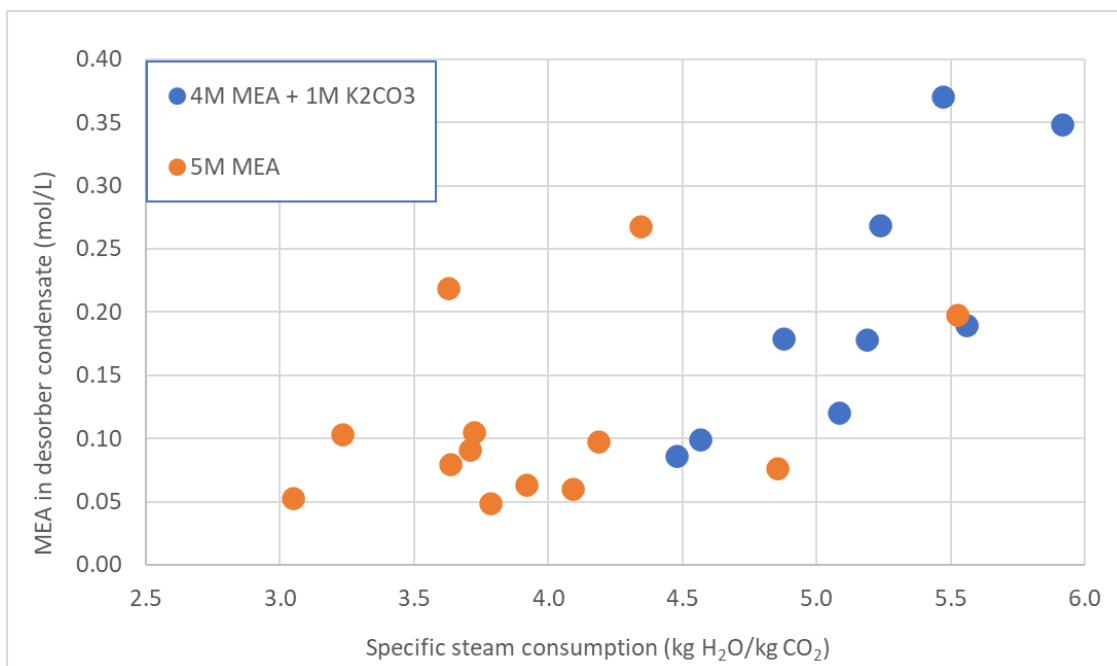


Figure 40 MEA concentration in desorber condensate at different steam consumption

6.3 Taurate-carbonate PCC pilot plant campaign

A total of 18 PCC pilot plant runs were conducted with the 3M taurate/1.5M K_2CO_3 formulation. The main aim was to assess the quality of the condensate. Unlike the experiments with MEA there was an expectation that the carry-over of taurate would be minimal given the lack of an amine vapour pressure for the amino-acid salt. However, there could be carry-over in the form of droplets and the condensate was also analysed for the presence of potassium ions. The operational target of most runs was to achieve 90% CO_2 -capture at different settings of the liquid flow rate for a given flue gas

flow rate. The average capture rate during the experiments was ~86%. The CO₂-content in the flue gas typically varied between 7.34 % and 11.2% for these runs as determined by the power plant operation.

The amount of steam required for regeneration of the 3M taurate/1.5M K₂CO₃ formulation is shown in Figure 41, in which the results are compared with 5M MEA. The data indicates that the taurate-carbonate solution is more difficult to regenerate than MEA and cyclic loadings will be lower. This is because of the lower concentration of amine in solution and the higher pH of the solution as a result of the carbonate addition, which, similar to the MEA-carbonate mixture will hamper the release of CO₂. While the pilot plant is not optimised for operation with the chosen absorption liquids, it appears that the taurate-carbonate solution is less attractive than MEA as a capture agent.

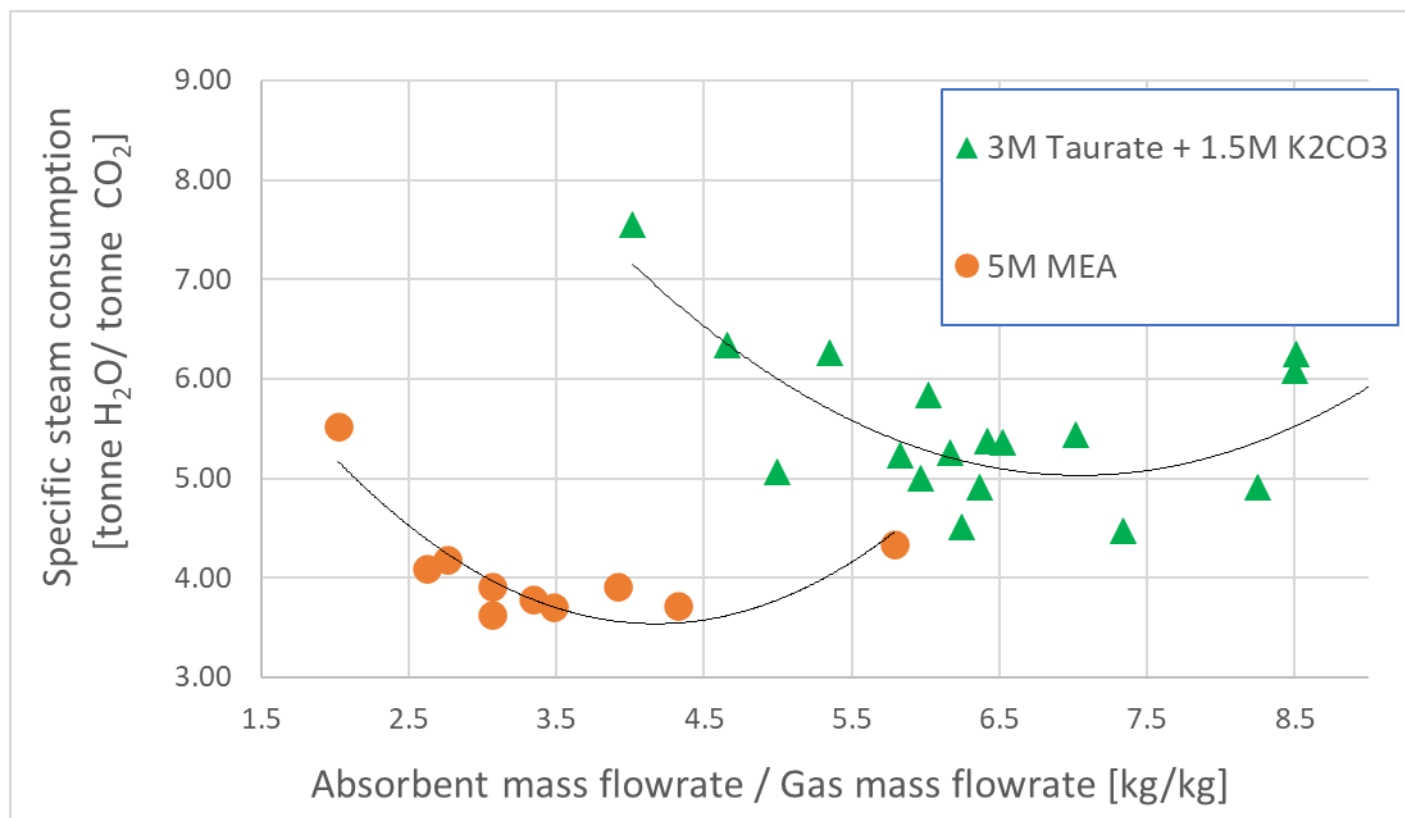


Figure 41 Specific steam flow into the reboiler at different values of the liquid/gas ratio in absorber for 5M MEA and 3M taurate + 1.5M K₂CO₃

During the experimental campaign samples were taken from the condenser after the desorber when the PCC pilot plant was in stable operation and sent to the CSIRO laboratory in Newcastle. Measurement of conductivity and pH was used to provide a coarse indicator for condensate quality with results shown in Figure 42. Most samples exhibited conductivity in the range 700 – 2300 μS/cm (somewhat higher than tap water: around 400 μS/cm) and neutral pH in the range 5.9 – 6.4. There were several outliers that exhibited higher conductivity (~ 10,000 μS/cm) and higher pH. We have not been able to correlate these with changes in the pilot plant operational conditions or the sampling methods used.

Further analysis was conducted using Ion Chromatography with a conductivity detector. The average potassium (K⁺) thus determined was quite low at 20 ppm (standard deviation=12 ppm). Other ions were determined at much lower concentration levels, i.e. sodium (Na⁺) and chloride (Cl⁻)

), at concentration levels of 0.66 ppm (standard deviation=0.53 ppm) and 1.54 ppm (standard deviation=1.43 ppm), respectively. As the potassium concentration was higher than for these other ions, we hypothesised that there was limited transfer of the absorption liquid in the form of droplets from the CO₂-desorber to the CO₂-product, which were subsequently collected in the condenser. However, as MEA was also detected in the condensate at an average level of 17 ppm (standard deviation=9 ppm), contamination with absorption liquid from previous runs with the MEA-carbonate mixtures was another source for the potassium found in the condensate. The analysis indicated levels of NH₄⁺ between 1,000 and 5,000 ppm in the condensate which was considered to be the main impurity. The most likely source of this product is the degradation of taurate in solution with the ammonia product captured in the condenser.

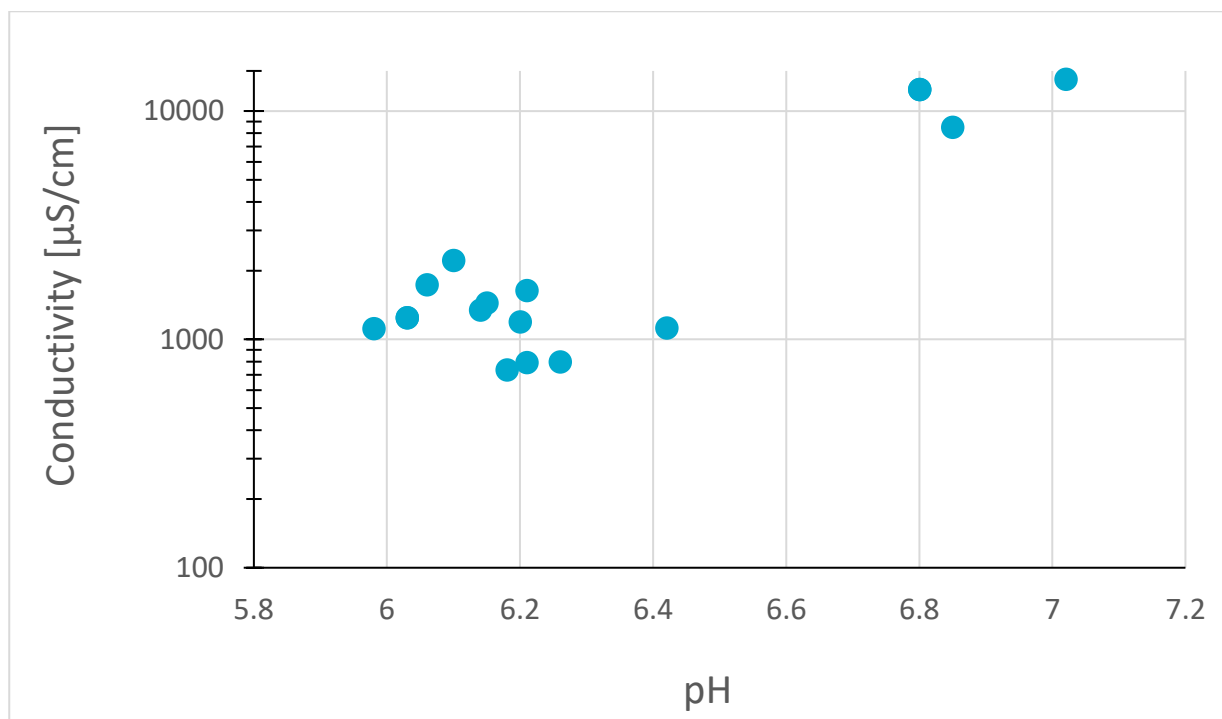


Figure 42 Conductivity versus pH of condensate samples from campaign with 3M taurate + 1.5M K₂CO₃

7 Vales Point Forward Osmosis rig experimental evaluation

7.1 Forward Osmosis rig design basis

The Forward Osmosis (FO) unit is at the core of the combined desalination-CO₂-capture process in which it replaces the trim cooler before the CO₂-absorber to transfer water from the cooling water to the amine solution. The FO rig design was based on a continuous operation in connection with the PCC pilot plant at Vales Point Power Station, transferring water from the saline water stream to the liquid absorbent solution. The design specification was based on the anticipated performance of a 5M MEA solution capturing 90% of the CO₂ present in the flue gas. This would result in a CO₂-production of 137.5 kg/h at the design flue gas conditions of the Vales Point PCC pilot plant. A key principle of the process concept is that water is produced at negligible additional energy requirement to the CO₂-capture process. Therefore, a water recovery of 0.4 kg/kg CO₂ was targeted from the desorber overhead, which represents an upper boundary for the amount of water produced per tonne of CO₂ captured. A higher amount would result in an increase of the reboiler duty of the capture process, which is to be avoided. At the PCC design conditions this meant that the FO rig would need to transfer 55 kg/h of water from the saline water to the MEA solution. The FO experimental results presented in

Table 7 indicated water fluxes in the range 7.3 – 10.4 L/m²h for MEA solutions (including solutions with addition of carbonate salts) in combination with a 3.5% NaCl solution. This enabled us to develop the design basis for the FO rig, in particular the required membrane area, applied to the PCC pilot plant at Vales Point (Table 13). The required membrane area was in the range 5.3 – 7.5 m².

Table 13 Design basis for Forward Osmosis rig at Vales Point.

CO ₂ capture	90%
Design flue gas flow (Vales Point PCC pilot plant)	1000 kg/h
Liquid flow rate based on Liquid to Gas ratio equal to 2.5	2500 kg/h
CO ₂ production based on 5M MEA at 0.25 mol/mol cyclic loading	137.5 kg/h
Water production (at 0.4 kg/kg CO ₂)	55 kg/h
Membrane area range	5.3 – 7.5 m ²

The design basis indicated the amount of water transferred is a relatively small, i.e. 2.2%, fraction of the absorption liquid flow. FO membrane modules are normally designed to operate at much higher recovery factors i.e. 30%, and would therefore have a significant excess water production. During the design phase a concern was raised that the water production may be hampered by the impurities from the targeted solvents accumulated through the standard PCC operation. Hence, two elements with a total membrane area of 14 m² were installed for each module. Two modules were installed in parallel for redundancy and the ability to cover a wide range of operating conditions. Each module could be individually operated with the use of built-in isolation valves within the skid. The two modules could also be operated in parallel.

7.2 Forward Osmosis rig integration with PCC pilot plant

Figure 43 shows the forward osmosis (FO) membrane module replacing the lean absorbent trim cooler in an amine-based CO₂-capture process. The absorbent flow from the lean/rich heat exchanger is redirected through the FO membrane module and then flows to the absorber. Any saline water such as seawater or other sources of surface water like lake water can be used to cool the liquid absorbent solution and as a result of the higher osmotic pressure of the absorbent solution water will transfer from the saline water source to the absorption liquid.

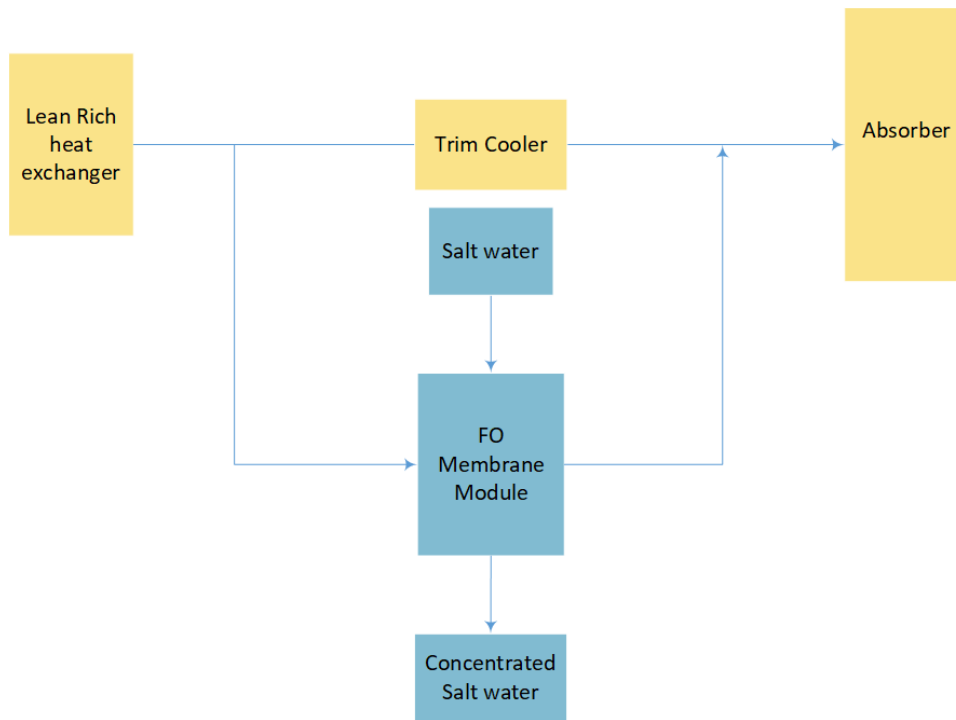
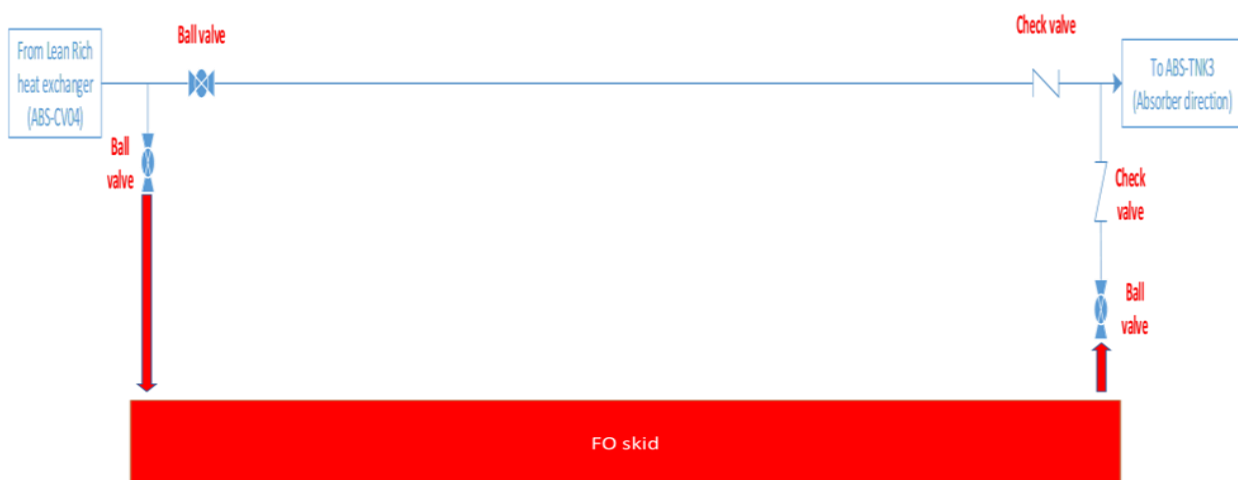


Figure 43 Basic Flow Diagram of Forward Osmosis Rig integration into the PCC pilot plant lay-out

The tie in line must reduce the disturbance to the existing process line. The FO unit cannot be exposed to high pressure conditions to avoid membrane damage, e.g. avoid installing membrane unit upstream of a large suction pump.

Based on the above assessment of process conditions and existing piping condition, the tie in points for both inlet and outlet of the module unit have been chosen at the downstream of control valve ABS-AV01 and ABS-TNK3. The two points are separated by a check valve to limit back flow of diluted solvent entering the FO unit. Figure 44 shows the tie in location for both inlet and outlet of the membrane module. It also depicts the modification of the existing line required to integrate the membrane system. The connection between the existing process line and the FO unit was joined by stainless steel braided line to allow for flexibility.



7.3 Forward Osmosis process design

The process flow diagram in Figure 45 contains the major equipment and indicates the main process flows. The Draw Solution (DS) represents the absorption liquid flow and the saline water flow is named the Feed Solution (FS), consistent with terminology use in FO processes. A pump was needed upstream of the FO membrane set to transfer the draw solution to the FO rig from the PCC pilot plant. A separate pump was installed at the saline water inlet end which carried the saline water solution to the membrane. A flow meter was included at both the inlet and outlet of the absorption liquid and the inlet saline stream which provided a basis for the water flux determination. As the membranes are vulnerable to large solid particles that may be present in the absorption liquid in the PCC pilot plant and saline liquids, separate 5 μm filters were included as part of the design.

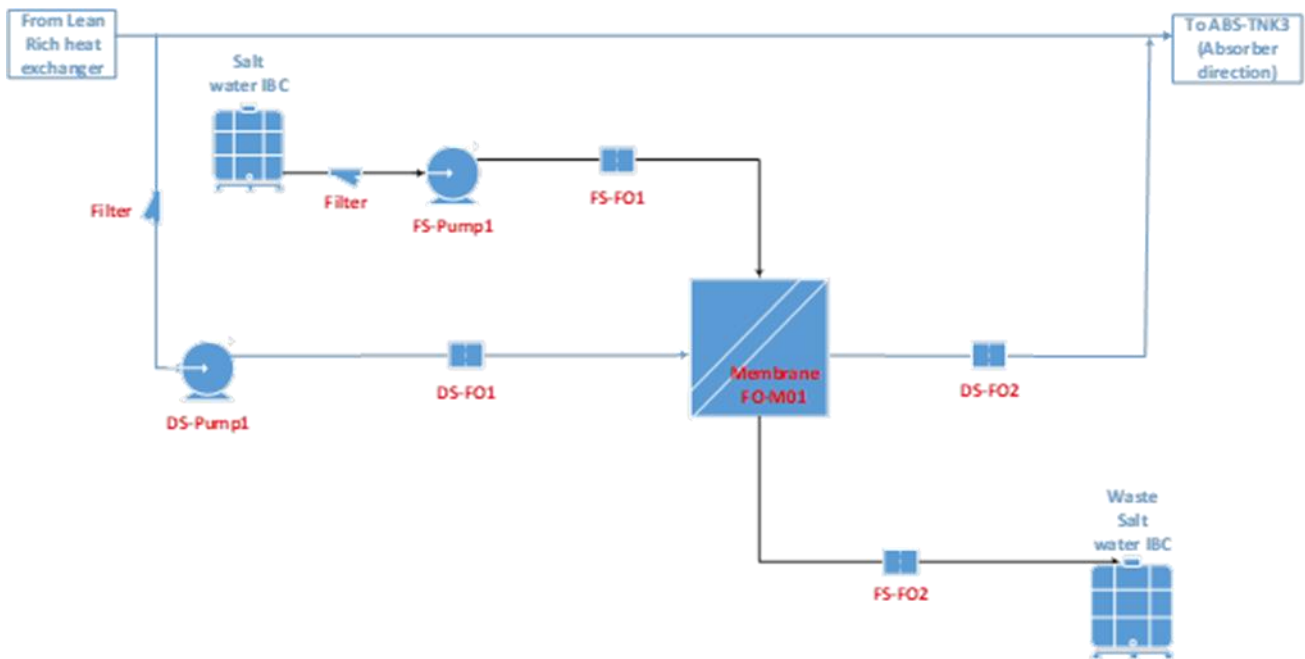


Figure 45 Process Flow Diagram of Forward Osmosis System

The piping and instrumentation diagram (P&ID) covers the piping and instrumentation of the FO module and the connecting PCC pilot plant (Figure 46). Various temperature and pressure sensors were included to report the process conditions, further aiding in the basis of membrane performance calculation. pH-Sensors and conductivity meters were installed at each stream to provide the timely feedback of the changes before and after the module. These instruments gave an early signal for potential membrane damage resulting in leakages or liquid transfer to the other side of the process line. Isolation valves have been detailed in the P&ID. The valves served to isolate major equipment such as filters, pumps and membrane for maintenance purpose.

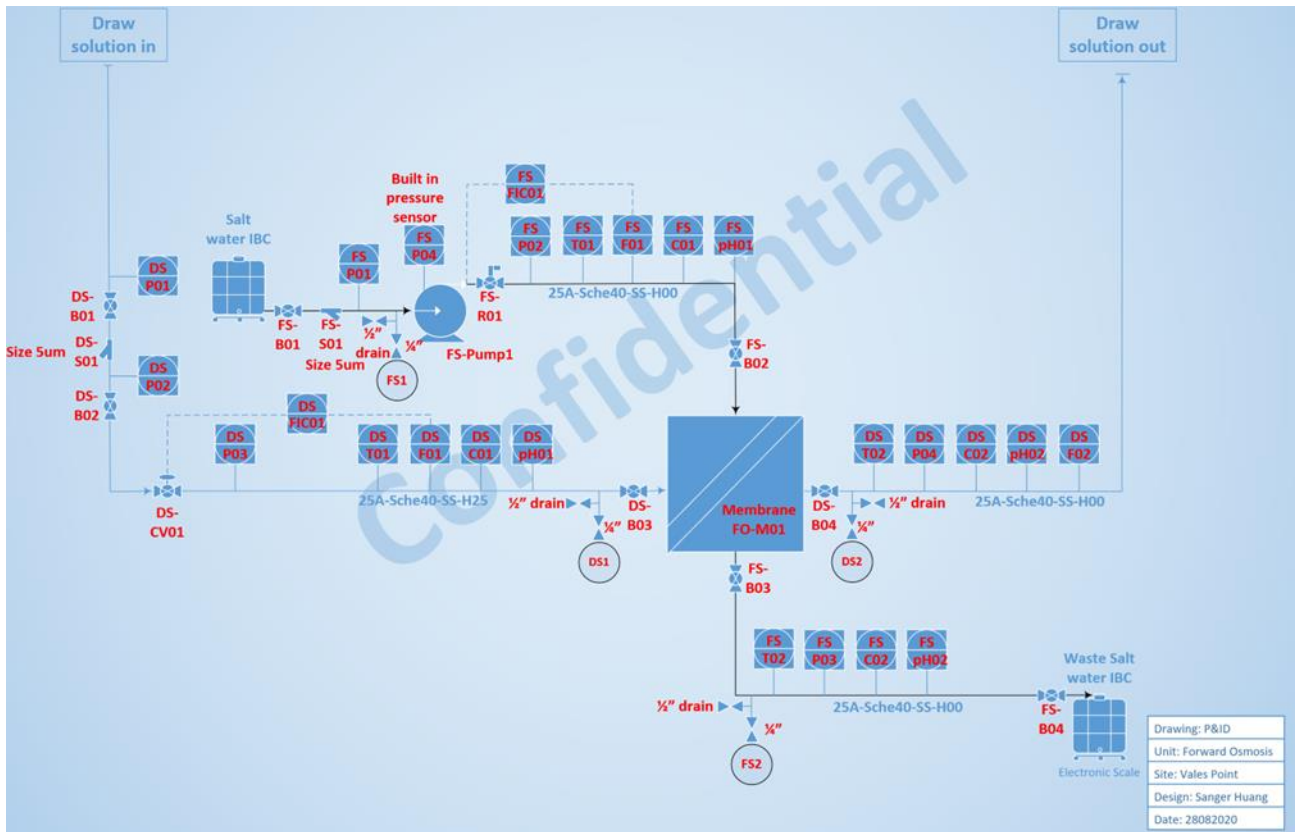


Figure 46 Piping and instrumentation diagram for Forward Osmosis unit

The detailed 3D lay-out (Figure 47) was developed from the piping workshop based on the P&ID, hydraulic and space consideration. The original design concept was to have all major equipment and pipe on the skid floor. The geometric of the layout was reconfigured to allow for better access for operation and maintenance purpose. As a result, most pipes were elevated by pipe supports to create the needed space.

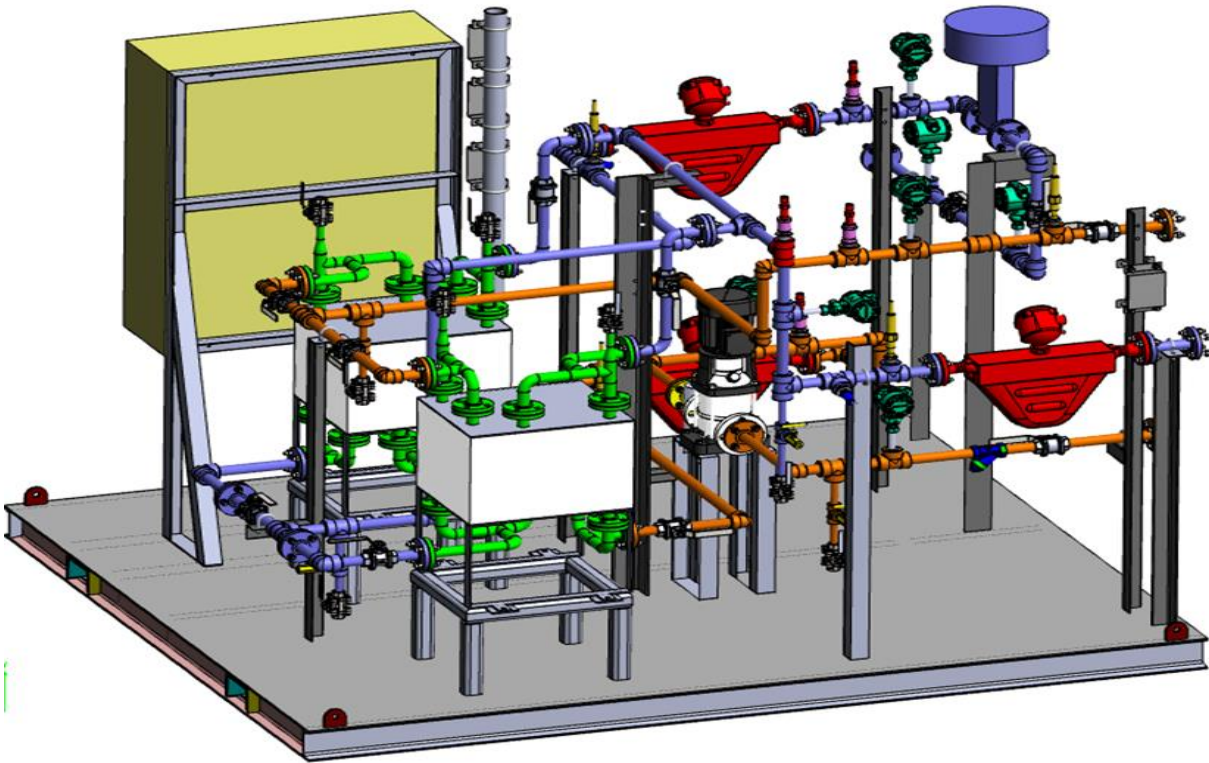


Figure 47 3D lay-out of Forward Osmosis unit

The Forward Osmosis unit was assembled on the CSIRO site in Pullenvale in Queensland and is shown in Figure 48, before being transported to the Vales Point site. Figure 49 shows the Forward Osmosis unit delivered on the Vales Point site.



Figure 48 Forward Osmosis rig with half of membrane modules installed (left side of picture)



Figure 49 Forward Osmosis unit delivered on site (with 2 membrane modules installed)

At the Vales Point site the Forward Osmosis unit was subsequently connected to the PCC pilot plant. This also involved the installation of a by-pass line to protect the membranes from high temperature (Figure 50), a heater to set the absorption liquid inlet temperature with steam from the boiler (Figure 51) and the installation of an additional sampling point at the outlet of the pumps.



Figure 51 : Heater to control solution temperature to the Forward Osmosis unit

The detailed FO unit specification can be found in Appendix B .

7.4 Overview results from Forward Osmosis experimental program

The experimental program consisted of two main components in which two different solutions were evaluated in accordance with the outcomes of the FO laboratory research (see section 4.6).

- Experiments using the MEA-carbonate mixture (Section 7.5)
- Experiments using a taurate-carbonate mixture (Section 7.6)

Both experimental campaigns were preceded by experiments using demineralised water and saline water to check the FO unit integrity before operation with the absorption liquids. Experiments also included thorough rinsing of the membranes at the end of each experimental day and filling the unit with a sodium bisulphite solution to prevent microbial growth inside the membrane module. The experiments were carried out in truncated campaigns because of limitations due to changing COVID19 restrictions throughout the campaigns.

The first campaign with MEA-carbonate solutions used a set of membrane modules that employed empty flow channels. Only a limited number of experiments could be carried out as MEA appeared to be present in large amounts on the saline water side. We suspected that the sealing used in the stacked membrane modules was not compatible with MEA. We hypothesised that reversible swelling of the seals caused them to become compromised as the FO membrane worked as expected with saline water solutions after the experiments with MEA-carbonate solutions. The FO membrane unit supplier provided new membrane modules that incorporated EPDM sealings which are compatible with MEA. The membrane modules also incorporated spacers in the flow channels for improved mass transfer. The experiments with taurate-carbonate solutions were subsequently conducted using the new membrane modules. While we did not see any evidence of swelling of sealings the membrane module pressure drop increased significantly, as a result of the presence of the spacers. As the membranes have limited tolerance for excess pressure these experiments had to be operated at reduced flow rate.

After the unexpected pass-over of MEA into the saline water, the risk of operating the FO unit continuously in conjunction with the PCC was considered unacceptably high. There was a risk that the amine solutions would be lost to the saline water at a high rate or vice versa that the saline water would enter the PCC plant circuit and render the PCC plant inoperable, and possibly damaged. So all experiments were conducted with a batch of absorption liquid and saline water, either in a once through mode or recirculation mode.

The main performance parameter, the water flux through the membranes, was determined in two ways:

- By measurement of flow difference between the draw solution (absorption solution under operational conditions) liquid flow going into the membrane module and out of the membrane. The feed (saline water under operational conditions) solution flow was only measured at the inlet and the exit flow derived from the mass balance.
- By weight measurement of the available metal tanks that were placed on load cells

Both methods provided equivalent results and were used interchangeably. As one of the load cells failed during the experimental campaigns, the flow measurement was used mostly. During the campaign with taurate-carbonate solution one of the flow meters failed and sample analysis via Ion Chromatography was relied upon to provide estimates for the water fluxes.

Other performance parameters covered the amine/amino-acid salt concentration in the saline water to determine the Specific Reverse Amine Flux (SRAF) and the salt concentration in the absorption liquid to determine the Specific Forward Salt Flux (SFSF). In support of the work at Vales Point a range of different analytical techniques were used and/or developed as shown in Table 14.

Table 14 Overview of analytical techniques used for determination of liquid concentrations

Component type	Liquids	
	Saline water	Amine/amino-acid solution
Salts	<ul style="list-style-type: none"> • Conductivity measurement for prepared solutions • Externally provided information for lake water 	<ul style="list-style-type: none"> • Ion Chromatography (IC) – for Na, K, Cl in MEA-carbonate solutions • Ion Chromatography (IC) – for Na, Cl in taurate-carbonate solutions (K not possible due overlapping peaks)
Amine/amino-acids	<ul style="list-style-type: none"> • Potentiometric titration for low concentration levels (> 400 ppm) • Fourier Transform Infrared (FTIR) spectroscopy for high concentration levels 	<ul style="list-style-type: none"> • Fourier Transform Infrared (FTIR) spectroscopy (only high concentrations)

The experimental program was carefully rolled out as indicated in Table 15. It involved a step-wise change in the feed and draw solution, progressing towards the ultimate aim of operating with the amine/amino-acid-carbonate solutions and saline water. The preceding experiments were necessary for hydraulic and sensor testing and familiarisation with the unit’s operation, providing checks for the system integrity and resolve any issues. Saline water was mostly made up from commercial pool salt (NaCl) with some experiments carried out with lake water.

Table 15 Scope of experimental program

Draw	Feed	Purpose
Water	Water	Hydraulic testing; sensor testing
Saline water	Water	Forward Osmosis operation familiarisation
Saline water	Saline water	Forward Osmosis operation familiarisation
MEA-carbonate solution Taurate-carbonate solution	Water	Process operation with simple feed
MEA-carbonate solution Taurate-carbonate solution	Saline water	Intended process operation

Section 7.5 reports on the results from the experimental campaign with the MEA-carbonate solutions whereas Section 7.6 reports on the results gathered from the campaign with taurate-carbonate solutions.

7.5 MEA-carbonate campaign results

Operation of the FO unit required a feedstock of 1000 L of saline water. The water was circulated for re-use over several experiments. This water was treated as process waste and disposed of through a hazardous waste contractor as it was expected to contain low levels of absorbent chemicals by the end of experiments. All the experiments were carried out in recirculation mode with liquids returned to the storage vessels.

Figure 52 shows the orientation of the membranes within the module. One side of the membrane has the active, separation layer as well as a baffle for liquid distribution. This side would normally face the draw solution line. The support layer of the membranes is facing the feed solution line. In our intended operation, the draw solution is the amine/amino-acid-carbonate solution and the feed solution will be the saline solution.

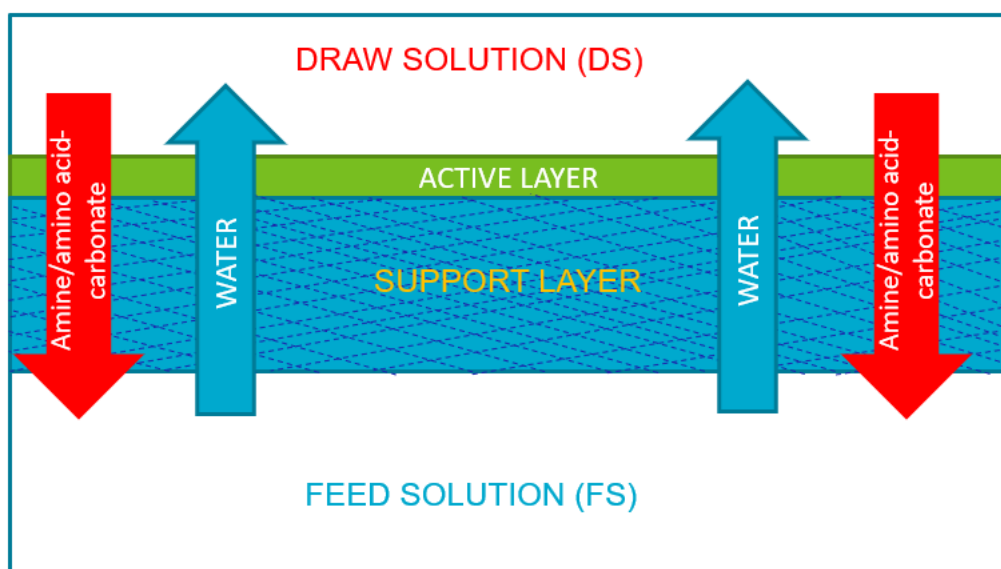


Figure 52: Orientation of the membrane module

7.5.1 Saline water experiment

A 30 wt.% aqueous MEA solution has an electrical conductivity of approximately 1 mS/cm. In this experiment, an NaCl solution with a similar electrical conductivity was prepared and run as the draw solution. On the other side of the module (i.e. in the feed solution line), an NaCl solution with the concentration close to that of seawater was run. The intent was to mimic the electrical conductivities of an absorption liquid and seawater using NaCl solutions and run them through the module before actually running the real-world fluids. The corresponding results of the experiment are shown in Figure 53.

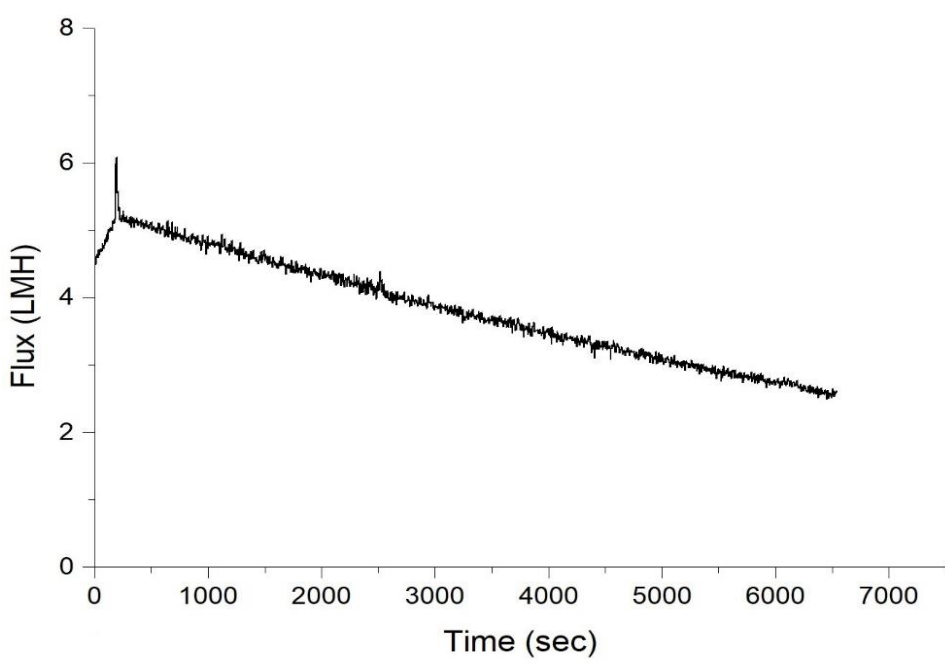


Figure 53 FO performance with NaCl solutions mimicking the conductivity of 30 wt.% aqueous MEA and seawater. FS flowrate = 40 lit/min; DS flowrate = 40 lit/min; NaCl concentration in the DS = 8.7 wt.%; NaCl concentration in the FS = 2.7 wt.%

Figure 53 shows the variation in water flux with time when two aqueous NaCl solutions, one mimicking 30 wt.% aqueous MEA, the other mimicking seawater, were run through the module. The experiment was run for at least one hour under steady state conditions. Overall, with the progression of the experiment, the FO flux gradually dropped from ca. 5.2 LMH to 3 LMH (LMH=L/m²h) within ca. 1.8 hours. As water was transferred from the feed side to the draw side, the draw solution became diluted and the feed solution more concentrated resulting in a reduced osmotic pressure difference and hence a lowered water flux.

7.5.2 MEA-carbonate – saline water

In this set of experiments, the MEA-carbonate solution from the PCC pilot plant was used as the draw solution and an NaCl solution, representing the seawater concentration, was used as the feed solution. Inlet flowrates for both the streams were 40 L/min each. The water flux through the FO membranes was determined by two complementary methods. In the first method, the mass change of the storage vessel of the NaCl solution was monitored to determine the water flux. In the second method, the flowrates obtained from the inline flow meters on the inlet and outlet of the draw solution were used to determine the water flux.

Figure 54 shows the results when a solution consisting of 3.5M MEA, 0.7M K₂CO₃ and 0.2 CO₂ loading was run on the draw side, whereas 3.5% NaCl solution was run on the feed side. Figure 54 shows the weight change in the NaCl solution's storage vessel over time. As this is the lower osmotic pressure liquid, the weight should decline over time with normal FO operation. The slope of the mass loss rate in the vessel represents the water flux through the membranes.

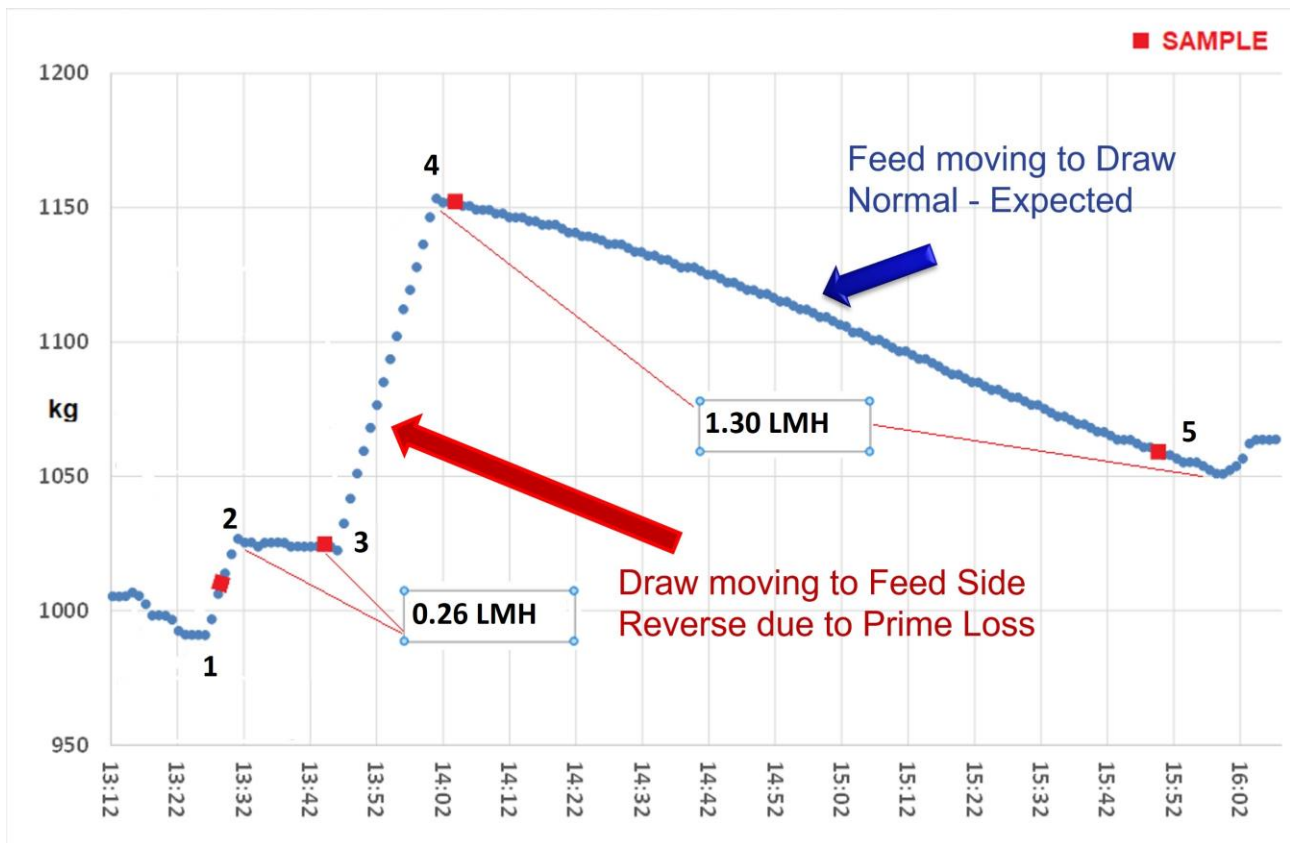


Figure 54: Variation in the mass of the saline feed solution tank with time

During the experiment, as can be seen from Figure 54, prior to Point 1, the liquid moved from the saline solution towards the draw solution line (herein called the ‘normal’ or ‘expected’ flux) during 13:15 – 13:27 Hrs. However, between Points 1 and 2 (as shown in Figure 54), the mass of the vessel increased, indicating that liquid moved from draw solution towards the saline solution (herein called the ‘reverse’ flux). This was triggered by sampling of liquid before the feed solution pump (FS1), which resulted in the pump losing prime and pressure being reversed. This resulted in the reverse or abnormal flux within the module. However, during Points 2 and 3, as the pump started delivering the flow, a ‘normal’ flux was observed from FS line to the DS line. Nevertheless, at around 13:45, when another attempt was made to collect a liquid sample, the feed solution pump lost prime again, resulting in reverse flux between Points 3 and 4. After Point 4, we see ‘normal’ flux of around 0.9 LMH (also confirmed from results in Figure 55) between Points 4 and 5.

Figure 55 provides information on the pH, conductivity of the draw solutions as well as the water flux as determined by the difference between the outlet and inlet flowmeters. A positive flux value would indicate movement of water from lower osmotic pressure liquid (salt solution) towards the higher osmotic pressure liquid (the CO₂ loaded absorption liquid consisting of MEA and K₂CO₃), which is what was expected.

During periods of “normal” operation the pH and conductivity are expected to decrease due to the dilution with water of the draw solutions, which is what indeed occurred. During periods of reverse flux (Points 1 to 2, and Points 3 to 4) both pH and conductivity do not vary much which is consistent with draw solution not being diluted but lost to the feed solution.

It is worth mentioning here that the maximum flux observed in Figure 55 is 1.47 LMH, whereas the minimum is 0.3 LMH, both of which are represented by horizontal dashed lines. These values are quite close to the flux values seen in Figure 54 (values of 0.26 and 1.30 LMH) during normal FO operation. The difference in values is due to the results in Figure 54 being averaged and based upon the slope of the corresponding section of the graph, whereas the results in Figure 55 are obtained directly from the difference of flowrates obtained from the flowmeters.

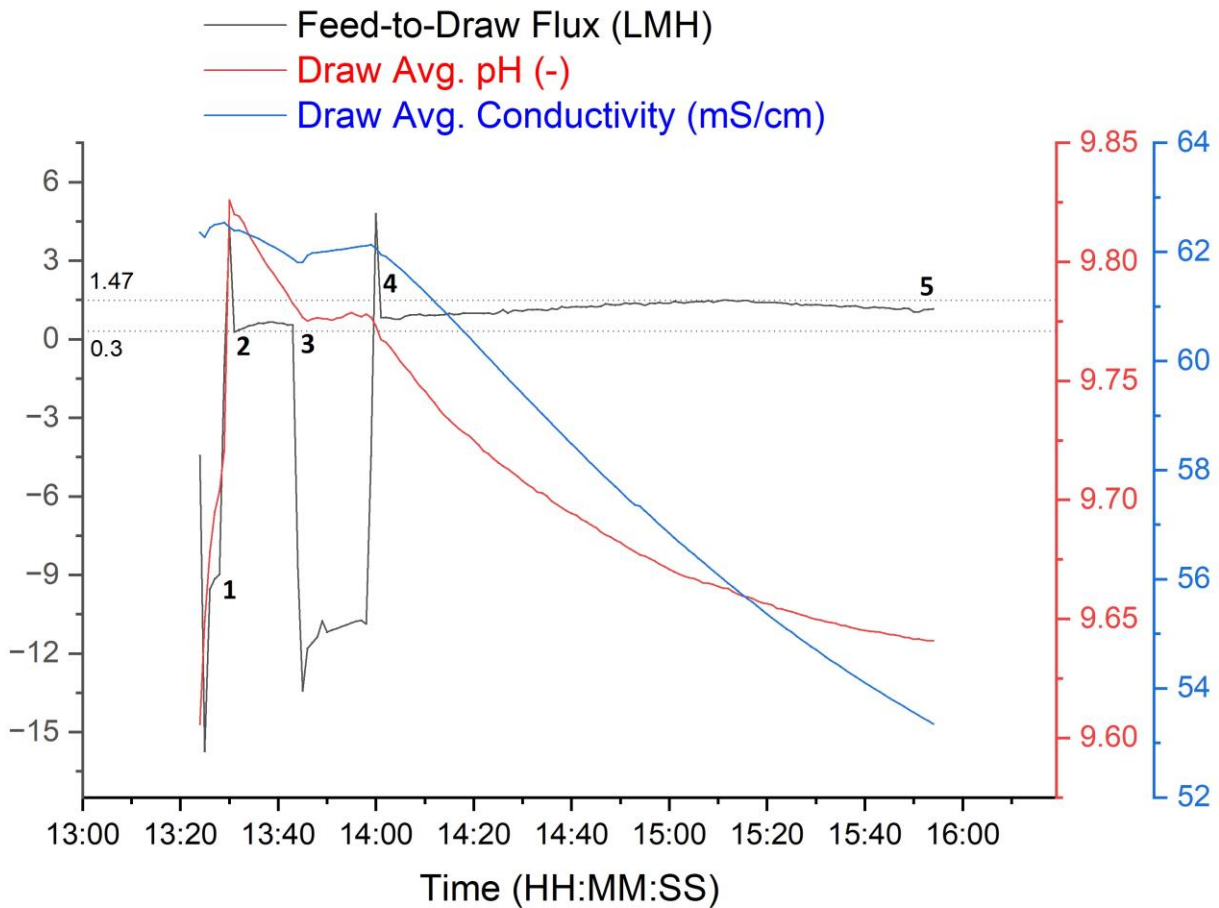


Figure 55: Variation in Flux, Average DS line conductivity and pH values with time

In order to address the loss of prime during liquid sampling, the sample collection point (FS1) was moved downstream of the feed solution pump. After this change, another experiment was performed to test the functioning of the membrane with the MEA-carbonate solution.

In the repeat experiment, the MEA-carbonate solution was used as the draw solution, whereas a 3.9 wt.% aqueous NaCl solution (simulating the seawater concentration) was used as the feed solution. The flowrates for the DS and FS lines were 40 L/min each.

Figure 57: Variation in Flux and the conductivities of draw and feed lines

and

Figure 57 show the results for the repeat experiment, with extra details about various symbols given within

Figure 57: Variation in Flux and the conductivities of draw and feed lines

. Similar to Figure 54, in

Figure 57: Variation in Flux and the conductivities of draw and feed lines

, any increase in the mass of the vessel is regarded as 'reverse' or 'abnormal' flux, whereas any decrease in the mass of the vessel is called as the 'normal' flux. The result showed that, when the experiment started, a 'reverse' flux of ca. 1 – 2 LMH was observed, indicating that MEA-carbonate solution was moving towards the salt solution side (high osmotic pressure liquid moving into lower osmotic pressure liquid across membrane). The trend continued for more than an hour between 12:14 Hrs and 13:55 Hrs. The table in the inset of

Figure 57: Variation in Flux and the conductivities of draw and feed lines

shows the salt, MEA and potassium carbonate fluxes, as calculated from their mass balances. The table also shows their direction. It was speculated that the 'reverse' flux appeared because MEA reacted with the sealing materials within the module, causing the module to lose hydraulic integrity.

Having concluded that the membrane module was struggling to function appropriately with the MEA-carbonate solution, it was decided to test the effect of back-pressurisation on the direction of the flux. At around 13:55 Hrs during the experiment, the feed solution was back-pressurised by only 2 kPa. The back-pressurization was able to reverse the direction of the flow of flux, and a 'normal' forward osmosis flux of ca. 0.4 – 0.5 LMH was observed, i.e. that water was flowing from the feed solution towards the draw solution. When this back-pressure was removed at around 15:30 Hrs, the flux reversed its direction again, and a reverse flux of ca. 3 LMH was observed through the module. This also supported the hypothesis that some part of the membrane module exhibited leaks between the draw and feed solutions, which might have been induced by the MEA-carbonate solution.

The membrane supplier suggested to supply a set of new membrane modules with different sealing materials (EPDM instead of Viton) that was known from previous experience to be compatible with MEA. The new set also included spacers in the membrane channels that were considered to be helpful for the promotion of mass transfer. Given COVID-19 lock-down project delays, these new membrane modules were used for the experiments with taurate-carbonate solutions rather than for experiments with MEA-carbonate solutions. Further experimentation with MEA-carbonate would also require the purchase of a new solution inventory as a significant part of the solution inventory was lost to the saline solution.

Following the COVID-19 lock-downs, an integrity check of the original set of membrane modules using saline water solutions was carried out at the Vales Point pilot plant. The check, although not extensive, indicated that the membrane unit exhibited normal Forward Osmosis operation and that they were not irreversibly damaged (see

Figure 57). The leakage found in MEA-carbonate operation might well be a swelling phenomenon caused by MEA that is reversible, i.e. in the absence of the amine it does not occur.

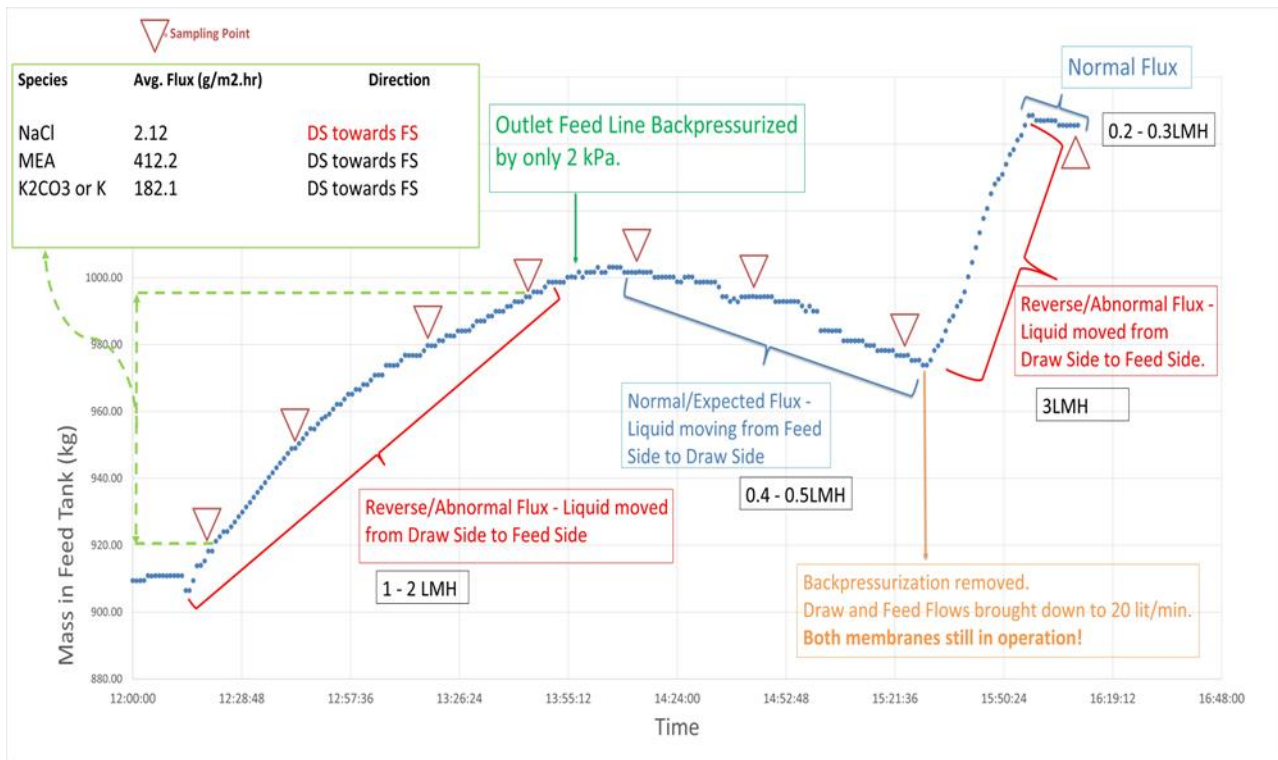


Figure 56: Variation in the mass of the salt solution with time

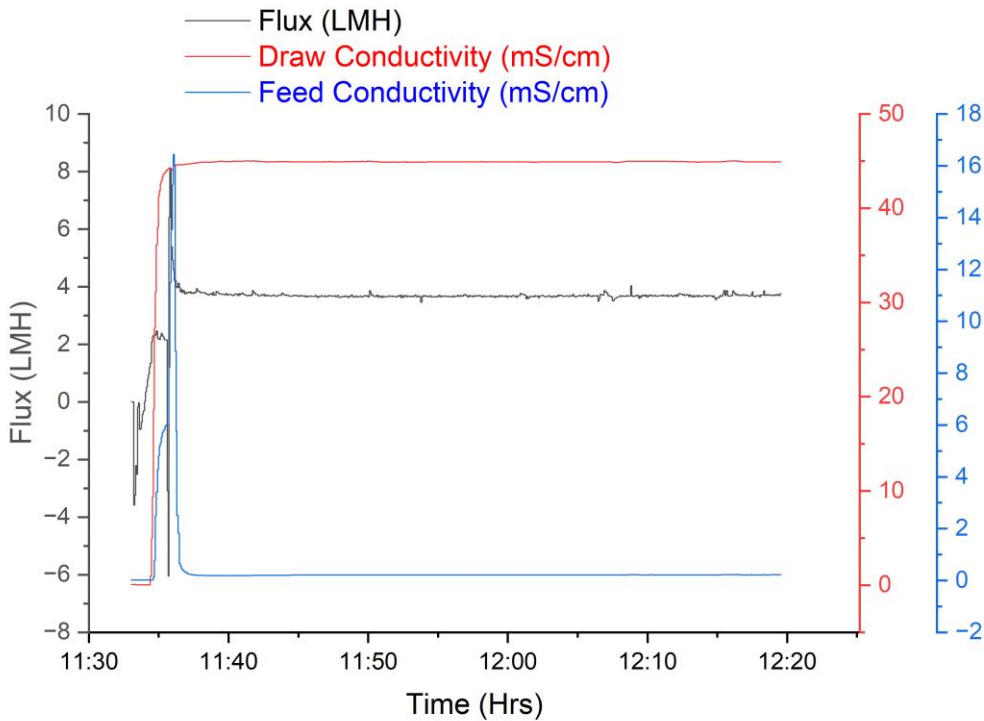


Figure 57: Variation in Flux and the conductivities of draw and feed lines

7.6 Taurate-Carbonate campaign results

7.6.1 Saline water experiments

The experiments using saline water (and de-ionised water) in draw and feed were intended as preparation for the experiments with taurate-carbonate solutions. They were carried out to characterise the FO membrane unit and to further familiarise the team with its operation. The 14 experiments reported here covered a wide range of saline concentrations as draw and feed solutions, including some experiments at elevated temperature.

The experimental conditions are described in Table 16, with the following overview:

- Experiments 1-6 described conditions where saline water with a conductivity equivalent to that of seawater was used as the draw solution and de-ionised water as the feed solution with a variation in the draw-feed flow rate ratio. The conductivity varied somewhat depending on any residual material left in the unit after rinsing between experiments. The experiments were carried out at ambient temperature.
- Experiments 7-8 described conditions where concentrated saline water with high conductivity was used as the draw solution and saline water with a conductivity equivalent to that of seawater as the feed solution with a variation in the draw-feed flow rate ratio. The experiments were carried out at ambient temperature.
- Experiments 9-10 described conditions where concentrated saline water with high conductivity was used as the draw solution and saline water with a conductivity equivalent to that of seawater as the feed solution with a variation in the draw-feed flow rate ratio. The experiments were carried out at elevated temperature.
- Experiments 11-13 described conditions where draw and feed solution had similar conductivity. The experiments were carried out elevated temperature and ambient temperature, aiming at conditions where the water flux would be negligible, mimicking heat transfer only operation.
- Experiment 14 was aimed at repeating the conditions of experiment 1-6 but at elevated temperature.

Throughout the campaign normal Forward Osmosis operation was observed, i.e. the flow through the membranes was always from the low osmotic pressure (low concentration) to the high osmotic pressure (high concentration) side. The salt balance was slightly over 100% during the experiments, as shown in Table 16, which also lists the water flux data. Water recovery ranged from 39% and 67% which was higher than intended, as a result of the low flow rates. The choice of flow rate was determined by the necessity to maintain the pressured drop below 20 kPa. The higher pressure drop was the result of the use of spacers in the membrane channels.

The water flux will be a function of the osmotic pressure difference between draw and feed solutions. The osmotic pressure will increase with increasing concentration. The water flux data are presented in Figure 58 at different values of the differential concentration difference between the draw solution and feed solution, which is a proxy for the osmotic pressure difference. The concentration difference between draw and feed is the arithmetic average of inlet and outlet concentration difference.

The results from experiment 1-6 indicate that an increase in concentration difference between draw and feed solutions results in a higher water flux. However, experiment 14 resulted in a significantly higher water flux at a similar concentration difference.

The comparison between experiments 7-8 (at ambient temperature) and 9-10 (elevated temperature) and the comparison between experiment 14 and experiments 1-6 indicates that water flux will increase with temperature.

The experiments at elevated temperature showed the temperatures at the draw and feed outlet were quite close. This was caused by the high water recovery which meant that significant amounts of the cold feed solution were simply, but selectively mixed through the membrane, leading to significant equilibration of temperature. In realistic applications the water recovery will be much lower and hence this effect will not occur. Therefore experiments 11-13 were carried out to understand the heat transfer in case there was minimum transfer of liquid through the membranes. Experiments 11 and 12 indeed indicate a noticeable temperature difference between draw and feed outlets. Surprisingly the feed outlet temperature was higher than the draw outlet. If the flow patterns as truly co-current this would not be possible. Further knowledge on the internal hydraulic design would be necessary to fully understand this. As this is covered by the intellectual property of the supplier, we have not investigated this further.

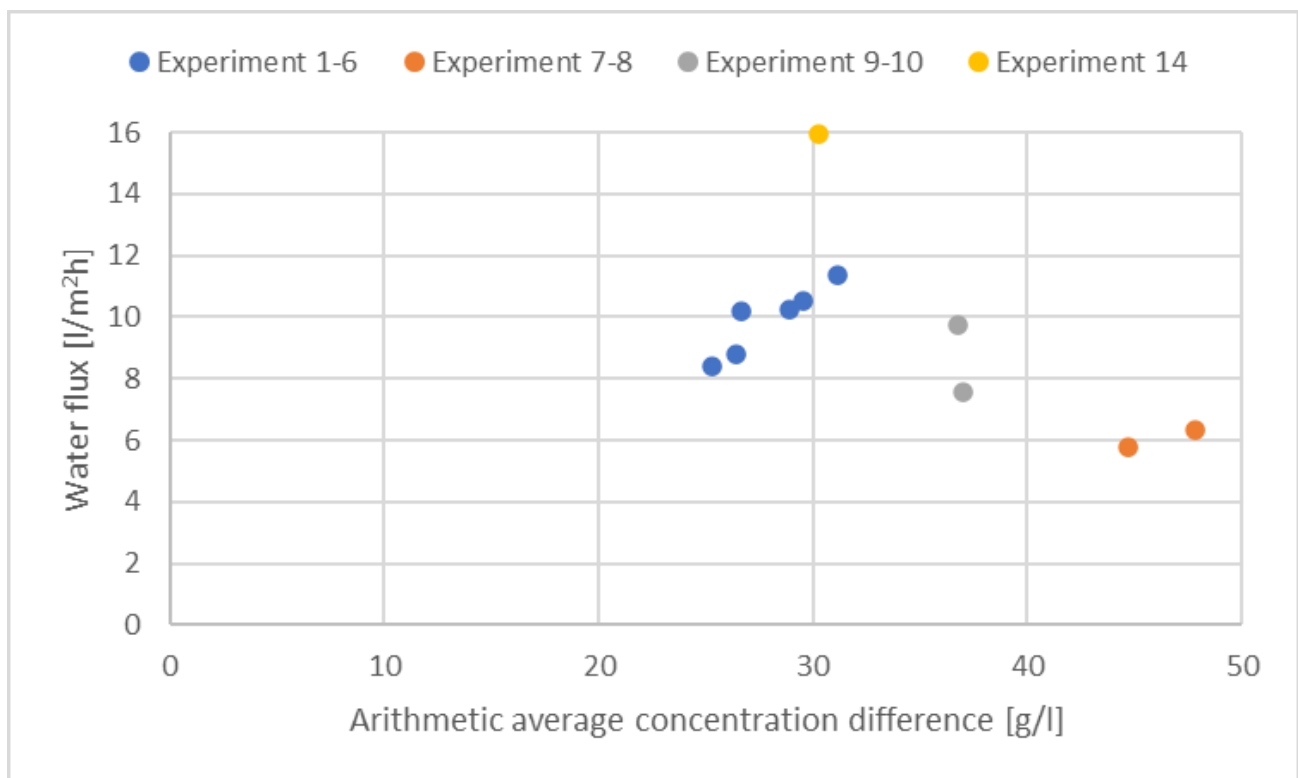


Figure 58 Experimentally determined water flux at average differential NaCl concentration levels

Table 16 Overview of Forward Osmosis experiments using saline solution as draw solution and de-ionised/saline water as the feed solution

No.	Date	Draw solution (D)	Feed solution (F)	Water flux [l/m ² h]	Water recovery [%]	Salt balance Out/in [%]	Comment
1	26 July 2022	NaCl-solution Flow _{in} = 10.86 l/min: Flow _{out} = 12.91 l/min σ _{in} = 52807 μS/cm ; σ _{out} = 45604 μS/cm T _{in} = 13.7 °C; T _{out} = 13.9 °C	DI-water Flow _{in} = 4.73 l/min: Flow _{out} = 2.68 l/min σ _{in} = 5513 μS/cm ; σ _{out} = 9191 μS/cm T _{in} = 13.9 °C; T _{out} = 14.1 °C	8.8	43	102	Seawater-like conductivity on draw side; DI on feed side; ambient temperature;
2	29 July 2022	NaCl-solution Flow _{in} = 11.13 l/min: Flow _{out} = 13.78 l/min σ _{in} = 54568 μS/cm ; σ _{out} = 45591 μS/cm T _{in} = 13.6 °C; T _{out} = 13.9 °C	DI-water Flow _{in} = 3.93 l/min: Flow _{out} = 1.28 l/min σ _{in} = 17 μS/cm ; σ _{out} = 1370 μS/cm T _{in} = 14.6 °C; T _{out} = 14.0 °C	11.4	67	104	Seawater-like conductivity on draw side; DI on feed side; ambient temperature;
3	1 August 2022	NaCl-solution Flow _{in} = 4.07 l/min: Flow _{out} = 6.45 l/min σ _{in} = 51454 μS/cm ; σ _{out} = 34005 μS/cm T _{in} = 14.8 °C; T _{out} = 15.3 °C	DI-water Flow _{in} = 4.23 l/min: Flow _{out} = 1.85 l/min σ _{in} = 18 μS/cm ; σ _{out} = 842 μS/cm T _{in} = 15.2 °C; T _{out} = 15.7 °C	10.2	56	105	Seawater-like conductivity on draw side; DI on feed side; ambient temperature;
4	2 August 2022	NaCl-solution Flow _{in} = 1.96 l/min: Flow _{out} = 3.93 l/min σ _{in} = 52809 μS/cm ; σ _{out} = 28031 μS/cm	DI-water Flow _{in} = 4.06 l/min: Flow _{out} = 2.09 l/min σ _{in} = 43 μS/cm ; σ _{out} = 638 μS/cm	8.4	48	107	Seawater-like conductivity on draw side; DI on

		$T_{in} = 13.3\text{ }^{\circ}\text{C}; T_{out} = 12.6\text{ }^{\circ}\text{C}$	$T_{in} = 12.1\text{ }^{\circ}\text{C}; T_{out} = 12.7\text{ }^{\circ}\text{C}$				feed side; ambient temperature;
5	2 August 2022	NaCl-solution Flow _{in} = 8.16 l/min: Flow _{out} = 10.61 l/min $\sigma_{in} = 52789\text{ }\mu\text{S/cm}$; $\sigma_{out} = 42104\text{ }\mu\text{S/cm}$ $T_{in} = 13.5\text{ }^{\circ}\text{C}; T_{out} = 13.2\text{ }^{\circ}\text{C}$	DI-water Flow _{in} = 4.04 l/min: Flow _{out} = 1.59 l/min $\sigma_{in} = 43\text{ }\mu\text{S/cm}$; $\sigma_{out} = 1046\text{ }\mu\text{S/cm}$ $T_{in} = 12.2\text{ }^{\circ}\text{C}; T_{out} = 13.3\text{ }^{\circ}\text{C}$	10.5	61	104	Seawater-like conductivity on draw side; DI on feed side; ambient temperature;
6	2 August 2022	NaCl-solution Flow _{in} = 6.45 l/min: Flow _{out} = 8.85 l/min $\sigma_{in} = 52725\text{ }\mu\text{S/cm}$; $\sigma_{out} = 39987\text{ }\mu\text{S/cm}$ $T_{in} = 13.7\text{ }^{\circ}\text{C}; T_{out} = 13.3\text{ }^{\circ}\text{C}$	DI-water Flow _{in} = 4.23 l/min: Flow _{out} = 1.84 l/min $\sigma_{in} = 43\text{ }\mu\text{S/cm}$; $\sigma_{out} = 884\text{ }\mu\text{S/cm}$ $T_{in} = 12.3\text{ }^{\circ}\text{C}; T_{out} = 13.5\text{ }^{\circ}\text{C}$	10.3	57	104	Seawater-like conductivity; DI on feed side; ambient temperature;
7	3 August 2022	NaCl-solution Flow _{in} = 8.93 l/min: Flow _{out} = 10.41 l/min $\sigma_{in} = 153724\text{ }\mu\text{S/cm}$; $\sigma_{out} = 137743\text{ }\mu\text{S/cm}$ $T_{in} = 13.3\text{ }^{\circ}\text{C}; T_{out} = 13.5\text{ }^{\circ}\text{C}$	NaCl-solution Flow _{in} = 3.31 l/min: Flow _{out} = 1.83 l/min $\sigma_{in} = 50673\text{ }\mu\text{S/cm}$; $\sigma_{out} = 88986\text{ }\mu\text{S/cm}$ $T_{in} = 13.4\text{ }^{\circ}\text{C}; T_{out} = 13.6\text{ }^{\circ}\text{C}$	6.3	45	104	Concentrated saline water conductivity on draw side; seawater-like conductivity DI on feed side; ambient temperature;
8	3 August 2022	NaCl-solution Flow _{in} = 3.67 l/min: Flow _{out} = 5.01 l/min $\sigma_{in} = 153398\text{ }\mu\text{S/cm}$; $\sigma_{out} = 120542\text{ }\mu\text{S/cm}$ $T_{in} = 13.6\text{ }^{\circ}\text{C}; T_{out} = 13.6\text{ }^{\circ}\text{C}$	NaCl-solution Flow _{in} = 3.56 l/min: Flow _{out} = 2.22 l/min $\sigma_{in} = 50632\text{ }\mu\text{S/cm}$; $\sigma_{out} = 81481\text{ }\mu\text{S/cm}$ $T_{in} = 13.5\text{ }^{\circ}\text{C}; T_{out} = 13.8\text{ }^{\circ}\text{C}$	5.8	38	106	Concentrated saline water conductivity on draw side; seawater-like conductivity DI on

							feed side; ambient temperature
9	8 August 2022	NaCl-solution Flow _{in} = 4.34 l/min: Flow _{out} = 6.10 l/min σ _{in} = 142675 μS/cm ; σ _{out} = 107580 μS/cm T _{in} = 44.1 °C; T _{out} = 27.4 °C	NaCl-solution Flow _{in} = 4.50 l/min: Flow _{out} = 2.73 l/min σ _{in} = 50274 μS/cm ; σ _{out} = 82616 μS/cm T _{in} = 14.2 °C; T _{out} = 27.6 °C	7.6	39	104	Concentrated saline water conductivity on draw side; seawater-like conductivity DI on feed side; elevated temperature
10	8 August 2022	NaCl-solution Flow _{in} = 12.85 l/min: Flow _{out} = 15.11 l/min σ _{in} = 142206 μS/cm ; σ _{out} = 125413 μS/cm T _{in} = 44.5 °C; T _{out} = 36.0 °C	NaCl-solution Flow _{in} = 4.49 l/min: Flow _{out} = 2.22 l/min σ _{in} = 50282 μS/cm ; σ _{out} = 100729 μS/cm T _{in} = 14.2 °C; T _{out} = 33.8 °C	9.7	51	103	Concentrated saline water conductivity on draw side; seawater-like conductivity DI on feed side; elevated temperature
11	11 August 2022	NaCl-solution Flow _{in} = 2.66 l/min: Flow _{out} = 2.61 l/min σ _{in} = 17 μS/cm ; σ _{out} = 18 μS/cm T _{in} = 42.9 °C; T _{out} = 24.2 °C	NaCl-solution Flow _{in} = 2.64 l/min: Flow _{out} = 2.69 l/min σ _{in} = 9 μS/cm ; σ _{out} = 10 μS/cm T _{in} = 13.9 °C; T _{out} = 27.3 °C	-0.2	ND	106	Feed and draw at equivalent conductivity; elevated temperature
12	15 August 2022	NaCl-solution Flow _{in} = 3.00 l/min: Flow _{out} = 3.01 l/min	NaCl-solution Flow _{in} = 2.99 l/min: Flow _{out} = 2.98 l/min	0.1	ND	101	Feed and draw at equivalent conductivity;

		$\sigma_{in} = 52098 \mu\text{S/cm}$; $\sigma_{out} = 52271 \mu\text{S/cm}$ $T_{in} = 42.4 \text{ }^\circ\text{C}$; $T_{out} = 26.7 \text{ }^\circ\text{C}$	$\sigma_{in} = 52154 \mu\text{S/cm}$; $\sigma_{out} = 53170 \mu\text{S/cm}$ $T_{in} = 17.4 \text{ }^\circ\text{C}$; $T_{out} = 29.1 \text{ }^\circ\text{C}$				elevated temperature
13	16 August 2022	NaCl-solution $\text{Flow}_{in} = 10.49 \text{ l/min}$: $\text{Flow}_{out} = 10.43 \text{ l/min}$ $\sigma_{in} = 51385 \mu\text{S/cm}$; $\sigma_{out} = 52189 \mu\text{S/cm}$ $T_{in} = 18.6 \text{ }^\circ\text{C}$; $T_{out} = 18.4 \text{ }^\circ\text{C}$	NaCl-solution $\text{Flow}_{in} = 3.38 \text{ l/min}$: $\text{Flow}_{out} = 3.43 \text{ l/min}$ $\sigma_{in} = 52168 \mu\text{S/cm}$; $\sigma_{out} = 52987 \mu\text{S/cm}$ $T_{in} = 18.4 \text{ }^\circ\text{C}$; $T_{out} = 18.5 \text{ }^\circ\text{C}$	-0.2	ND	102	Feed and draw at equivalent conductivity; ambient temperature
14	17 August 2022	NaCl-solution $\text{Flow}_{in} = 5.39 \text{ l/min}$: $\text{Flow}_{out} = 9.11 \text{ l/min}$ $\sigma_{in} = 60522 \mu\text{S/cm}$; $\sigma_{out} = 37289 \mu\text{S/cm}$ $T_{in} = 43.3 \text{ }^\circ\text{C}$; $T_{out} = 27.8 \text{ }^\circ\text{C}$	DI-water $\text{Flow}_{in} = 5.39 \text{ l/min}$: $\text{Flow}_{out} = 1.67 \text{ l/min}$ $\sigma_{in} = 31 \mu\text{S/cm}$; $\sigma_{out} = 1763 \mu\text{S/cm}$ $T_{in} = 14.2 \text{ }^\circ\text{C}$; $T_{out} = 27.5 \text{ }^\circ\text{C}$	15.9	69	105	Seawater-like conductivity on draw side; DI on feed side; ambient temperature

7.6.2 Taurate-carbonate experiments

A total of 11 experiments (see complete list in Table 17) were carried out using the taurate-carbonate solutions; four with deionised (DI) water; six with a saline (NaCl) solution and one with power plant cooling water extracted from Lake Macquarie as the feed solutions representing cooling water. In four experiments fresh taurate-carbonate solution was used; in all other experiments the solution was taken from the PCC plant inventory that was essentially a lean or rich solution that contained CO₂ and most likely some degradation products as well. Apart from the first experiment, eight experiments were carried out at approximately equivalent draw and feed flow rate. For two experiments the draw solution flow rate was twice that of the feed flow.

Throughout the campaign there was no evidence of abnormal operation such as the flow of draw solution to the feed solution through compromised seals, experienced in the campaign with MEA-carbonate solutions. Normal Forward Osmosis operation was observed throughout the campaign.

Liquid flow rates through the membrane modules were, however, significantly lower compared to the previous campaign. The choice of the flow rates was determined by the pressure drop through the membrane not exceeding a value of 20 kPa to prevent membrane damage. This does mean that the flow meters were operated at below 5% of their full range, reducing the accuracy of the flow rate measurement. As a consequence of the low flow rates, the water recovery from the feed solutions was high, i.e., between 47% and 58% for those experiments where it was reported, with a high recovery of 90% for the first experiment. For the envisaged combined CO₂-capture and desalination process the water recovery will be less than 5%. The changes in concentrations encountered during the experiments are much larger than would be the case in an optimal process. As a consequence, the water fluxes will be lower and salt fluxes higher.

The flow meter on the outlet of the draw solution provided erroneous results during the course of the campaign and could not be relied upon to calculate the water flux for all but experiment 1. In case of the saline feed solution experiments (experiment 6-11), we therefore relied on the chloride balance between inlet/outlet feed flow and draw flow and the known inlet flow rates to calculate the water flux through the membranes. The chloride concentrations were determined by ion chromatography using the collected samples after the campaign was finished. It appeared that the conductivity changes in the feed flow could also be used to calculate the NaCl concentration change and hence derive flow rate changes. However, both methods could not be used for the experiments with deionised water. We were not able to use the taurate concentration changes in the draw solution as the basis for an estimate of the water flux as they resulted in flow rates that were infeasible, i.e. higher than the combined inlet flows. Therefore, we provided an upper estimate for the water flux on the assumption that all of the feed solution was transferred to the draw solution.

The taurate balance, defined as taurate mass flow divided by taurate mass outflow out was variable ranging from 61% and 97%, i.e. always below 100%, except for experiment 1. The limited accuracy of the flow rate measurements at the low end was the most likely reason for this. Also, interference from degradation products in the sample analysis could not be ruled out.

Table 17 Overview of Forward Osmosis experiments using taurate-carbonate mixtures as draw solution and de-ionised/saline water as the feed solution

No.	Date	Draw (D) solution	Feed (F) solution representing cooling water	Draw-Feed flow ratio	Comment on experimental conditions
1	1 September 2022	Fresh unloaded solution	DI water	0.8	Only experiment with three flow meters operating
2	2 September 2022	CO ₂ -loaded solution – lean	DI water	1.0	Loading: 0.23 M/M; Liquid mass balance incomplete;
3	2 September 2022	CO ₂ -loaded solution - rich	DI water	1.0	Loading: 0.35 M/M; Liquid mass balance incomplete;
4	5 September 2022	CO ₂ -loaded solution - lean	DI water	1.0	Loading: 0.23 M/M; Liquid mass balance incomplete; Warm draw solution
5	6 September 2022	CO ₂ -loaded solution – lean	3.5% NaCl solution	2.0	Loading: 0.35 M/M; Warm draw solution
6	6 September 2022	Fresh unloaded solution	3.5% NaCl solution	1.0	Warm draw solution
7	6 September 2022	Fresh unloaded solution	3.5% NaCl solution	2.0	Ambient temperature
8	6 September 2022	Fresh unloaded solution	3.5% NaCl solution	1.0	Ambient temperature

9	7 September 2022	CO ₂ -loaded solution - rich	3.5% NaCl solution	1.0	Loading: 0.35 M/M; Ambient temperature
10	13 September 2022	CO ₂ -loaded solution – lean	3.5% NaCl solution	1.0	Loading: 0.23 M/M; “Bucket and stopwatch” check applied; Ambient temperature
11	15 September 2022	CO ₂ -loaded solution - lean	Cooling water Lake Macquarie	1.0	Loading: 0.23 M/M; “Bucket and stopwatch” check applied.

An overview of results from the Forward Osmosis experiments is given in Table 18, providing performance data for the experiments listed in Table 17. Further experimental results are provided in Appendix C . The performance data reported are:

- Water flux (l/m^2h) from feed solution to draw solution
The water flux determines the membrane area required and is therefore a design parameter.
- Taurate concentration in feed solution outlet (g/l)
The taurate concentration at the outlet is needed to understand any issues with the water discharge into the environment.
- Taurate flux (g/m^2h) from draw solution to feed solution
The taurate flux represents the transfer of taurate to the feed solution and will determine the loss of amino-acid from the CO_2 -absorbent loop.
- Specific Reverse Amine Flux – SRAF (g/l)
The SRAF is the ratio of amino-acid flux and water flux. A specification for the SRAF was developed on in Section 4.2 on the basis of amine tolerable losses and water recovery per unit CO_2 -captured. The SRAF should be ideally below 1.0 and preferably below 0.25.
- Potassium flux (g/m^2h) from draw solution to feed solution
The potassium flux represents the transfer of potassium to the feed solution and should be low.
- Salt flux (g/m^2h) from feed solution to draw solution, determined by the transfer of Na^+ , expressed as a NaCl salt flux
The salt flux describes transfer of salt as NaCl to the CO_2 -absorbent loop and will add to the build-up of heat stable salts and should therefore be limited.
- Specific Forward Salt Flux – SFSF – Na-basis (g/l)
The SFSF is the ratio of salt flux and water flux and effectively represents the quality of the water transferred to the CO_2 -absorbent loop.
- Salt flux (g/m^2h) from feed solution to draw solution, determined by the transfer of Cl^- , expressed as a NaCl salt flux
The salt flux describes transfer of salt as NaCl to the CO_2 -absorbent loop and will add to the build-up of heat stable salts and should therefore be limited.
- Specific Forward Salt Flux – SFSF – Cl-basis (g/l)
The SFSF is the ratio of salt flux and water flux and effectively represents the quality of the water transferred to the CO_2 -absorbent loop.

Water flux

The water flux results for the experiments with 3.5% NaCl feed solution varied between 4.4 and 10.6 l/m²h which was lower than the laboratory experiments with different taurate solutions (15 – 21 l/m²h; see

Table 7). One reason was the higher water recovery resulting in more dilution of the draw solution and more concentration in the feed solution that will reduce the osmotic pressure difference. It is also quite customary for membrane fluxes to be lower when technology is scaled up from single sheet membranes and optimal flow conditions to industrial membrane units. The FO unit had a membrane area that was 3000 larger than the laboratory set-up and it is evident that a massive process scale increase was realised in this project.

Water fluxes were highest in the experiments using the warm inlet streams. As expected, the experiment using DI water gave the highest water flux. The water flux determined with lake water was in agreement with the result obtained from the model NaCl solutions.

It was not possible to confirm any effect of the CO₂-loading on the water flux, with the limited data set.

Taurate

The taurate concentrations in the feed solution at the exit were always at a low level, between 0.26 and 0.52 g/L for the experiments using saline solutions as the feed solution. The resulting values for the SRAF were between 0.26 and 0.75 g/l, which were lower than the desired threshold and also lower than the experimental results obtained in the laboratory (

Table 7). For the experiment with lake water the potentiometric titration was not able to provide an estimate for the concentration due to interference from components present in the lake water.

Potassium

The potassium concentration in the feed solution at the exit appeared to be much higher than the taurate concentration. As potassium is present in large concentration in the draw solutions there is a large concentration difference across the membrane that drives this. It was also thought that the reverse permeation of carbonate added to the potassium permeation, as the charge balance needed to be maintained. While carbonate concentrations were not determined in our analysis, our online FT-IR equipment recorded a concentration of the order of 0.2 M. This instrument has limited accuracy at low concentration level and is used to determine amine concentration in the absorption liquids. The high concentration of carbonate ions has probably contributed to the high permeation of potassium.

Sodium and Chloride

The separate analysis of sodium and chloride provided data that were converted to a single NaCl permeation rate and the SFSF, which is a proxy for the purity of the water permeating from the feed to the draw solution. The SFSF was higher than anticipated and varied between 0.7 and 7 g/l based on sodium ion concentration measurement, and between 0.4 and 2.7 g/l for the chloride ion concentration measurement. The sodium ion permeation appeared to be higher than the chloride permeation. It was hypothesised that the SFSF could be reduced by replacing the potassium by sodium in the formulation of the amino-acid salts and by the omission of potassium carbonate in the solutions in the first place.

It needs to be stressed that the high recovery from the feed solutions aggravated the undesired permeation of salts and led to lower water fluxes, i.e., under realistic process conditions the overall process performance is anticipated to be better.

Heat transfer

Temperatures were measured at the inlet and outlet points of the membrane module. As the draw and feed solution were flowing in a co-current mode, in most experiments the temperatures of the outlet flows were quite similar. Even in the experiments with warm draw solution this was the case. Given the high water recovery ratio from the feed solution, there was a significant flow of water from the feed to the draw side, which essentially meant that the flows were mixed.

Table 18 Overview of results from Forward Osmosis experiments using taurate-carbonate mixtures as draw solution and de-ionised/saline water as the feed solution

No.	Draw solution	Feed solution representing cooling water	Water flux [l/m ² h]	Taurate concentration at feed outlet [g/l]	Taurate flux [g/m ² h]	SRAF [g/l]	Potassium flux [g/m ² h]	Salt flux As NaCl based on sodium [g/m ² h]	SFSF As NaCl based on sodium [g/L]	Salt flux [g/m ² h] As NaCl based on chloride	SFSF As NaCl based on chloride [g/L]
1	Fresh unloaded solution	DI water	21.6	0.6	1.35	0.06	11.4	NA	NA	NA	NA
2	CO ₂ -loaded solution – lean	DI water	< 21.0	0.28	ND	ND	ND	NA	NA	NA	NA
3	CO ₂ -loaded solution - rich	DI water	< 21.3	0.36	ND	ND	ND	NA	NA	NA	NA
4	CO ₂ -loaded solution - lean	DI water	< 21.3	1.27	ND	ND	ND	NA	NA	NA	NA
5	CO ₂ -loaded	3.5% NaCl solution	10.6	0.47	3.79	0.36	100	48.1	4.5	28.7	2.7

	solution – lean										
6	Fresh unloaded solution	3.5% NaCl solution	8.9	0.28	2.69	0.30	114	61.6	6.9	13.6	1.5
7	Fresh unloaded solution	3.5% NaCl solution	5.3	0.34	2.82	0.53	115	3.88	0.73	2.17	0.41
8	Fresh unloaded solution	3.5% NaCl solution	8.6	0.26	2.23	0.26	111	34.7	4.0	3.82	0.45
9	CO ₂ -loaded solution - rich	3.5% NaCl solution	4.9	0.33	1.55	0.31	69.6	23.4	4.8	6.39	1.3
10	CO ₂ -loaded solution – lean	3.5% NaCl solution	4.4	0.52	3.38	0.75	39.0	19.4	4.5	5.37	1.2
11	CO ₂ -loaded solution - lean	Cooling water from Lake Macquarie	7.1	ND	ND	ND	-18.5 (flow from salt water to absorbent)	5.23	0.74	6.3	0.88

8 Techno-economic and Greenhouse-Gas Life Cycle Analysis

8.1 Design basis of combined CO₂-capture-desalination process

The process design is based on the ultra-supercritical coal fired power station described in Section 1.2 to which a PCC process is retrofitted that captures 90% of the CO₂ present in the flue gas.

For the capture system we assumed that the PCC process performance was equivalent to the state-of-the-art PCC process and the performance estimates are not based on a detailed integration. The addition of the PCC process also required flue gas desulphurisation to be installed. Previous process simulations²⁰ indicate that around 1% of the power output will be needed for the flue gas desulphurisation. The PCC process will also reduce the power output of the power station. Here we simply assumed that the energy requirement for capture and compression equalled 0.244 MWh/tonne CO₂ which, at 90% CO₂ capture, result in a 17.07% output reduction. Overall, an output reduction of 18.07% is therefore anticipated.

For the water consumption we assumed a 22% increase in absolute water consumption after the addition of 90% CO₂-capture, resulting in an increase of 250 m³/h mainly for cooling and an increase of 42 m³/h (based on 0.064 m³/MWh) as a result of the flue gas desulphurisation. In total the increase in water consumption was 292 m³/h equivalent to an increase of 25.7%.

Based on this analysis we found that the combined desalination – CO₂-capture system would be most beneficial if it could produce 0.64 m³/tonne CO₂ captured to provide the overall additional water requirement for PCC and flue gas desulphurisation with a lower limit of 0.1 m³/tonne CO₂ sufficient for flue gas desulphurisation only. Our previous process modelling work based on 5 M MEA¹ indicated that 0.41 m³/tonne CO₂ could be recovered from the desorber only, without an increase in the reboiler duty and without major additional investment apart from the replacement of the lean absorption liquid heat exchanger by the Forward Osmosis unit. We considered the cases of 0.1 and 0.4 m³/tonne CO₂ as representative cases for the techno-economic analysis, with results presented in Table 19. At the maximum production capacity, around 60% of the additional water requirement (PCC cooling and FGD) could be supplied by the combined CO₂-capture-desalination process.

Given relative immaturity of the Membrane Distillation technology, i.e., in comparison with Forward Osmosis technology, the recovery of water from the CO₂ absorber was not considered in the techno-economic analysis.

²⁰ CSIRO internal report ET/IR – 1083; Assessing post-combustion capture for coal fired power stations in APP countries, N. Dave, T. Do and D. Palfreyman, November 2008

Table 19: Performance overview for ultra-supercritical coal fired power plant with evaporative cooling used in this study; Results for 90% CO₂-capture estimated for state-of-the-art PCC process

Power plant	No capture	90% CO ₂ capture
Net electric power output [MW _e]	650	532.6
Net electrical efficiency, LHV [%]	42.88	35.13
Net electrical efficiency, HHV [%]	41.36	33.89
CO ₂ -emissions [tonne/h]	505.3	50.5
Specific CO ₂ emissions [tonne/MWh]	0.777	0.095
Water consumption [m ³ /h]	1137 (cooling water and boiler feedwater)	1429 (cooling water and boiler feedwater, FGD, PCC plant)
Water consumption [m ³ /MWh]	1.777	2.699
Water production for FGD only [m ³ /h] (based on 0.1 m ³ /tonne CO ₂ captured)	-	45.5
Water production for FGD and PCC cooling [m ³ /h] (based on 0.4 m ³ /tonne CO ₂ captured)	-	182

8.2 Techno-economic analysis Forward Osmosis process

The techno-economic analysis used the design basis defined in Section 8.1 8.1. Two water production cases were defined: 0.1 m³/tonne CO₂, sufficient to supply water to the FGD and 0.4 m³/tonne CO₂ as a typical maximum amount that could be produced from the desorber only. The FO water flux will be dependent on the type of amine, its lean CO₂-loading, temperature and the salinity of the feedwater. Given that the design water recovery was less than 4%, i.e. ten times less than the recovery worked with in both our laboratory and pilot plant experiments a design water flux of 10 l/m²h was thought to be realistic. This resulted in the overall design requirements for the Forward Osmosis unit in Table 20.

Table 20: Design requirements for Forward Osmosis unit

Specific Water production [m ³ /tonne CO ₂ captured]	0.1	0.4
Lean absorption liquid flow into FO unit [m ³ /h]	4730	4730
Absolute water production [m ³ /h]	45.5	182
Area FO membranes [m ²]	4550	18200

The techno-economic analysis was based on the technical and economic premises provided in Table 21. The maximum water production equivalent to 0.4 m³/tonne CO₂ was assumed. The Forward Osmosis process cost estimates used information applicable to Reverse Osmosis processes as the nearest comparative process, to estimate chemical cost and membrane replacement cost. The total investment included costs for pretreatment, piping, pumps, control system, construction and installation. Table 21 provides the comparative information for the Forward and Reverse Osmosis process. The reduced complexity of the Forward Osmosis process leads to some cost advantages for maintenance and labour costs. Given the lower maturity of the Forward Osmosis technology the chemical and membrane replacement costs are taken higher than for the Reverse Osmosis process. A significant advantage of the Forward Osmosis process is the much lower power consumption as the feedwater does not require pressurisation.

Table 21: Technical and economic premises for a Forward Osmosis and a Reverse Osmosis process

Parameter	Forward Osmosis	Reverse Osmosis	Unit	Notes
	Value			
Water production	4,368		m ³ /day	(=24x182)
Electricity cost coal – no capture	0.14		A\$/kWh	CSIRO GenCost report ²¹
Electricity cost coal – with capture	0.23		A\$/kWh	CSIRO GenCost report ²¹
Operation period	24		h/day	
Amortisation period	20		Yrs	
Interest rate	6		%	
Plant personnel	4	7 ²²	No.	RO: Average of high and low automation
Operational cost basis				
Power consumption	0.5	3.3 ^{22,23,24}	kWh/m ³	
Chemical cost	0.07	0.06 ^{21,25}	A\$/m ³	20% use more than RO as basis
Membrane replacement cost	0.09	0.06 ^{22,24}	A\$/m ³	50% more than RO as basis
Maintenance	0.25	0.42 ^{24,26}	A\$/m ³	2% of installed equipment cost for the processing capacity
Labour	77,948		A\$/year/person	AWOTE, average of last 8 yrs.
Capital cost basis				
Membrane cost	438	22	A\$/m ²	Basis from recent small-scale purchase and factor for scaleup, no pressure vessel, 1 US\$ =1.46 A\$

²¹ Graham, P., Hayward, J., Foster J. and Havas, L. 2022, GenCost 2022-23: Consultation draft, CSIRO, Australia.

²² Voutchkov, N., Desalination engineering planning and design. 2013, USA: The McGraw-Hill Companies

²³ WSAA 2013, Seawater desalination, Water Services Association Australia

²⁴ Qasim et al 2019, Desalination, 459, 59-104

²⁵ Fritzmann et al. 2007, Desalination, 216, 1-76

²⁶ Bhojwani et al. 2019, Sci Total Env., 6651, 2749-2761

The total capital costs estimation (Table 22) for the Forward Osmosis process is based on the capital costs for a Reverse Osmosis plant of the same capacity for which the capital costs were estimated using data available in the literature^{27,28,29}. The various cost components, other than the membranes, are generally lower for Forward Osmosis compared to Reverse Osmosis as a result of the lower operating pressure, the ability to use lower cost materials and reduced complexity. The disposal for brines and post-treatment, as well as the project contingency are assumed to be equivalent. While Reverse Osmosis generates highly concentrated brine streams as a result of the high water recovery, Forward Osmosis generates only slightly concentrated streams as water recovery is much less. However post-treatment in case of Forward Osmosis might have to deal with low concentrations of amines in the cooling water and there might be increased costs in handling the salts that transfer into the absorbent solution. On balance and despite the much higher membrane costs, the capital costs for the Forward Osmosis process are 11% lower than the Reverse Osmosis process.

In our analysis we distinguished three water production cases, i.e. two base cases using stand-alone Reverse Osmosis:

1. a standard coal fired power plant without PCC (low electricity cost – high CO₂-emission), and,
2. a coal fired power plant with PCC (higher electricity cost – low CO₂-emission).

These cases were compared the case where water was produced by Forward Osmosis through the PCC process (high electricity cost – low CO₂-emission).

²⁷ Crisp 2012, Desalination in Australia

²⁸ Wolf et al. 2005, Desalination, 182, 293-300

²⁹ Hafez and El-Manharawy 2002, Desalination, 153, 335-347

Table 22 Estimated capital costs for a Forward Osmosis and a Reverse Osmosis process

Component	Forward Osmosis capital cost, A\$	Reverse Osmosis capital cost, A\$	Comment
	Water production = 4,368 m ³ /day		
Membrane element	7,971,600	471,763	FO requires more expensive membranes as membrane and module manufacturing is not on the scale of RO membranes.
Pressure vessel	-	235,881	No pressure vessels require for FO
Intake and pre-treatment	3,382,357	6,980,242	Less pre-treatment needed for FO
Pumps and energy recovery system and monitoring equipment	1,127,452	2,702,029	Pumps on FO are low pressure
Piping & valves	676,471	1,125,845	Simpler materials for FO due the low pressure
Construction, Installation, Electrical & Instrumentation	3,382,357	7,430,580	FO process has lower complexity
Brine disposal & post treatment	2,254,905	2,254,905	Assumed same cost for disposal of brine
Others & contingency	1,127,452	1,125,845	Similar cost
Total	20.0 M	22.5 M	Rounded up numbers

Next the water production costs for the Forward Osmosis process were calculated and compared with the costs for the reference Reverse Osmosis process with the same capacity, assuming the feedwater was seawater.

The FO plant investment amounts to nearly A\$20M for the capacity of 4,368 m³/day, as shown in Table 23, with the RO plant investment being 12.5% higher. The resulting FO water production costs are calculated to be \$1.82/m³ with the largest contribution (60%) determined by the capital costs. The operational costs (40%) are largely determined by maintenance and labour costs. The equivalent costs for the RO process in a coal fired power plant with PCC were 58% higher at \$2.88/m³ and 42% for the RO process in a coal fired power without PCC. The FO process exhibited much lower maintenance and electricity cost and also lower capital cost (Table 23). As the electricity costs for the FO process stem from the pumping of absorption liquid and cooling water, it can be argued that these are not additional cost but already part of the CO₂-capture plant cost.

Finally, given that there is significant potential for FO membrane cost reduction, it is likely that the costs for the FO process will come down with further deployment. The RO membrane costs have

already been reduced to very low levels through its deployment over the past fifty years and the potential for further reduction is limited.

Table 23: Preliminary Forward Osmosis process cost estimate with a Reverse Osmosis process as reference

Parameter	Forward Osmosis (with PCC)	Reverse Osmosis (with PCC)	Reverse Osmosis (No PCC)	Unit
	Value			
Water production	4,368			m ³ /day
Membrane area	18,200	17,390	17,390	m ²
Plant investment	19.9	22.5	22.5	MA\$
Total operating cost	0.73	1.65	1.35	A\$/m ³
Membrane replacement cost	0.09	0.06	0.06	A\$/m ³
Maintenance	0.25	0.42	0.42	A\$/m ³
Chemical cost	0.07	0.06	0.06	A\$/m ³
Labour	0.20	0.34	0.34	A\$/m ³
Electricity	0.12	0.76	0.46	A\$/m ³
Capital cost	1.09	1.23	1.23	A\$/m ³
Total water cost	1.82	2.88	2.58	A\$/m ³

8.3 Greenhouse-gas lifecycle analysis

Forward Osmosis systems are not yet widespread and can be applied in diverse applications like wastewater treatment and energy harvesting from concentration differences. The lifecycle analysis will therefore need to be quite specific to the application. The greenhouse-gas (GHG) life cycle analysis for the combined desalination-CO₂-capture application has focused on the comparison between the Reverse Osmosis process and the Forward Osmosis process to provide desalinated water from the saline cooling water. With this scope for the GHG lifecycle analysis it was assumed that the production processes for Reverse Osmosis and Forward Osmosis equipment were quite similar, as well as the post- and pre-treatment of produced water and other liquids during operation. Given the lack of a detailed process design for the combined desalination-CO₂-capture process, this assumption was considered to be justified. The functional unit for the GHG lifecycle analysis was 1 m³ of produced water.

The greenhouse-gas impacts of Reverse Osmosis processes are normally dominated by the energy requirement and the emissions intensity of the energy source³⁰. The non-energy use greenhouse-gas impacts originate from the embedded energy in the equipment used, chemicals used in the desalination process and the maintenance activities. These were estimated by extrapolation of literature data³¹ that were provide at different energy consumption for the Reverse Osmosis process, which resulted in a GHG-emission of 0.04 kg CO_{2,e}/m³ water produced. The energy consumption related emissions were determined by multiplication of the power consumption and the specific CO₂ emissions, which were taken as the emissions from the coal fired power plant after installation of the PCC process. The GHG emissions are given in Table 24.

³⁰ A comparative life cycle assessment of hybrid osmotic dilution desalination and established seawater desalination and wastewater reclamation processes, Nathan T. Hancock, Nathan D. Black, Tzahi Y. Cath, Water Research, Volume 46, Issue 4, 15 March 2012, Pages 1145-1154

³¹ Life Cycle Assessment of Water Production Technologies; Part 2: Reverse Osmosis Desalination versus the Ebro River Water Transfer, R. Gemma Raluy, Luis Serra, Javier Uche and Antonio Valero, Int J LCA 10 (5) 2005

Table 24 Greenhouse gas emission for water production from the Forward Osmosis and Reverse Osmosis process

Parameter	Forward Osmosis (With PCC)	Reverse Osmosis (With PCC)	Reverse Osmosis (No PCC)	Unit
	Value			
Water production	4,368			m ³ /day
Specific CO ₂ emissions	0.095		0.777	kg/kWh
Power consumption	0.5	3.3	3.3	kWh/m ³
Non-energy GHG emissions	0.04	0.04	0.04	kg CO _{2,eq} /m ³ or tonne CO _{2,eq} /ML
Energy GHG emissions	0.05	0.31	2.56	
Total specific GHG emissions	0.09	0.35	2.60	
Total annual emissions	130	510	3696	Tonne/year (330 days/year)

The total GHG emissions are lowest for the Forward Osmosis process. They are only one quarter of the GHG emissions for the Reverse Osmosis process for the coal fired power station with PCC. The GHG emissions for the Forward Osmosis represent a 96.5 % reduction compared to the water production by Reverse Osmosis using electricity from the coal fired power station without PCC. The low emissions for the Forward Osmosis process result from both the low electricity consumption and the use of low-emission electricity from the power station with PCC.

Next, we combined the results from Table 23 and Table 24 into a single graph (Figure 59) that enabled us to determine the costs per tonne CO₂-avoided. This is generally defined as the specific cost differential between a reference case production process and a case with lower CO₂-emissions divided by the differential of the CO₂-emissions intensity.

As the Forward Osmosis process has lower water production costs, the change over from the reference case using the Reverse Osmosis process results in negative values for the CO₂-avoidance cost. This means that process does not require a carbon premium to assist with its implementation. The implementation of Reverse Osmosis on coal fired power station that has PCC retrofitted would require a carbon premium to be equivalent cost. In that case the emission reduction would be significant, but it would come at increased water production costs. This is not the situation if the Forward Osmosis process were implemented.

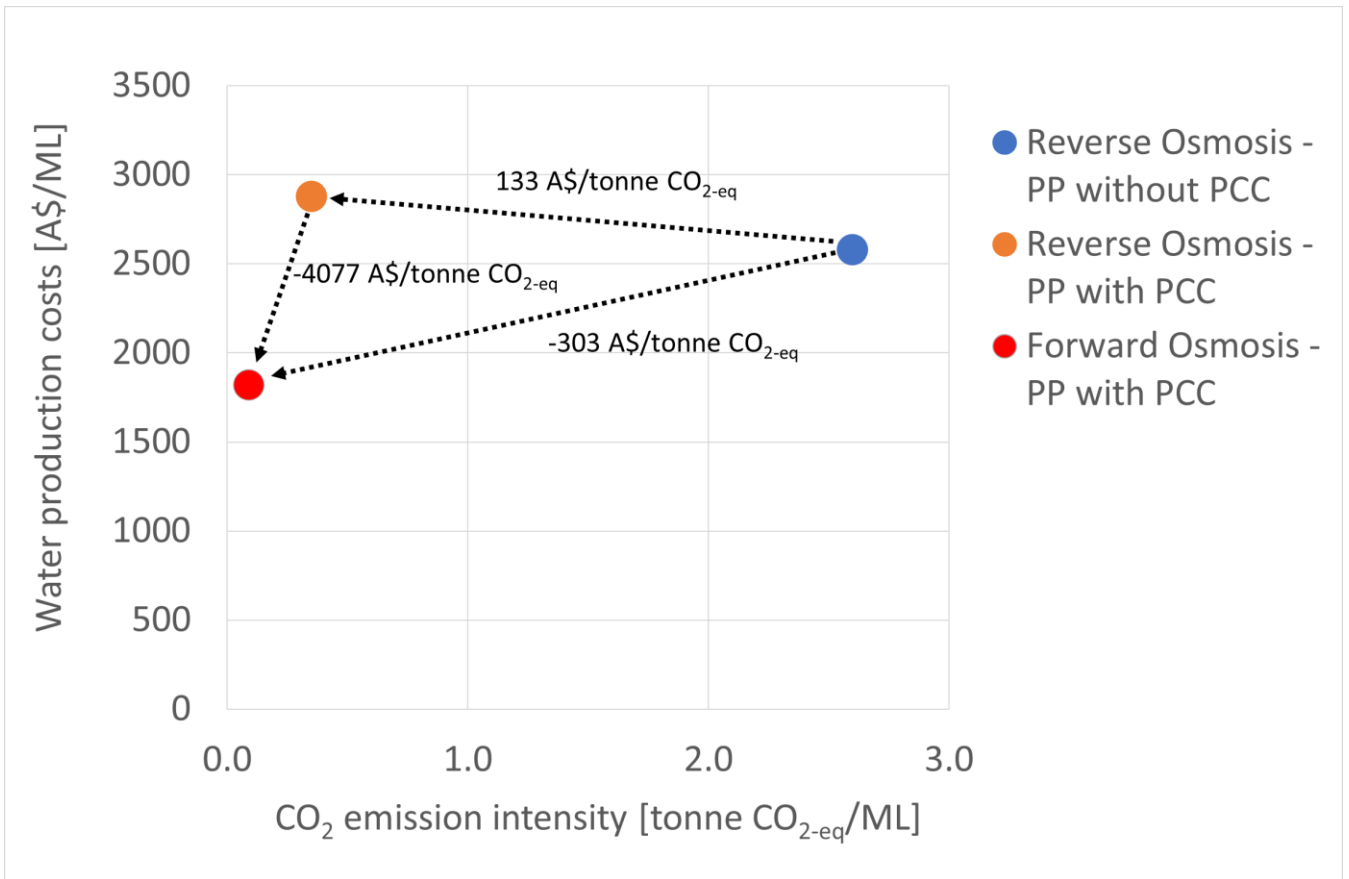


Figure 59 Water production cost versus CO₂-emission intensity

9 Conclusions

The project investigated the application of a combined desalination – amine-based CO₂-capture process, consisting of a Forward Osmosis unit that transferred water from saline cooling water to the absorption liquid, using water recovery via the desorber condensate or via a Membrane Distillation unit from the absorber. Each of these process steps were assessed during the project.

Forward Osmosis

Laboratory research using six representative absorption liquids and two commercially available membranes and modules showed the effectiveness of the FO membranes in transferring water from a saline solution to the absorption liquids. Amino-acid salt solutions appeared to exhibit the best performance in terms of water flux and specific reverse amine flux, which is a measure of amine loss to the cooling water.

The Forward Osmosis process has been successfully demonstrated using a taurate-carbonate solution with the PCC pilot plant at Vales Point Power Station in a membrane unit that represented a 3000 times increase in membrane area compared to the laboratory work.

Experiments with an MEA-carbonate solution were not successful, most likely because of interactions between the flat sheet membrane sealing and MEA.

Water fluxes determined for the taurate-carbonate solutions in the technology demonstration at Vales Point were lower than those determined in the laboratory experiments, whereas the Specific Reverse Amine Flux Process performances met the specifications previously defined and were lower than the laboratory experiments. The Specific Forward Salt Flux (not determined in the laboratory studies) was variable and higher than previously assumed.

While it is clear that the FO membrane unit operated as a heat exchanger, its operation was not further optimised or investigated in-depth as the high water flux through the membranes that dominated the heat transfer.

The conclusions around the technology performance were unfavourably affected by the high water recovery from the saline feed solutions in both the laboratory experiments and the technology demonstration. As lower water recovery will be aimed for in real applications, water fluxes will be higher and the impact of the reverse amine flux and the forward salt flux is anticipated to be lower.

Water recovery from the absorber through Membrane Distillation

The laboratory research investigated a range of membrane geometries (flat sheet, hollow fibre, capillary), membrane modules (contactor and filtration type) and membrane materials (porous Poly-Tetra-Fluoro-Ethylene and Polypropylene) for their suitability to recover water via evaporation through the membrane and subsequent condensation.

Apart from the assessment of the technical performance (water flux and amine flux) the objective was to also identify the preferred membrane configuration that had potential for technology demonstration at Vales Point. It was concluded that it was too soon for this due to a lack of reliable

commercially available membrane module or poor membrane performance (membrane leakage or low water flux) for those membrane modules that were commercially available.

It was concluded that for amino-acid salt solutions (taurate solutions as proxy) the porous polypropylene membranes were useable as there was limited permeation of the amino-acids through the membranes. For amine-solutions poly-tetrafluorethylene membranes were required to avoid amine permeation. However, the evaporative losses of amines will lead to significant contamination of the product water and the use of amino-acid salts (no amine vapour pressure) is preferred.

Water recovery from desorber

The experiments with the PCC pilot plant at Vales Point with MEA and MEA-carbonate solution indicated that the product water retrieved from the condenser incorporated significant amounts of MEA as a result of the amine vapour pressure. Depending on its end use, further clean-up might therefore be required.

The pilot plant experiments using taurate-carbonate mixtures indicated that the product water did not contain significant amounts of the absorption liquid. There was evidence that degradation products were present in the condensate obtained in these experiments.

10 Recommendations

Forward Osmosis process

- The project has systematically investigated several aspects of the combined desalination – CO₂-capture process. The methodology thus developed can be used as a recommended protocol to assess the process performance for different absorption liquids and different Forward Osmosis membranes. This involves the FO process characterisation in terms of water flux, Specific Reverse Amine Flux and Specific Forward Salt Flux and the assessment of product water through pilot plant operation.
- As the next development step, an integrated FO process is recommended that would operate in-line with a PCC pilot plant or on a slip stream of a larger capture plant. The objective would be to investigate the long term operation and performance of the FO membrane under realistic conditions and assess its robustness under variable conditions and changes in the absorption liquids over time. This activity needs to be based on combinations of FO membranes and absorption liquids that have been successfully evaluated using the aforementioned protocol. It would also need to consider the quality of water produced, the build-up salts in the absorption liquids and the potential slip of absorption liquid constituents to the cooling water.
- To enable optimum performance from the process, in terms of water production and heat transfer, the water recovery should generally be low to enable the water production to require no additional thermal energy. This requires a new membrane module design with low water recovery.
- Close collaboration with an FO membrane supplier is needed to ensure best performance from the process and resolution of issues encountered during process operation. A wider variety of membrane geometries and types for further investigation is also recommended.
- Further optimisation of the desorber and condenser operation would be required to determine the minimum reflux rates necessary to recover amine vapours and optimise produced water quality from the condenser. This can be assessed through process modelling as a first step.
- The impact of the Forward Salt Flux on the PCC plant in terms of added build-up of heat stable salts requires further attention.

Membrane distillation process

- Further work with suppliers of Membrane Distillation equipment is recommended to assess the potential for water recovery from the absorber. The work can start using amino-acid salt solutions as they exhibited no vapour pressure and the water produced should be of adequate purity. Using these solutions, a first demonstration would be feasible using commercially available membrane contactors. This could also support the exploration of other benefits such as using the device for absorber intercooling and removal of oxygen.

Appendix A Conference presentations and publications

Conference presentations

Seawater desalination with an amine-based CO₂-capture process, Paul Feron, Ramesh Thiruvengatchari, Sanger Huang, Jun-Seok Bae, Ashleigh Cousins, Debra Fernandes, Anne Tibbett, poster presentation at GHGT-15, 15-18 March 2021, Abu Dhabi, UAE

Reclamation of Water from Carbon Capture Process (Absorption Liquid) using Vacuum Membrane Distillation (VMD), Nouman Mirza, Robert Taylor, Paul Feron, Oral presentation at PCCC6, 19-21 October 2021, Virtual conference, Sheffield, UK

Combined desalination and CO₂-Capture: Results from pilot plant experiments, Paul Feron, Ramesh Thiruvengatchari, Sanger Huang, Nouman Mirza, Debra Fernandes, Dan Maher, Phil Green, Will Conway, Jun-Seok Bae, Ashleigh Cousins, Ali Pourkhesalian, Oral presentation at GHGT-16, 23-27 October 2022, Lyon, France

Publications

Reclaiming water from a direct air capture plant using vacuum Membrane Distillation – A bench-scale study, Nouman Rafique Mirza, Debra Fernandes, Qiyuan Li, Amr Omar, Shuaifei Zhao, Zongli Xie, Robert Taylor, Jessica Allen, Paul Feron, Separation and Purification Technology 305 (2023) 122418

Gas flow enhanced mass transfer in vacuum Membrane Distillation, Shuaifei Zhao, Paul H.M. Feron, Xiao Chen, Inci Boztepe, Jianhua Zhang, Nouman Rafique Mirza, Lingxue Kong, Desalination 552 (2023) 116434

Appendix B Combined Desalination & CO₂ capture – Pilot plant equipment specification



B.1 Design and Features

- Handle Draw and Feed solutions range from 20L/m to 40L/m
- Water Production Capacity of 55kg/hr of water @ 40L/min (Draw & Feed)
- Capture 2.2% of the water from Feed solution
- Capable of operating with MEA and Amino Acid respectively

B.2 Main Equipment

B.2.1 Membrane module (FO-MO1-1 and FO-MO1-2)

- Porifera Pro-100
- Flat Sheet

- Standard Membrane Area 7 m² / element
- 2 elements / module, 2 modules installed in parallel
- Physical Dimension 460mm X 390mm X 145mm
- ½" NPT Connection port

B.2.2 Pumping equipment

Feed solution pump (FS-PUMP1)

- Grundfos CRNE 3-4
- 40L/min @ 12 m, max temperature 90°C
- 316 wet end construction
- Powered by 0.55 kW motor
- Controlled via built in VSD

B.2.3 Filters (connected to inlet of DS and FS)

Draw Solution Filter (DS-FXX)

- Aquastream FPBH 3-25
- 5 um filtration
- Max capacity 300L/m
- bag filter
- SS 304/316 housing
- Seal Material EPDM
- 1" BSP process connection

Feed Solution Filter (FS-FXX)

- Pentek HSN-1000 BB20PR
- 5 um filtration
- Max capacity 200L/m
- polyester pleated sediment cartridge filter
- Polypropylene housing
- Seal Material Buna-N
- 1" BSP process connection

B.3 Piping

- 316 stainless steel schedule 40 pipe for draw solution line
- 316 stainless steel schedule 40 pipe for feed solution line
- 316 stainless steel flanges RF 150lb and assorted schedule 40 fittings

B.4 Utility

B.4.1 Instrument air (to Control Valve DS-CV01)

- Delta Power Station supplies at 6 bar G
- ACT8T AIR Dryer
- With a flow rate of 14.1 L/s
- Power supply 240V
- ¼" BSP connection needed for DS-CV01
- 3 Micron air filter attached.

Appendix C Overview of Forward Osmosis experimental results with taurate-carbonate solutions

Data provided for inlet and outlet streams:

- Flow rates (data in red is calculated from other experimental results)
- Taurate concentration
- Potassium concentration
- Sodium concentration
- Chloride concentration
- Temperature
- Conductivity (for cooling/feed streams)

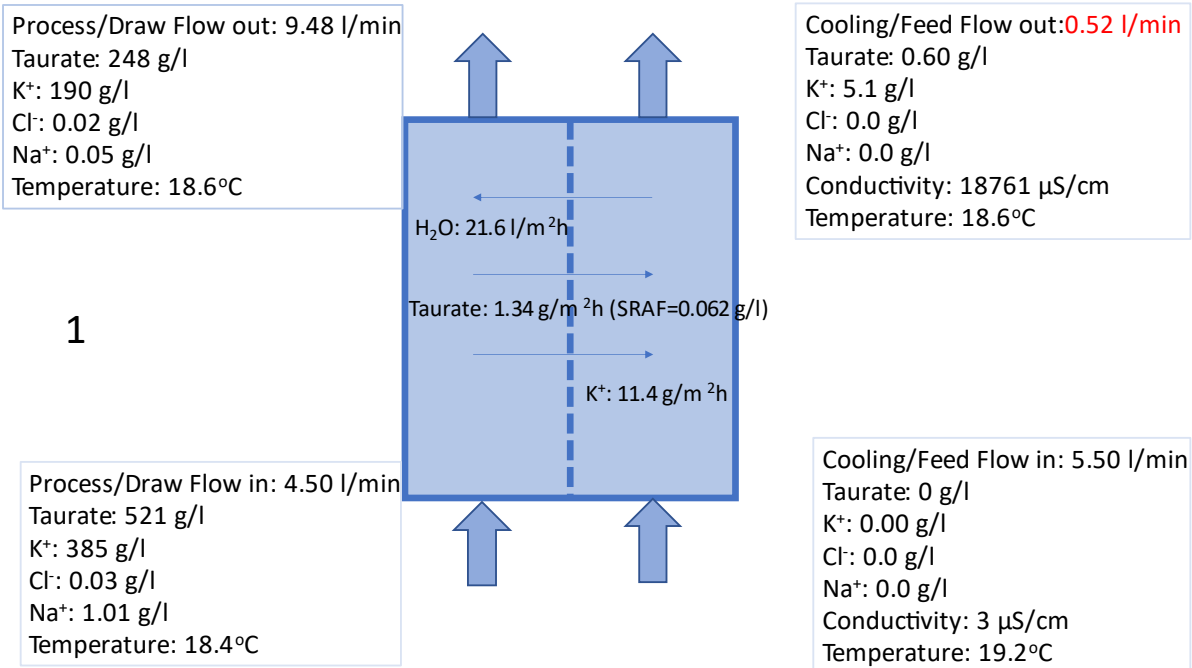
Fluxes calculated:

- Water flux
- Taurate flux, including Specific Reverse Amine Flux (SRAF)
- Potassium flux
- Salt flux as NaCl – sodium-based, including Specific Forward Salt Flux (SFSF)
- Salt flux as NaCl – chloride-based, including Specific Forward Salt Flux (SFSF)

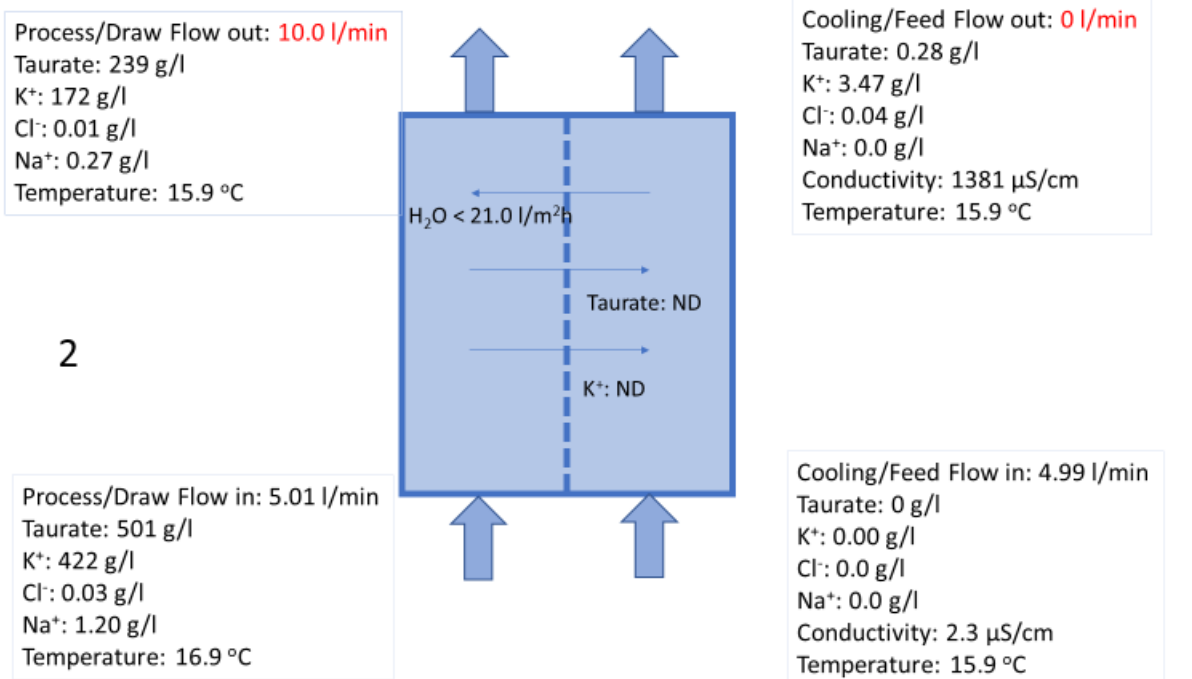
ND means Not Determined

Refer to Table 17 for description of experimental conditions for each experiment.

C.1 Experiment 1



C.2 Experiment 2

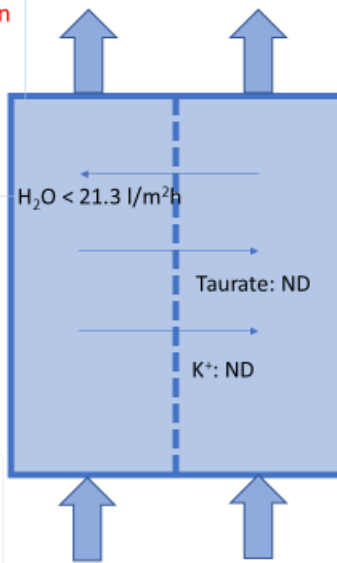


C.3 Experiment 3

Process/Draw Flow out: **10.16 l/min**
 Taurate: 226 g/l
 K⁺: 157 g/l
 Cl⁻: 0.07 g/l
 Na⁺: 0.30 g/l
 Temperature: 17.7 °C

3

Process/Draw Flow in: 5.18 l/min
 Taurate: 523 g/l
 K⁺: 379 g/l
 Cl⁻: 0.05 g/l
 Na⁺: 1.07 g/l
 Temperature: 22.0 °C



Cooling/Feed Flow out: **0 l/min**
 Taurate: 0.36 g/l
 K⁺: 0.62 g/l
 Cl⁻: 0.00 g/l
 Na⁺: 0.0 g/l
 Conductivity: 1699 μS/cm
 Temperature: 17.8 °C

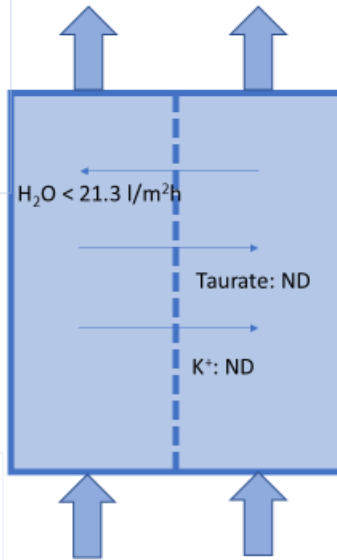
Cooling/Feed Flow in: 4.98 l/min
 Taurate: 0 g/l
 K⁺: 0.00 g/l
 Cl⁻: 0.0 g/l
 Na⁺: 0.0 g/l
 Conductivity: 2.3 μS/cm
 Temperature: 16.9 °C

C.4 Experiment 4

Process/Draw Flow out: **9.99 l/min**
 Taurate: 159 g/l
 K⁺: 145 g/l
 Cl⁻: 0.02 g/l
 Na⁺: 0.41 g/l
 Temperature: 19.6 °C

4

Process/Draw Flow in: 5.02 l/min
 Taurate: 533 g/l
 K⁺: 440 g/l
 Cl⁻: 0.12 g/l
 Na⁺: 1.27 g/l
 Temperature: 35.2 °C



Cooling/Feed Flow out: **0 l/min**
 Taurate: 1.27 g/l
 K⁺: 1.10 g/l
 Cl⁻: 0.01 g/l
 Na⁺: 0.0 g/l
 Conductivity: 1421 μS/cm
 Temperature: 19.3 °C

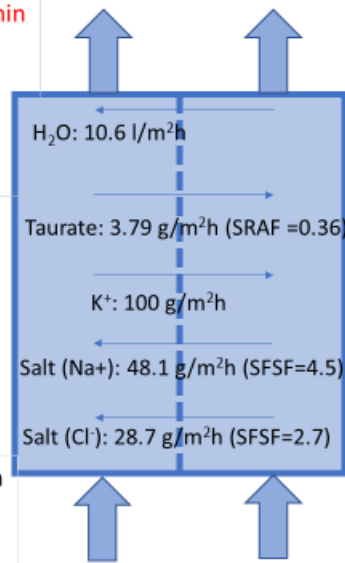
Cooling/Feed Flow in: 4.97 l/min
 Taurate: 0 g/l
 K⁺: 0.00 g/l
 Cl⁻: 0.0 g/l
 Na⁺: 0.0 g/l
 Conductivity: 2.2 μS/cm
 Temperature: 14.8 °C

C.5 Experiment 5

Process/Draw Flow out: **11.48 l/min**
 Taurate: 222 g/l
 K⁺: 146 g/l
 Cl⁻: 1.70 g/l
 Na⁺: 2.89 g/l
 Temperature: 20.9 °C

5

Process/Draw Flow in: 8.86 l/min
 Taurate: 473.3 g/l
 K⁺: 380 g/l
 Cl⁻: 0.15 g/l
 Na⁺: 1.20 g/l
 Temperature: 39.8 °C



Cooling/Feed Flow out: **1.87 l/min**
 Taurate: 0.47 g/l
 K⁺: 14.97 g/l
 Cl⁻: 37.72 g/l
 Na⁺: 20.25 g/l
 Conductivity: 96857 μS/cm
 Temperature: 20.9 °C

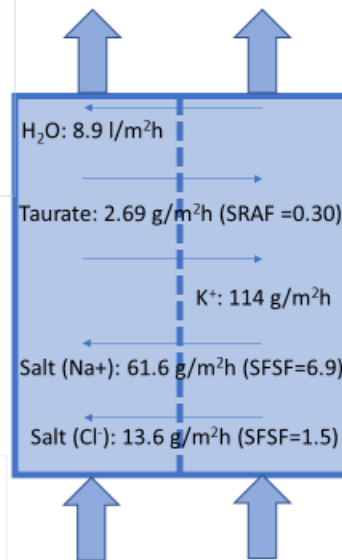
Cooling/Feed Flow in: 4.48 l/min
 Taurate: 0.0 g/l
 K⁺: 1.03 g/l
 Cl⁻: 19.80 g/l
 Na⁺: 14.02 g/l
 Conductivity: 52544 μS/cm
 Temperature: 14.2 °C

C.6 Experiment 6

Process/Draw Flow out: **6.72 l/min**
 Taurate: 224 g/l
 K⁺: 195 g/l
 Cl⁻: 1.01 g/l
 Na⁺: 3.75 g/l
 Temperature: 22.3 °C

6

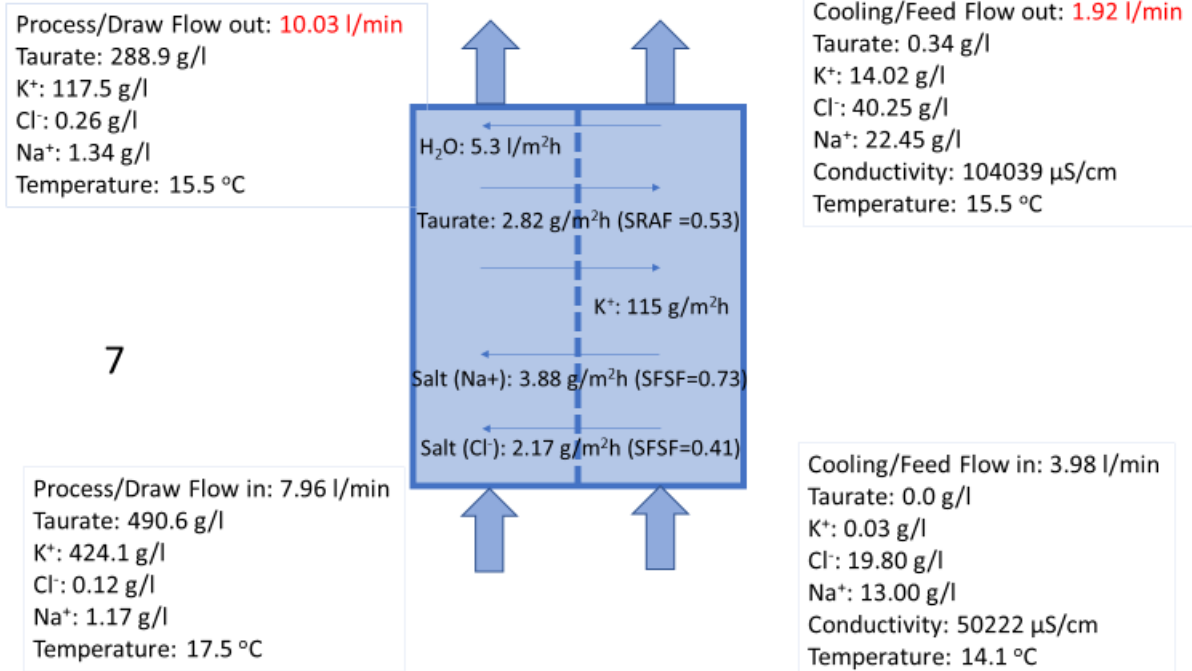
Process/Draw Flow in: 4.50 l/min
 Taurate: 473 g/l
 K⁺: 380 g/l
 Cl⁻: 0.15 g/l
 Na⁺: 1.20 g/l
 Temperature: 42.9 °C



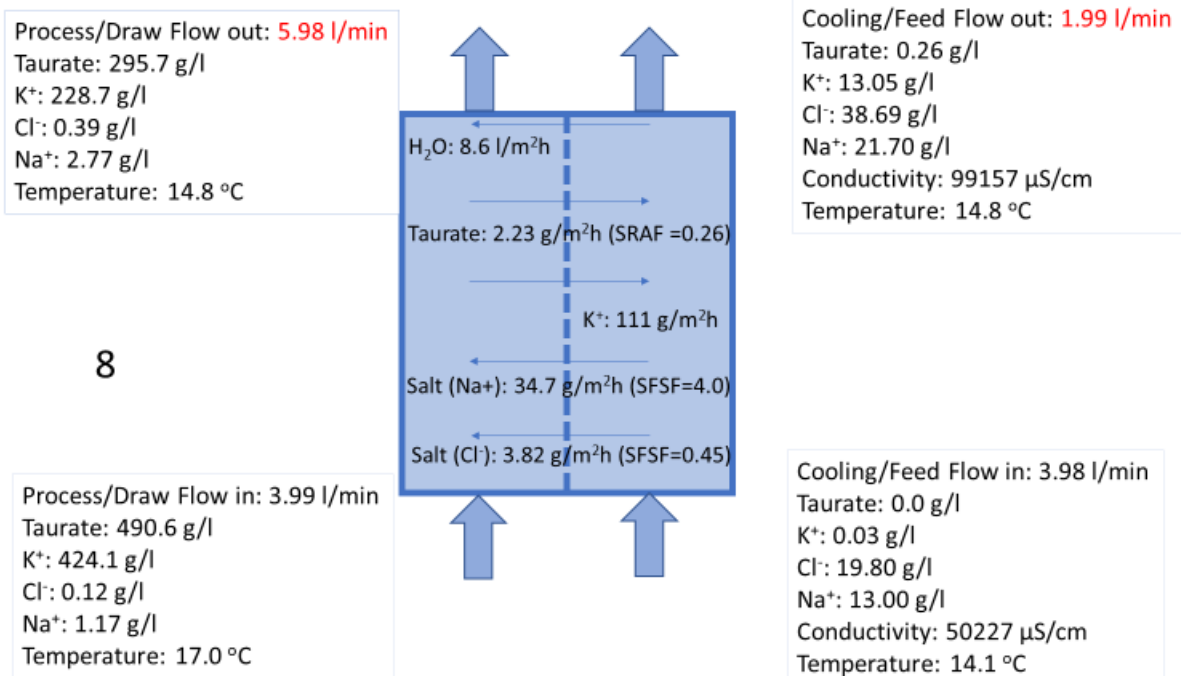
Cooling/Feed Flow out: **2.26 l/min**
 Taurate: 0.28 g/l
 K⁺: 13.77 g/l
 Cl⁻: 36.51 g/l
 Na⁺: 19.90 g/l
 Conductivity: 93926 μS/cm
 Temperature: 22.4 °C

Cooling/Feed Flow in: 4.48 l/min
 Taurate: 0.0 g/l
 K⁺: 1.03 g/l
 Cl⁻: 19.80 g/l
 Na⁺: 14.02 g/l
 Conductivity: 502544 μS/cm
 Temperature: 14.2 °C

C.7 Experiment 7



C.8 Experiment 8

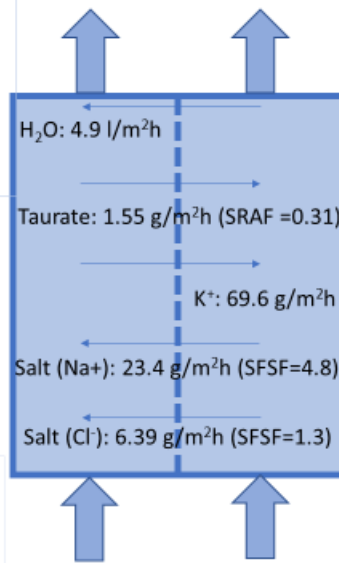


C.9 Experiment 9

Process/Draw Flow out: **3.65 l/min**
 Taurate: 274.9 g/l
 K⁺: 246.45 g/l
 Cl⁻: 0.97 g/l
 Na⁺: 2.90 g/l
 Temperature: 17.0 °C

9

Process/Draw Flow in: 2.39 l/min
 Taurate: 464.6 g/l
 K⁺: 384.9 g/l
 Cl⁻: 0.26 g/l
 Na⁺: 1.20 g/l
 Temperature: 20.6 °C



Cooling/Feed Flow out: **1.11 l/min**
 Taurate: 0.33 g/l
 K⁺: 14.82 g/l
 Cl⁻: 40.36 g/l
 Na⁺: 22.17 g/l
 Conductivity: 105163 μS/cm
 Temperature: 16.3 °C

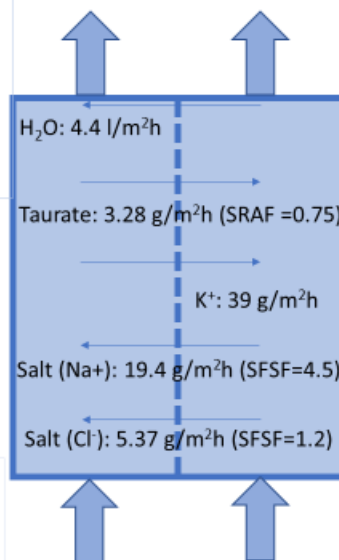
Cooling Flow in: 2.37 l/min
 Taurate: 0.0 g/l
 K⁺: 0.09 g/l
 Cl⁻: 20.07 g/l
 Na⁺: 13.26 g/l
 Conductivity: 50798 μS/cm
 Temperature: 14.6 °C

C.10 Experiment 10

Process/Draw Flow out: **4.11 l/min**
 Taurate: 333.1 g/l
 K⁺: 224.2 g/l
 Cl⁻: 0.66 g/l
 Na⁺: 2.44 g/l
 Temperature: 15.8 °C

10

Process/Draw Flow in: 2.80 l/min
 Taurate: 504.5 g/l
 K⁺: 384 g/l
 Cl⁻: 0.08 g/l
 Na⁺: 1.09 g/l
 Temperature: 18.2 °C



Cooling/Feed Flow out: **1.47 l/min**
 Taurate: 0.52 g/l
 K⁺: 13.24 g/l
 Cl⁻: 37.35 g/l
 Na⁺: 21.53 g/l
 Conductivity: 103675 μS/cm
 Temperature: 15.7 °C

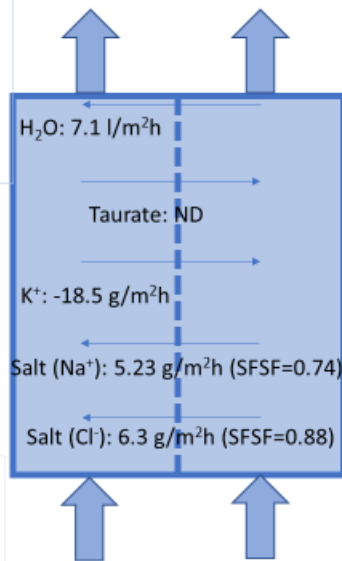
Cooling/Feed Flow in: 2.78 l/min
 Taurate: 0.0 g/l
 K⁺: 3.77 g/l
 Cl⁻: 20.58 g/l
 Na⁺: 12.04 g/l
 Conductivity: 49996 μS/cm
 Temperature: 15.1 °C

C.11 Experiment 11

Process/Draw Flow out: **5.04 l/min**
 Taurate: 305.7 g/l
 K⁺: 221.6 g/l
 Cl⁻: 0.56 g/l
 Na⁺: 1.77 g/l
 Temperature: 15.9 °C


11

Process/Draw Flow in: 3.20 l/min
 Taurate: 519.6 g/l
 K⁺: 391.9 g/l
 Cl⁻: 0.08 g/l
 Na⁺: 1.51 g/l
 Temperature: 17.3 °C



Cooling/Feed Flow out: **1.35 l/min**
 Taurate: ND
 K⁺: 10.84 g/l
 Cl⁻: 40.27g/l
 Na⁺: 20.62 g/l
 Conductivity: 103675µS/cm
 Temperature: 16.5 °C

Cooling/Feed Flow in: 3.19 l/min
 Taurate: ND
 K⁺: 5.94 g/l
 Cl⁻: 17.83 g/l
 Na⁺: 10.36 g/l
 Conductivity: 51224 µS/cm
 Temperature: 17.4 °C



As Australia's national science agency and innovation catalyst, CSIRO is solving the greatest challenges through innovative science and technology.

CSIRO. Unlocking a better future for everyone.

Contact us

1300 363 400
+61 3 9545 2176
csiro.au/contact
csiro.au

For further information

Energy

Paul Feron
+61 0 447688747
paul.feron@csiro.au
csiro.au/Energy